

# **DNA-Based Asymmetric Catalysis as a Synthetic Tool.**

Rik Megens

The research described in this thesis was carried out at the Stratingh Institute for Chemistry, University of Groningen, The Netherlands. It was financially supported by the Dutch Organization for Scientific Research (NWO).

Printing of this thesis was financially supported by the University Library and the Graduate School of Science (Faculty of Mathematics and Natural Sciences, University of Groningen, The Netherlands).

ISBN: 978-90-367-5775-1 (printed version)

ISBN: 978-90-367-5776-8 (electronic version)

Printed by: Ipskamp Drukkers B.V., Enschede, The Netherlands

**RIJKSUNIVERSITEIT GRONINGEN**

**DNA-Based Asymmetric Catalysis as a Synthetic Tool**

**Proefschrift**

ter verkrijging van het doctoraat in de  
Wiskunde en Natuurwetenschappen  
aan de Rijksuniversiteit Groningen  
op gezag van de  
Rector Magnificus, dr. E. Sterken,  
in het openbaar te verdedigen op  
vrijdag 7 december 2012  
om 16.15 uur

door

Rikkert Pepijn Megens

geboren op 25 september 1984  
te Harderwijk

Promotor : Prof. dr. J.G. Roelfes

Beoordelingscommissie : Prof. dr. B.L. Feringa  
Prof. dr. F.P.J.T. Rutjes  
Prof. dr. J.G. de Vries

ISBN: 978-90-367-5775-1 (printed version)

ISBN: 978-90-367-5776-8 (electronic version)

## Table of Content

---

|  |          |
|--|----------|
| <b>Chapter 1 Asymmetric Catalysis with Helical (Bio-) Polymers</b> | <b>7</b> |
| 1.1 Introduction   | 8        |
| 1.2 Static helical polymers  | 8        |
| 1.3 DNA-based catalysis  | 18       |
| 1.4 Dynamic and chirality-responsive helical polymers              | 23       |
| 1.5 Summary and outlook  | 25       |
| 1.6 Aims and outline   | 26       |
| 1.7 References   | 26       |

---

|  |           |
|--|-----------|
| <b>Chapter 2 DNA-Au Nanoparticles in Catalysis</b> | <b>29</b> |
| 2.1 Introduction                                   | 30        |
| 2.2 Applications                                   | 30        |
| 2.3 DNA-based catalysis with DNA-Au np's           | 33        |
| 2.4 Synthesis of DNA-Au np's                       | 34        |
| 2.5 DNA-Au nanoparticle based catalysis            | 36        |
| 2.6 Linker synthesis                               | 38        |
| 2.7 Conclusions                                    | 40        |
| 2.8 Experimental Section                           | 41        |
| 2.9 References                                     | 43        |

---

|  |           |
|--|-----------|
| <b>Chapter 3 Organic Co-Solvents in Aqueous DNA-Based Asymmetric Catalysis</b> | <b>47</b> |
| 3.1 Introduction   | 48        |
| 3.2 Solvents scope   | 48        |
| 3.3 Influence on Reaction Rate   | 52        |
| 3.4 Substrate scope  | 55        |
| 3.5 Lower temperature  | 57        |
| 3.6 Larger scale   | 57        |
| 3.7 Conclusions  | 59        |
| 3.8 Experimental Section   | 59        |
| 3.9 References   | 62        |

---

**Chapter 4 DNA-Based Catalytic Enantioselective Intermolecular Oxa-Michael Addition Reactions 65**

|  |    |
|--|----|
| 4.1 Introduction   | 66 |
| 4.2 DNA-based catalytic enantioselective intermolecular Oxa-Michael addition reactions | 68 |
| 4.3 Conclusions  | 73 |
| 4.4 Experimental Section   | 73 |
| 4.5 References   | 75 |

---

**Chapter 5 DNA-Based Catalytic Enantioselective Protonation in Water 77**

|  |     |
|--|-----|
| 5.1 Introduction   | 78  |
| 5.2 Catalytic enantioselective protonation                     | 80  |
| 5.3 Enantioselective catalytic protonations in protic solvents | 83  |
| 5.4 DNA-based catalytic enantioselective protonation in water  | 86  |
| 5.5 Substrate scope  | 92  |
| 5.6 Nucleophile scope  | 93  |
| 5.7 DNA sequence selectivity                                   | 94  |
| 5.8 Conclusions  | 94  |
| 5.9 Experimental Section                                       | 95  |
| 5.10 References  | 101 |

---

**Chapter 6 Conclusions and Perspective 105**

|                         |     |
|-------------------------|-----|
| 6.1 Introduction        | 106 |
| 6.2 DNA-based catalysis | 107 |
| 6.3 Future prospects    | 111 |
| 6.4 Concluding remarks  | 114 |
| 6.5 References          | 114 |

---

**Dutch summary 115**

---

**Dankwoord 119**

---

# Chapter 1

## Asymmetric Catalysis with Helical (Bio-)Polymers

*Inspired by Nature, the use of helical (bio)-polymer catalysts has emerged over the last years as a new approach to asymmetric catalysis. The use of helical polymers does not only open the ability to catalyze reactions asymmetrically but also enables easier recovery of the catalyst. In this chapter the various approaches and designs and their application in asymmetric catalysis will be discussed.*

Parts of this chapter have been published: R.P. Megens, G. Roelfes, *Chem. Eur. J* **2011**, *17*, 8514-8523 and A.J. Boersma, R.P. Megens, B.L. Feringa, G. Roelfes *Chem. Soc. Rev.* **2010** *39*, 2083-2092

## 1.1 Introduction

The helical structure has always had a special attraction to chemists, especially since the discovery of the peptidic  $\alpha$ -helix<sup>1</sup> and the DNA double helix structures<sup>2</sup>, which have shown that helicity is a key element of biomolecular structure. Many efforts have been dedicated to re-creating these helical structures with synthetic macromolecules. This has resulted in a variety of helical polymers that have found widespread applications because of their interesting material properties.<sup>3</sup> Inspired by nature, the use of helical (bio-)polymers in enantioselective catalysis is starting to be explored. In this chapter this emerging field will be introduced. We have chosen not to distinguish between biopolymers, such as peptides, polynucleotides and other polymers. Instead, a more conceptual approach will be presented, focussing on the various design strategies that can be used to achieve asymmetric catalysis with helical (bio-)polymers.

Helical polymers can be divided in two main classes. First, there are the static helical polymers. These are polymers in which the helical sense is "fixed", that is, which cannot interconvert. This class can be subdivided in 1) polymers in which the helicity originates from the chirality in the side chains and 2) helical polymers that do not rely on chiral side chains; these include polymers with stereogenic centres in the main chain as a result of the use of chiral monomers and stable helical polymers of achiral monomers that were polymerized in a helix sense specific manner.

The second main class is that of the dynamic and/or responsive helical polymers. Responsive polymers respond to external physical, chemical or electrical stimuli resulting in a dramatic change in morphology, structure, shape or function.<sup>4</sup> These polymers become helical under specific reaction conditions and can interconvert to give the opposite helicity.

## 1.2 Static helical polymers

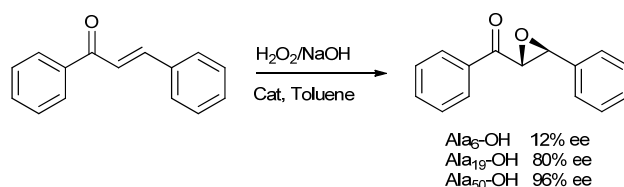
### 1.2.1 Helical polymers with side chain chirality

A variety of polymers need to be equipped with chiral side chains in order to maintain a stable helical structure in an enantiomerically pure form. In the case of peptides, the choice of the side chains is crucial to obtain a helical structure. Other polymers, such as, for example, polyacetylenes and, polyisocyanates do form helical structures by themselves, but their inversion barriers are low. Therefore, to stabilize them, chiral side chains are required.<sup>3</sup>

One of the early demonstrations of chiral polymers in catalysis was the use of polypeptides as catalyst in the enantioselective nucleophilic epoxidation of chalcone with hydrogen peroxide, in what has become known as the Julia-Colonna epoxidation.<sup>5-8</sup> Using polyalanine as the



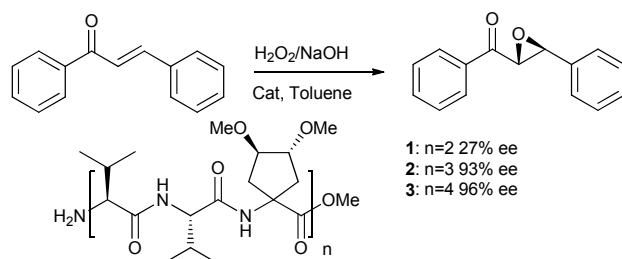
catalyst, the epoxide product could be obtained in up to 96 % ee, depending on the length of the polypeptide (Scheme 1.1). This was a first indication of a macromolecular amplification of chirality, albeit that a helical structure has not been proven for these peptides.



**Scheme 1.1** Epoxidation of chalcone catalyzed by polypeptides.

Poly-alanine, leucine and isoleucine are among the most efficient catalysts for the Julia-Colonna epoxidation with a preference for longer polymer chain in terms of reaction rates and enantiomeric excess.<sup>6</sup>

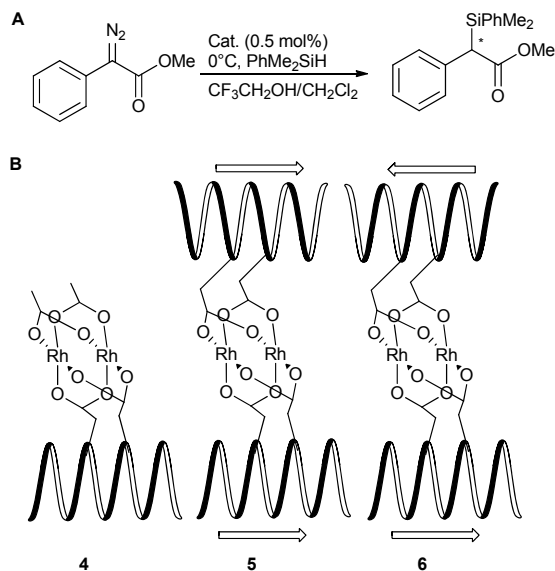
More recently, a chiral cyclic  $\alpha$ -amino acid oligopeptide for the asymmetric epoxidation of chalcone was reported. X-ray crystallographic analysis has shown that these oligopeptides (**1-3**) form  $\alpha$ -helical structures.<sup>9</sup> An increase in enantioselectivity was observed with increasing peptide length (Scheme 1.2). Which is a similar trend compared to the above mentioned peptides.



**Scheme 1.2** Epoxidation of chalcone catalyzed by polypeptides **1-3**.

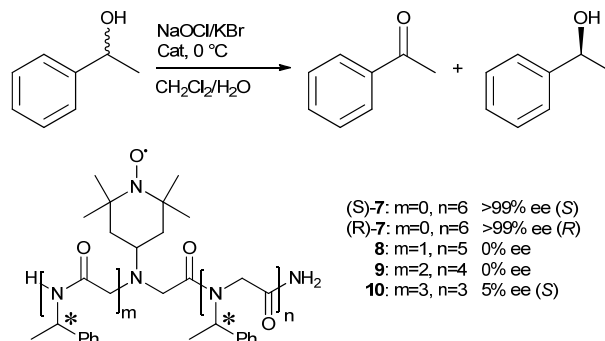
Whereas the Julia-Colonna type epoxidations represent an organocatalytic approach, also catalytically active transition metal complexes can be incorporated into a helical peptide structure. Ball and co-workers designed a peptide containing two carboxylate side chains which can coordinate to a di-rhodium metal center.<sup>10</sup> These metallopeptides proved to be active in diazo decomposition reactions,<sup>11</sup> however not in an asymmetric catalytic fashion. The design was changed slightly to nonapeptide (**4**), which catalyzed the insertion reaction of carbenes into PhMe<sub>2</sub>SiH (Scheme 1.3A) to afford the product in 32% ee.<sup>12</sup> To improve the chiral recognition, a *bis*-peptide catalyst was designed, in which the Asp side chains of two peptides were used to bridge the di-rhodium centre. (Scheme 1.3B).<sup>12</sup> The *bis*-peptide can be parallel (**5**) or antiparallel (**6**) isomers, albeit that to date it has not been established which isomer is which. The *bis*-peptide isomers afforded different enantioselectivity (20% and 45% ee, respectively)

which could be further improved by changing the peptide sequence (up to 92% ee). It was found that the residues adjacent to the catalytic moiety had the most significant effect on the enantioselectivity.



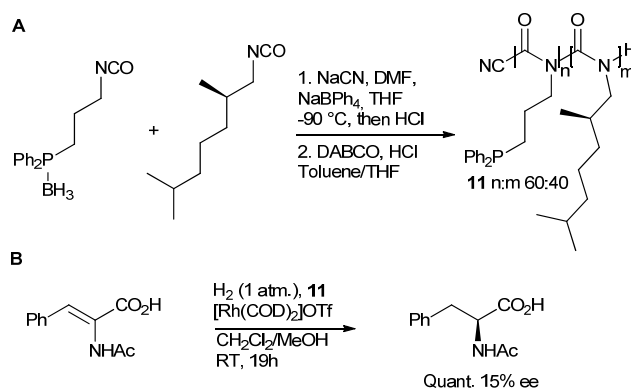
**Scheme 1.3** A; Insertion reaction of  $\text{PhMe}_2\text{SiH}$  into  $\alpha$ -diazophenylacetate, B; Different Rhodium peptides as catalysts in insertion reaction.

Small peptoids have been used in the oxidative kinetic resolution of 1-phenylethanol by attaching TEMPO, a well known oxidation catalyst<sup>13</sup> (Scheme 1.4).<sup>14</sup> It was found that right-handed helical **7** preferentially oxidized *S*-1-phenylethanol to acetophenone, while left-handed **7** preferentially oxidized *R*-1-phenylethanol. Furthermore, the enantioselectivity was dependent on the position of the catalytic moiety within the peptide. Replacing the chiral phenylethyl substituents of the peptoid with benzyl substituents decreased the selectivity of the TEMPO-terminated peptoid **7**, but an increased selectivity was found with the TEMPO in the central position (**10**).



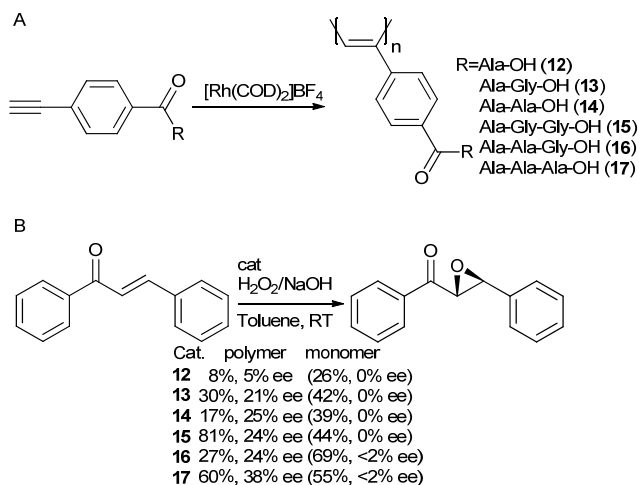
**Scheme 1.4** Oxidative kinetic resolution of 1-phenylethanol.

A first example using a non-peptidic polymer involved a polyisocyanate in which an achiral monomer containing a phosphine ligand was co-polymerized with a chiral non-metal binding monomer (Scheme 1.5A).<sup>15</sup> In this way a single-sense helical polymer was created using a sub-stoichiometric number of chiral units.



**Scheme 1.5** A; Synthesis of polyisocyanate co-polymers, B; Rhodium catalyzed asymmetric hydrogenation of N-acetamidocinnamic acid.

Upon complexation with [Rh(COD)<sub>2</sub>]OTf, the co-polymer catalyst (**11**) was applied in the asymmetric hydrogenation of N-acetamidocinnamic acid. However, only low enantioselectivity of the hydrogenated product was achieved (Scheme 1.5B).

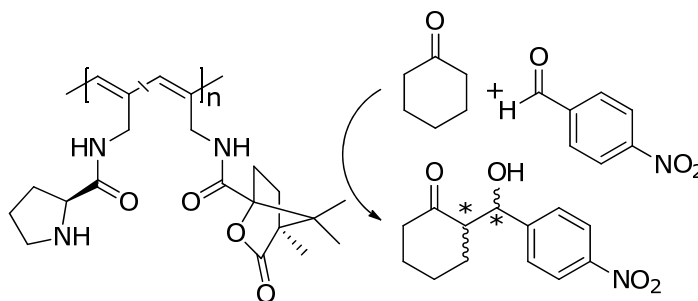


**Scheme 1.6** Helical poly(phenylacetylene)s bearing oligopeptide pendants; A; Polymer synthesis, B; Epoxidation of chalcone catalyzed by helical polymers **12-17**.

Peptides as side chains can have a dual role, they are used to stabilize the helical structure of the polymer but can also be used as organocatalyst.<sup>16</sup> For example, a poly(phenylacetylene) with pendant

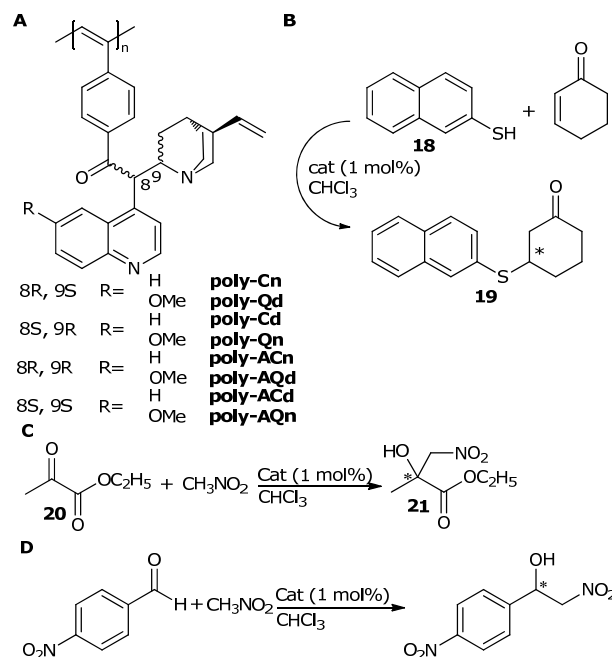
oligopeptide arms was shown to adopt a stable helical structure (Scheme 1.6A). Application of these polymers in the epoxidation of chalcones using  $\text{H}_2\text{O}_2$  gave rise to moderate enantioselectivities of up to 38% (Scheme 1.6B). Since with the corresponding monomers no significant ee was obtained, it was suggested that the selectivity originates directly from the helical polymer and not from the chiral peptides.<sup>17</sup>

Another example of a helical polymer bearing peptides as side chains has appeared recently. In this example a co-polymer of polyacetylenes bearing prolineamide pendant groups and chiral bicycloheptanones was synthesized<sup>18</sup> (Scheme 1.7). An induced CD signal was found for these polymers and they were used in the aldol reaction of cyclohexanone with *p*-nitrobenzaldehyde. Using a 1 to 1 co-polymer up to 80% conversion and 80% ee could be obtained. Unfortunately these results were not compared to proline itself. Furthermore, an unlikely mechanism was suggested that involved activation of the cyclohexanone via hydrogen bonding with the amide groups instead of formation of an enamine with benzaldehyde and proline.



**Scheme 1.7.** Aldol reaction of cyclohexanone with *p*-nitrobenzaldehyde catalyzed by a proline bearing helical co-polymer.

A similar approach was taken by Yashima and co-workers.<sup>19</sup> They synthesized poly(phenylacetylene) but now bearing chinchona alkaloids as pendant groups (Scheme 1.8A) instead of peptides. These polymers exhibited an induced circular dichroism in the UV-visible region of the polymer backbone indicating that they formed a preferred-handedness helical polymer. These polymers were used in both the asymmetric conjugate addition of 2-naphthalenethiol (**18**) to 2-cyclohexanone (Scheme 1.8B) as well as the Henry reaction of ethylpyruvate (**20**) with nitromethane (Scheme 1.8C).



**Scheme 1.8.** Helical polymers bearing cinchona alkaloid pendant groups.

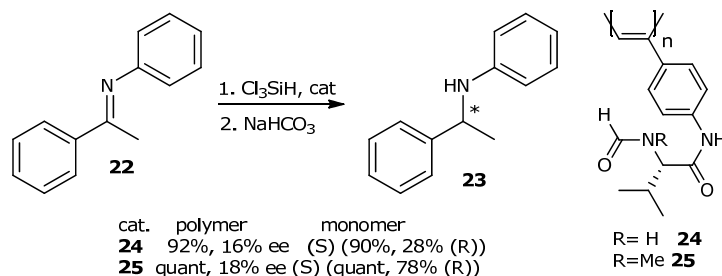
While all polymers gave conversions comparable to their monomers, only the polymer with cinchonidine pendant arms (**poly-Cd**) showed a slight increase in the enantioselectivity of the conjugate addition compared to the monomer, 32% vs. 14% ee, respectively.

The same trend holds for the Henry reaction of ethylpyruvate (**20**) with nitromethane. But now the polymer bearing the cinchonine pendant arms (**poly-Cn**) showed a slight increase in the enantioselectivity of the reaction, 26 and 14% ee, respectively.

More recently, the same alkaloid based helical polymers were used for the asymmetric Henry reaction of *p*-nitrobenzaldehyde with nitromethane (Scheme 1.8D).<sup>20</sup> In addition also amino-functionalized cinchona alkaloids (**ACd**, **ACn**, **AQn**, **AQd**) were prepared from commercially available natural cinchona alkaloids. **Poly-ACd** and **poly-ACn** gave similar results as the monomer whereas, **poly-AQn** and **poly-AQd** showed a much higher enantioselectivity compared to their monomeric counterparts. Using **poly-AQn** up to 94% ee of the Henry reaction product could be obtained.

However, when the chiral side chains themselves do give rise to enantioselectivity, there is the potential of a mismatch with the sense of helicity. This was observed in the reduction of ketimine (**22**) catalyzed by **24** or **25**.<sup>21</sup> The reaction catalyzed by the polymer gave a low ee of the opposite enantiomer compared to the monomer (Scheme 1.9). This indicates that the chirality of the side chain and the helicity of the main

chain of the polymer counteract each other (mismatched combination), resulting in low overall ee's.

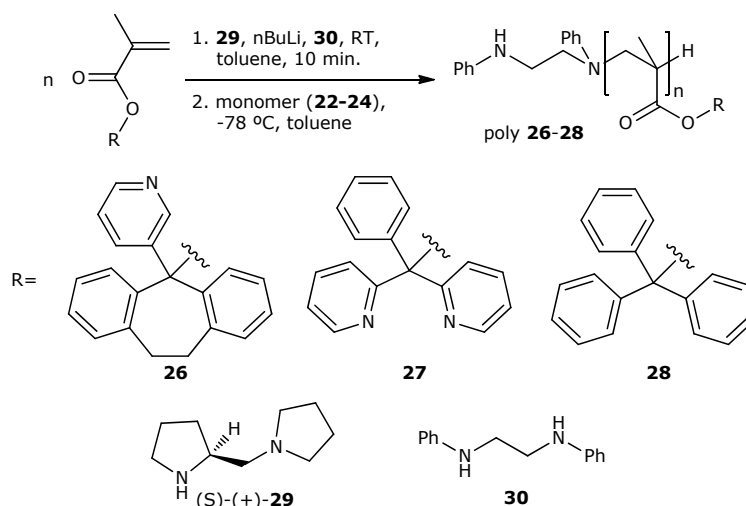


**Scheme 1.9** Asymmetric reduction of ketimine catalyzed by **24** or **25**.

### 1.2.2 Helical polymers with backbone chirality

Enantioselective polymerization can give access to helical polymers that do not require chiral side chains, provided that their helical structure is stable.<sup>22,23</sup> In this process, the chirality in the polymer is induced during the polymerization by using a chiral initiator.

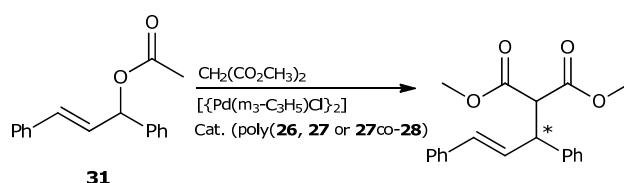
The group of Reggelin prepared helical polymers (poly **26-28**) by helix-sense selective anionic polymerization of methacrylates containing a pyridyl metal binding moiety using a chiral initiator. This initiator was made by treating a mixture of (*S*)- or (*R*)-1-(2-pyrrolidinomethyl)pyrrolidine (**29**) and *N,N'*-Diphenyl-ethylenediamine (**30**) with 1 eq. of *n*-BuLi (Scheme 1.10). This forms a chiral base complex which is able to initiate the helix-sense selective anionic polymerization.<sup>15,24</sup>



**Scheme 1.10** Anionic helix-sense selective polymerization of methacrylates.

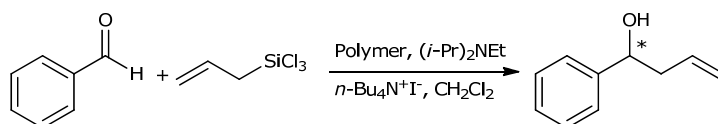
These polymers were used in the palladium-catalyzed enantioselective allylic substitution reaction of 1,3-diphenylprop-2-enyl acetate (**31**) with dimethylmalonate (Scheme 1.11). It was found that using **30** in catalysis did not give rise to any conversion.<sup>24</sup> Initiator **29** did result in conversion, with a slight enantiomeric excess of 10%. However, when (-)-poly-**26** was used, the product was obtained in 81% yield and 33% ee. Using the polymer with the opposite helicity resulted in preferred formation of the opposite enantiomer of the product with a similar enantioselectivity (32% ee).

Poly-**27**, which contains bidentate ligands, was designed because precipitation of palladium was observed when using the monodentate ligands.<sup>15</sup> A low optical activity was observed, which most likely indicates that a low excess of one of the helical forms of the polymer is present. Therefore also a co-polymer of **27** and **28** (poly(**27co-28**)) was prepared, which gave rise to an increased enantioselectivity of 60%.



**Scheme 1.11** Allylic alkylation of 1,3-diphenylprop-2-enyl acetate with dimethylmalonate.

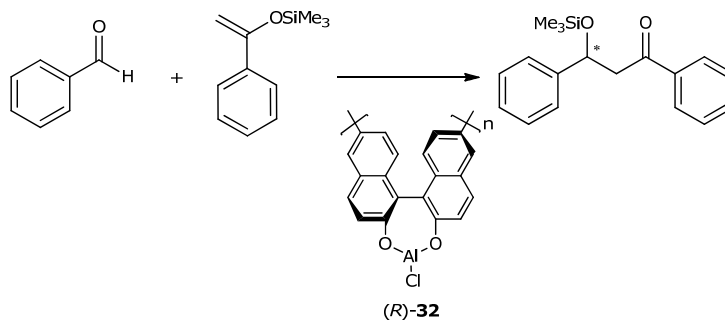
It was demonstrated that by oxidizing the pyridyl group to the corresponding pyridyl N-oxide with *m*-CPBA, these polymers could be used as Lewis base catalysts.<sup>25</sup> The N-oxide derived from polymer **26** proved to be active in the asymmetric allylation of benzaldehyde with allyltrichlorosilane (Scheme 1.12), resulting in the formation of the secondary alcohol in 56% yield and 19 % ee. In contrast, no reaction was observed with polymer **26**.



**Scheme 1.12** Asymmetric allylation of benzaldehyde with allyltrichlorosilane.

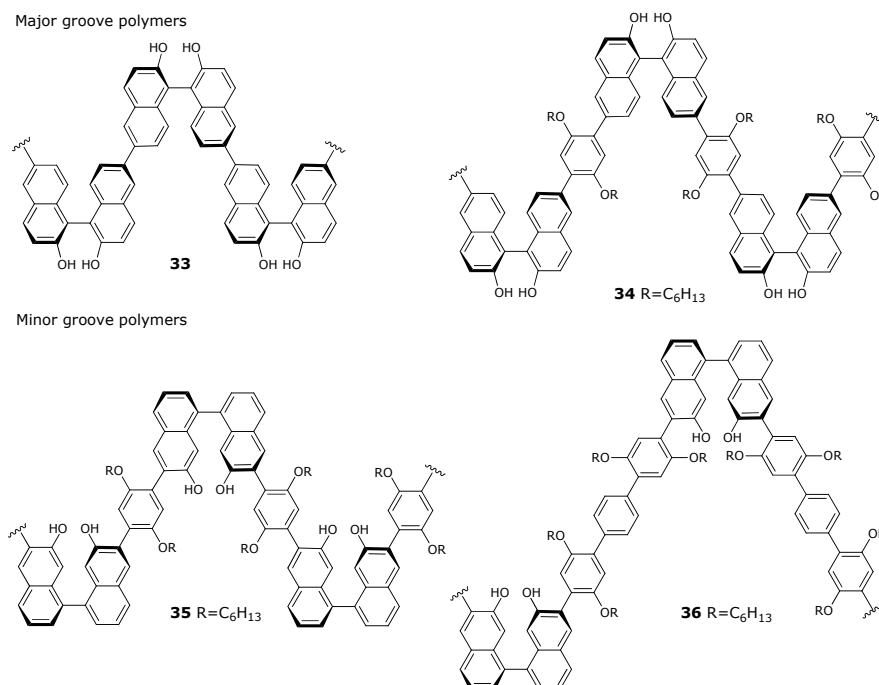
Using chiral monomers also results in the formation of conformationally stable helical polymers. Binaphthols have been applied extensively in asymmetric organic reactions and have been shown to induce excellent chiral selectivity in many reactions.<sup>26,27</sup> Pu and co-workers, have used polybinaphthols to form rigid and sterically regular polymers. The polybinaphthol was treated with aluminum chloride and then used as a Lewis acid catalyst in the Mukaiyama aldol reaction (Scheme 1.13).<sup>28,29</sup> With the polymer (**32**) full conversion was obtained after 3.5h, while the monomeric aluminum complex gave only ~5%

conversion in the same time. However no enantioselectivity was obtained in either case.



**Scheme 1.13** Mukaiyama aldol condensation.

Polybinaphthyl (**33-36**) has been proposed to possess a "major" and a "minor" groove.<sup>30,31</sup> The 6,6'-polymerized binaphthols, in which the hydroxy groups point outwards, are designated "major groove" polybinaphthyls. When the binaphthol is polymerized at the 3,3'-position, a "minor-groove" polymer is obtained, with the hydroxy groups pointing inwards in the helical structure. A variety of minor and major groove polymers have been prepared (Scheme 1.14).<sup>30-32</sup>

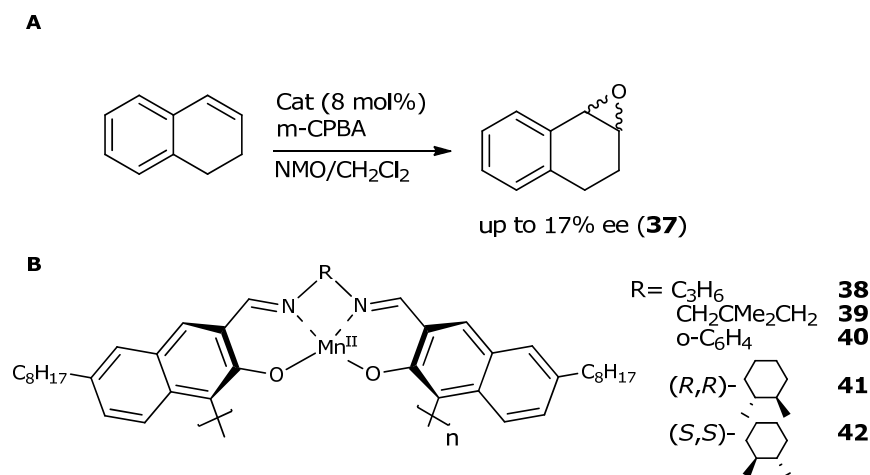


**Scheme 1.14** Variety of polybinaphthyls used in the reaction of benzaldehyde with diethylzinc.



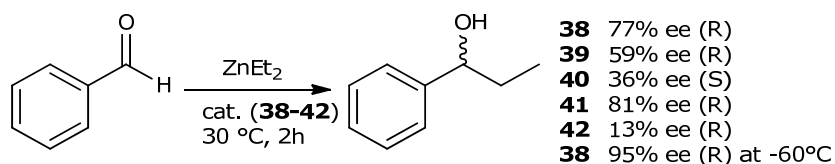
When the 1,2-addition reaction of benzaldehyde with diethylzinc was performed using the major groove polymers (**33**, **34**) a rather low enantioselectivity was obtained and also considerable amounts of benzylalcohol were found as a side product.<sup>30</sup> Using the minor groove polybinaphthyl (**35**), high chemo- and enantioselectivities were obtained; by extending the spacer between the binaphthyl units (**36**) the selectivity could be further increased up to 98% ee.<sup>32</sup> This demonstrates the importance of the position of the catalyst in the polymer. These polymers were recovered readily by precipitation with methanol and used again without loss of activity and selectivity.<sup>33</sup>

A similar approach was followed by Takata and co-workers, using a poly(binaphthyl salen metal complex).<sup>34,35</sup> Salen manganese complexes (**38-40**) were shown to be capable of oxidizing alkenes, albeit with low enantioselectivity (Scheme 1.15A).



**Scheme 1.15** A; Epoxidation of alkenes with **38-40**, B; Poly(binaphthyl salen) Manganese complexes (**38-42**).

When the same polymers were used in the 1,2-addition of diethylzinc to benzaldehyde, excellent yields and enantioselectivities, (i.e.) up to 81% ee for **37**, were obtained (Scheme 1.16), which could further be increased to 95% ee by lowering the temperature to -60 °C. Furthermore, a matched and mismatched combination was observed when introducing chirality in the amine linker.<sup>35</sup>



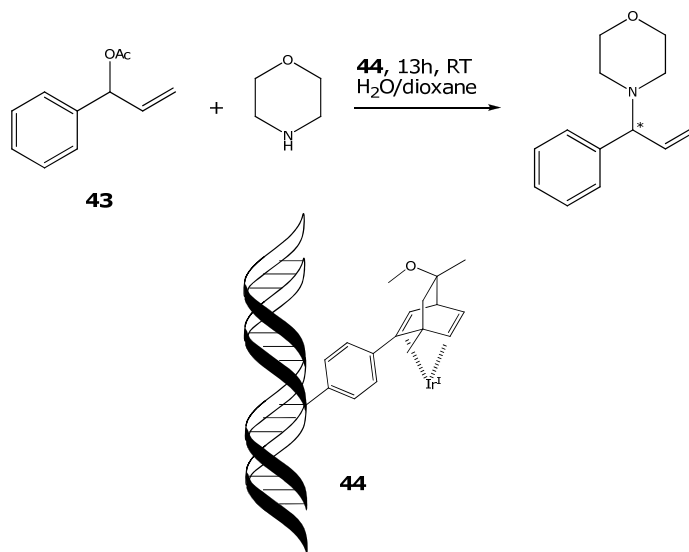
**Scheme 1.16** Addition of diethylzinc to benzaldehyde.

### 1.3 DNA-based catalysis

The archetype helical polymer undoubtedly is DNA. Its unique double helical structure has been a source of inspiration for catalyst design. Asymmetric catalysis with DNA can be divided into two classes, which differ in the mode of attachment of the catalytic moiety, that is, using a covalent linkage or via non-covalent interactions.<sup>36-38</sup>

#### 1.3.1 Covalent approach

Covalent anchoring involves binding of a transition metal complex via the ligand to the DNA using a small spacer moiety. Attachment sites in this case can be modified nucleobases or phosphate esters. Covalent anchoring is attractive since it allows for precise control over the positioning of the catalyst and, therefore, the structure and microenvironment of the catalytic site. However, covalent modification of DNA is laborious and very time consuming, which complicates the catalyst optimization process. This is illustrated by the fact that several approaches to the synthesis of ligand-DNA conjugates have been reported,<sup>39-41</sup> but in only a few cases successful catalysis has been achieved.

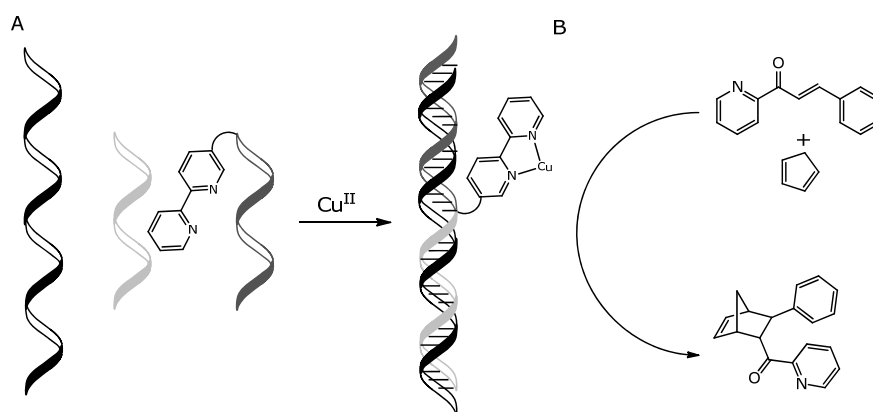


**Scheme 1.17** DNA-based Ir-catalyzed allylic amination.

Jäschke and co-workers covalently attached diene ligands to DNA via a coupling of the diene ligand with an activated nucleoside 4-triazolyldeoxyuridine, which was introduced by solid-phase synthesis.<sup>42</sup> The corresponding Ir-complex (**44**) proved to be an efficient catalyst for the allylic amination of **43** with morpholine, resulting in a kinetic resolution of **43** (Scheme 1.17). The enantioselectivity of this reaction was modest (23 %) and can be attributed to the chirality of the ligand itself which gives 28% ee in the allylic amination reaction. However,

when a complementary RNA strand was used the opposite enantiomer of the product was formed in 27 % ee, indicating that a relationship exists between the structure of the polynucleotide and the enantioselectivity of the catalyzed reaction.

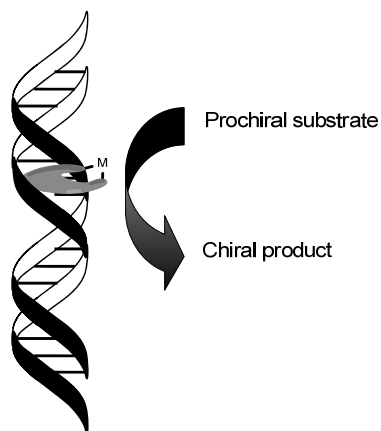
A method that allows for easier optimization involves the modular assembly of a DNA-based catalyst. This strategy involves two oligonucleotides, ON1 and ON2, with a covalently attached 2,2'-bipyridine ligand at the terminus of one of the strands (Scheme 1.18).<sup>43</sup> Upon hybridization of both oligonucleotides with a complementary template strand the catalytic moiety is placed in an internal position in the DNA duplex. Complexation of  $\text{Cu}^{\text{II}}$  to the bipyridine moiety produced the active DNA-based catalyst, which was found to be active in the asymmetric Diels-Alder reaction of azachalcone with cyclopentadiene. Ee's up to 93% were obtained, depending on the DNA sequence around the catalytic site and the length of the spacer.



**Scheme 1.18** A; Modular assembly of a DNA-based system as catalyst for the B; Diels-Alder reaction of azachalcone with cyclopentadiene.

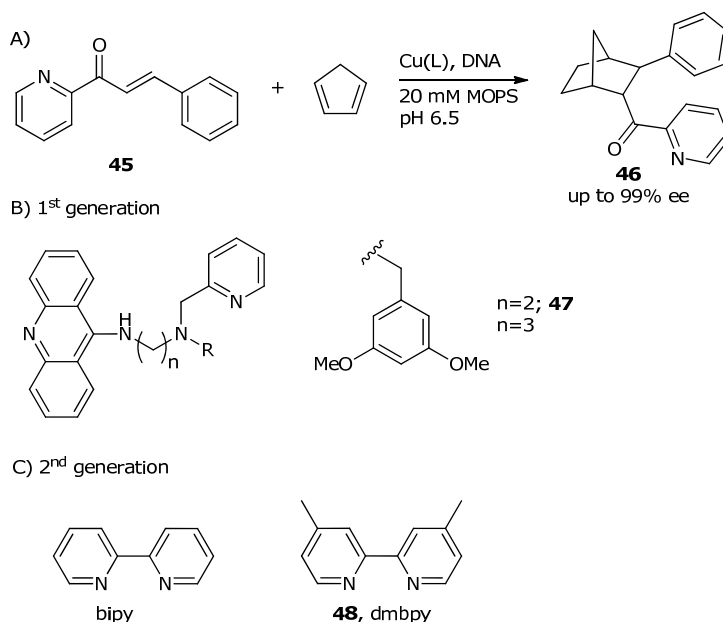
### 1.3.2 Non-covalent approach

Alternatively, a transition metal complex can be bound to the DNA using supramolecular interactions such as intercalation and/or groove binding. (Figure 1.1). The supramolecular anchoring approach is attractive because the catalyst is spontaneously self-assembled by combining the transition metal complex with the DNA, usually salmon testes DNA (st-DNA), which allows for rapid optimization. However, depending on the binding affinity and the DNA sequence selectivity, the catalyst may not be very well-defined; it is likely that the transition metal complex binds at multiple positions to the DNA. This method therefore results in a heterogeneous mixture of catalysts that reside in a different micro-environment and therefore will have different reactivity and selectivity.



**Figure 1.1** Schematic representation of non-covalent DNA-based catalysis.

The non-covalent approach to DNA-based catalysis has proven highly successful in a variety of reactions.<sup>[39,40]</sup> The Diels-Alder reaction of azachalcone (**45**) with cyclopentadiene was used initially to demonstrate the concept and has been used as the benchmark reaction for mechanistic studies. Using the first generation of ligands, which contain separated DNA intercalation and metal binding moieties that are connected via a spacer, up to 50% ee of **46** was found for this reaction (Scheme 1.19A and B).<sup>44</sup>

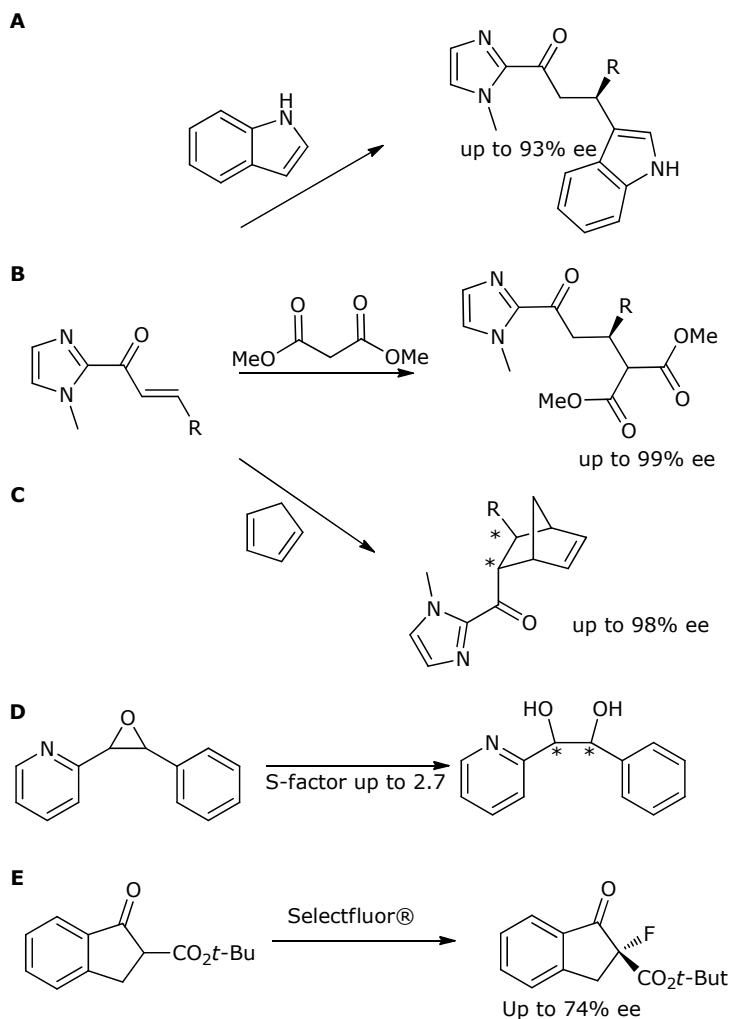


**Scheme 1.19.** A; Diels-Alder reaction of azachalcone (**45**) with cyclopentadiene catalyzed by 1<sup>st</sup> (B) and 2<sup>nd</sup> generation (C) DNA-binding ligands.

By changing the design of the ligand, in particular the length of the spacer, the opposite enantiomer of the product could be obtained, which is of interest since natural DNA is available in one chiral form only. With the second generation of ligands (Scheme 1.19C), which do not contain a separate DNA-binding moiety, up to 99 % ee was obtained in the case of 4,4'-dimethyl-bipyridine (**48**).<sup>45</sup> The corresponding Cu<sup>II</sup> complex, however, has only a moderate DNA-binding affinity and displays no sequence selectivity in binding. Moreover, the DNA-binding mode is not well-defined. In this light, the observed complete enantioselectivity is quite remarkable. This seeming paradox was solved by a kinetic and sequence dependence study, which revealed that the reaction is accelerated up to 2 orders of magnitude when the catalyst is bound to DNA. So the DNA is not just the chiral scaffold, but also participates actively in the reaction, most likely by providing favorable "second coordination sphere interactions".<sup>37,46</sup> Moreover, both the rate acceleration and the enantioselectivity were found to be sequence dependent, with the DNA sequences that give the highest ee, i.e. sequences containing G-tracts, also providing the largest rate acceleration.<sup>47,48</sup> Combined, this means that it is no problem that the catalyst is a heterogeneous mixture of many different species, since those that are in the optimum microenvironment which gives the highest ee's, dominate the outcome of the catalyzed reaction, since they also accelerate the reaction the most.

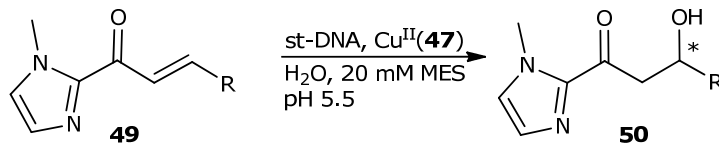
In addition to the Diels-Alder reaction, the Cu-dmbipy/st-DNA catalyst has been applied successfully in catalytic enantioselective Michael addition,<sup>49,50</sup> Friedel-Crafts alkylation,<sup>51</sup> fluorination<sup>52</sup> and epoxide ringopening reactions,<sup>53</sup> with in several cases ee's >90% (Scheme 1.20).

For the Friedel-Crafts alkylation and the Michael addition the same ligand and sequence dependency was obtained as with the Diels-Alder reaction. In these reactions dmbpy (**48**) gave the best results while 1<sup>st</sup> generation ligands gave much lower enantioselectivities. In these cases oligonucleotides containing G-tracts also proved to be the most effective with regard to the enantioselectivity. Furthermore, kinetics showed that the DNA, like in the Diels-Alder reaction, is beneficial for the reaction rate.



**Scheme 1.20** Reaction scope of DNA-based catalysis, A; Friedel-Crafts alkylation, B; Michael addition, C; Diels-Alder reaction, D; Kinetic resolution of pyridyloxiranes, E; Fluorination reaction.

Recently it has also been demonstrated that DNA-based catalysis can be applied to a reaction for which there is no precedent using synthetic catalyst, namely the catalytic enantioselective and diastereospecific *syn* hydration of enones (Scheme 1.21).<sup>54</sup>



**Scheme 1.21** Catalytic enantioselective *syn* hydration of enones.

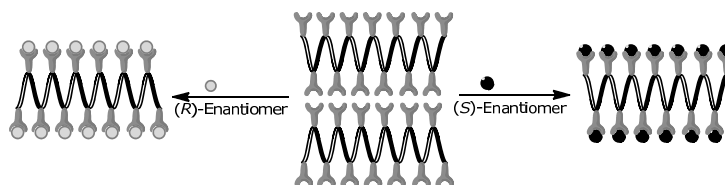
In contrast to the other examples of DNA-based catalysis, the first generation ligands, that is, those based on a 9-aminoacridine intercalating moiety proved to be the most effective ligands for this reaction giving up to 79% ee. Furthermore, oligonucleotide containing central AT fragments displayed the highest selectivities, while G-tracts were shown to be the best sequences for the former developed reactions.

By performing the reaction in D<sub>2</sub>O the ee could not only be improved to 82% ee but also the stereochemical course of the reaction could be elucidated, namely the addition of water goes in a *syn*-selective fashion. Interestingly, the reaction without DNA also results in the *syn*-selectivity, indicating that this might be dependent on the copper catalyst.

#### 1.4 Dynamic and chirality-responsive helical polymers

Responsive polymers are polymers that react to external physical, chemical or electrical stimuli, resulting in a dramatic change in morphology, structure, shape or function. Such as, for example, helix inversion.<sup>4</sup> To date, a significant number of stimuli responsive polymers have been synthesized. Most often the chirality responsive helical polymers contain functional pendant groups and upon addition of a chiral molecule, a conformational change of the polymer can be induced via non-covalent interactions (Figure 1.2).<sup>55</sup> These helical structures can be interconverted from right handed to the left handed and *vice versa* as in the case of polyisocyanates and poly(phenylacetylene).<sup>56,57</sup>

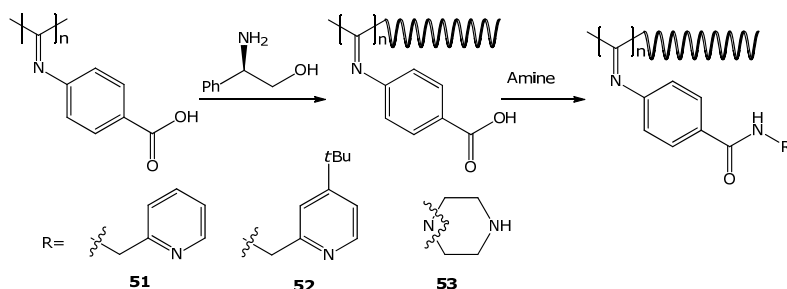
To date, only a few examples of asymmetric catalysis with responsive helical polymers have been reported. Yet, catalysts based on responsive helical polymers have great potential, since switching the helicity of the polymer with an external trigger makes it, in principle, possible to selectively obtain either enantiomer of a reaction product using the same catalyst.



**Figure 1.2** Schematic representation of a chirality-responsive polymer.

In a first example a poly(4-carboxyphenyl isocyanide) was prepared and upon addition of (*R*)-phenylglycinol a single-handed helical structure was induced with a molar ellipticity at 357 nm of  $-10.6 \text{ M}^{-1}\text{cm}^{-1}$ .<sup>58</sup> The induced helicity was memorized; after removal of the chiral amine and derivatization with an achiral amine containing a ligand moiety, the

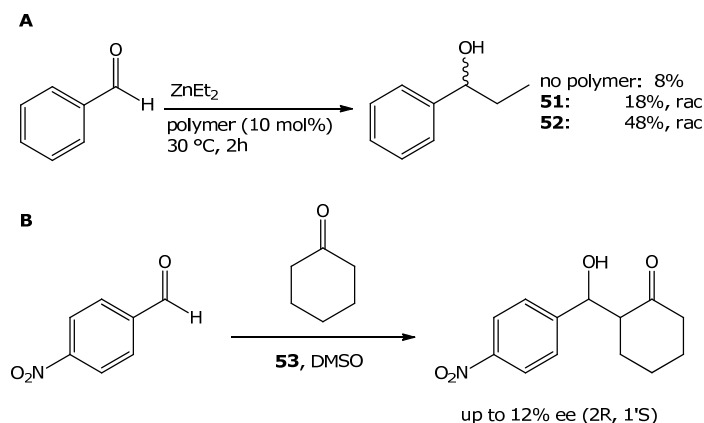
helical structure remained stable (Scheme 1.22); the amide moieties were found to increase the thermal stability of the helical polyisocyanide.<sup>59</sup>



**Scheme 1.22** Schematic illustration for the helicity induction and memory of poly(4-carboxyphenyl isocyanide).

Using the polymers derivatized with pyridyl amines in the 1,2-addition reaction of diethylzinc to benzaldehyde (Scheme 1.23A) an acceleration of the reaction rate was obtained. However, no enantioselectivity was observed, which was attributed to the distance of the pyridyl group from the helical polymer.

The piperazine bound helical polyisocyanide (**53**) was used as organocatalyst in the aldol reaction of benzaldehyde with cyclohexanone. Enantioselectivity was observed, albeit that the ee values were rather low, i.e. up to 12% (Scheme 1.23B).

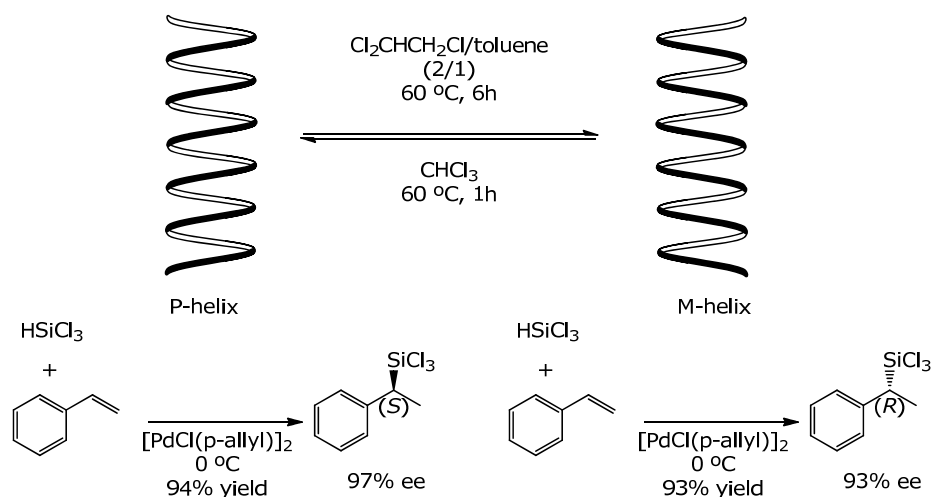


**Scheme 1.23** Reaction catalyzed by polymers with helical memory, A; Addition of diethylzinc to benzaldehyde, B; Aldol reaction of benzaldehyde with cyclohexanone.

An impressive demonstration of how helix interconversion can be used in asymmetric catalysis was recently reported by Suginome and co-workers.<sup>60</sup> They prepared a high-molecular-weight polymer based on a 20-mer polyquinoxaline-based phosphine (PQXphos) and used it in the palladium-catalyzed asymmetric hydrosilylation of styrenes (Scheme



1.24). Surprisingly, it was found that this polymer switches from P to M-helicity upon changing the solvent from chloroform to 1,1,2-trichloroethane/toluene (2:1). In catalysis, this resulted in 97% ee of the *S*-enantiomer with the P-helical form and 93% ee of the *R*-enantiomer with the M-helical form. Furthermore, the polymer was recycled up to 8 times without loss of selectivity, albeit that the palladium had to be recharged at the end of the 8<sup>th</sup> run, as a result of leaching.



**Scheme 1.24** Asymmetric hydrosilylation using chirality responsive polymer.

## 1.5 Summary and outlook

In catalysis, polymers were for a long time only considered as scaffolds to create “heterogeneous” versions of homogeneous catalysts, with the idea that this would facilitate catalyst recovery and recycling.<sup>61</sup> From the examples described here, it is clear that asymmetric catalysis using helical (bio-)polymers has started to emerge as an attractive new approach. This is mainly due to the fact that these helical polymers can provide a chiral microenvironment for a catalyst, analogous to an enzyme active site, that can be used to direct the catalyzed reaction towards the selective formation of one enantiomer of a product. To date, the biopolymer-based catalysts, e.g. peptide and polynucleotide based catalysts, have proven to be most versatile and can already be used in a variety of important catalytic enantioselective reactions. The synthetic polymers have to date generally not achieved the same level of activity and selectivity in catalysis. One main difference, of course, is that synthetic polymers presently have less functional diversity, as they are built up from a smaller number of different monomeric units, and are not mono-disperse and structurally less well-defined compared to biopolymers. However, further advances in polymer preparation to

address these issues can be envisioned. Using dynamic and responsive polymers, new avenues in catalysis can be explored, such as using one catalyst to selectively prepare either enantiomer of a product, just by triggering a helix interconversion. Taken together, it can be concluded that helical (bio-)polymers are a promising and attractive new approach to enantioselective catalysis.

## 1.6 Aims and outline

The goal of the research described in this thesis is to explore the concept of DNA-based catalysis for practical use in synthetically interesting reactions. Our efforts have focused in two different directions: 1) optimization of the reaction conditions in terms of recyclability of the DNA with copper-catalyst and scale of the reaction. 2) the development of new reactions which are unknown or difficult to perform using conventional transition metal catalysis.

In chapter 2, attempts for covalently attaching DNA strands to gold nanoparticles for the use in DNA-based catalysis are described.

In chapter 3 describes the influence of the addition of organic co-solvents to DNA-based catalysis. The effects of these co-solvents on DNA-structure, yield, enantioselectivity and kinetics are investigated. The use of water-miscible co-solvents has resulted in the reduction of the catalyst loading to 0.75 mol% and increase of the enantioselectivity by performing the reaction at  $-18^{\circ}\text{C}$ .

Chapter 4 describes the first transition metal catalyzed asymmetric intermolecular oxa-Michael addition of alcohols. This reaction was catalyzed by 1<sup>st</sup> generation DNA-based catalysts and provided ee's up to 86%.

In chapter 5, a novel approach to asymmetric protonation in water is presented. In our approach, 2<sup>nd</sup> generation DNA-based catalysis is used to perform a Friedel-Crafts alkylation/enantioselective protonation cascade with up to 60% ee.

Finally in chapter 6 the results in this thesis are summarized and combined with previous results. Furthermore an extensive future perspective is presented on the basis of ongoing projects.

## 1.7 References

1. L. Pauling, R. B. Corey, H. R. Branson, *Proc. Natl. Acad. Sci. U.S.A.* **1951**, *37*, 205.
2. J. D. Watson, F. H. Crick, *Nature* **1953**, *171*, 737.
3. E. Yashima, K. Maeda, H. Iida, Y. Furusho, K. Nagai, *Chem. Rev.* **2009**, *109*, 6102.
4. B. Jeong, A. Gutowska, *Trends Biotechnol.* **2002**, *20*, 305.
5. S. Banfi, S. Colonna, H. Molinari, S. Julia, J. Guixer, *Tetrahedron* **1984**, *40*, 5207.

6. G. Carrea, S. Colonna, D. R. Kelly, A. Lazcano, G. Ottolina, S. M. Roberts, *Trends Biotechnol.* **2005**, *23*, 507.
7. S. Colonna, H. Molinari, S. Banfi, S. Julia, J. Masana, A. Alvarez, *Tetrahedron* **1983**, *39*, 1635.
8. D. R. Kelly, S. M. Roberts, *Biopolymers* **2006**, *84*, 74.
9. M. Nagano, M. Doi, M. Kurihara, H. Suemune, M. Tanaka, *Org. Lett.* **2010**, *12*, 3564.
10. A. N. Zaykov, K. R. MacKenzie, Z. T. Ball, *Chem. Eur. J.* **2009**, *15*, 8961.
11. B. V. Popp, Z. T. Ball, *J. Am. Chem. Soc.* **2010**, *132*, 6660.
12. R. Sambasivan, Z. T. Ball, *J. Am. Chem. Soc.* **2010**, *132*, 9289.
13. P. L. Bragd, H. van Bekkum, A. C. Besemer, *Topics in Catalysis* **2004**, *27*, 49.
14. G. Maayan, M. D. Ward, K. Kirshenbaum, *Proc. Natl. Acad. Sci. U.S.A.* **2009**, *106*, 13679.
15. M. Reggelin, S. Doerr, M. Klussmann, M. Schultz, M. Holbach, *Proc. Natl. Acad. Sci. U.S.A.* **2004**, *101*, 5461.
16. E. A. C. Davie, S. M. Mennen, Y. Xu, S. J. Miller, *Chem. Rev.* **2007**, *107*, 5759.
17. K. Maeda, K. Tanaka, K. Morino, E. Yashima, *Macromolecules* **2007**, *40*, 6783.
18. D. Zhang, C. Ren, W. Yang, J. Deng, *Macromol. Rapid Commun.* **2012**, *33*, 652.
19. G. M. Miyake, H. Iida, H. Hu, Z. Tang, E. Y. - Chen, E. Yashima, *J. Polym. Sci., Part A: Polym. Chem.* **2011**, *49*, 5192.
20. Z. Tang, H. Iida, H. Hu, E. Yashima, *ACS Macro Lett.* **2012**, 261.
21. K. Terada, T. Masuda, F. Sanda, *J. Polym. Sci., Part A: Polym. Chem.* **2009**, *47*, 4971.
22. T. Nakano, Y. Okamoto, *Chem. Rev.* **2001**, *101*, 4013.
23. Y. Okamoto, T. Nakano, *Chem. Rev.* **1994**, *94*, 349.
24. M. Reggelin, M. Schultz, M. Holbach, *Angew. Chem. Int. Ed.* **2002**, *41*, 1614.
25. C. A. Muller, T. Hoffart, M. Holbach, M. Reggelin, *Macromolecules* **2005**, *38*, 5375.
26. C. Rosini, L. Franzini, A. Raffaelli, P. Salvadori, *Synthesis-Stuttgart* **1992**, 503.
27. Y. Canac, R. Chauvin, *Eur. J. Inorg. Chem.* **2010**, 2325.
28. Q. S. Hu, D. Vitharana, X. F. Zheng, C. Wu, C. M. S. Kwan, L. Pu, *J. Org. Chem.* **1996**, *61*, 8370.
29. Q. S. Hu, X. F. Zheng, L. Pu, *J. Org. Chem.* **1996**, *61*, 5200.
30. Q. S. Hu, W. S. Huang, D. Vitharana, X. F. Zheng, L. Pu, *J. Am. Chem. Soc.* **1997**, *119*, 12454.
31. W. S. Huang, Q. S. Hu, L. Pu, *J. Org. Chem.* **1998**, *63*, 1364.
32. Q. S. Hu, W. S. Huang, L. Pu, *J. Org. Chem.* **1998**, *63*, 2798.
33. W. S. Huang, Q. S. Hu, X. F. Zheng, J. Anderson, L. Pu, *J. Am. Chem. Soc.* **1997**, *119*, 4313.
34. T. Maeda, Y. Furusho, T. Takata, *Chirality* **2002**, *14*, 587.
35. T. Maeda, T. Takeuchi, Y. Furusho, T. Takata, *J. Polym. Sci., Part A: Polym. Chem.* **2004**, *42*, 4693.
36. A. J. Boersma, R. P. Megens, B. L. Feringa, G. Roelfes, *Chem. Soc. Rev.* **2010**, *39*, 2083.

37. F. Rosati, G. Roelfes, *Chemcatchem* **2010**, *2*, 916.
38. S. Park, H. Sugiyama, *Angew. Chem. Int. Ed.* **2010**, *49*, 3870.
39. M. Nuzzolo, A. Grabulosa, A. M. Z. Slawin, N. J. Meeuwenoord, G. A. van der Marel, P. C. J. Kamer, *Eur. J. Org. Chem.* **2010**, 3229.
40. L. Ropartz, N. J. Meeuwenoord, G. A. van der Marel, P. W. N. M. van Leeuwen, A. M. Z. Slawin, P. C. J. Kamer, *Chem. Commun.* **2007**, 1556.
41. M. Caprioara, R. Fiammengo, M. Engeser, A. Jäschke, *Chem. Eur. J.* **2007**, *13*, 2089.
42. P. Fournier, R. Fiammengo, A. Jäschke, *Angew. Chem. Int. Ed.* **2009**, *48*, 4426.
43. N. S. Oltra, G. Roelfes, *Chem. Commun.* **2008**, *45*, 6039.
44. G. Roelfes, B. L. Feringa, *Angew. Chem. Int. Ed.* **2005**, *44*, 3230.
45. G. Roelfes, A. J. Boersma, B. L. Feringa, *Chem. Commun.* **2006**, 1635.
46. T. Heinisch, T. R. Ward, *Curr. Opin. Chem. Biol.* **2010**, *14*, 184.
47. A. J. Boersma, J. E. Klijjn, B. L. Feringa, G. Roelfes, *J. Am. Chem. Soc.* **2008**, *130*, 11783.
48. F. Rosati, A. J. Boersma, J. E. Klijjn, A. Meetsma, B. L. Feringa, G. Roelfes, *Chem. Eur. J.* **2009**, *15*, 9596.
49. D. Coquière, B. L. Feringa, G. Roelfes, *Angew. Chem. Int. Ed.* **2007**, *46*, 9308.
50. E. W. Dijk, A. J. Boersma, B. L. Feringa, G. Roelfes, *Org. Biomol. Chem.* **2010**, *8*, 3868.
51. A. J. Boersma, B. L. Feringa, G. Roelfes, *Angew. Chem. Int. Ed.* **2009**, *48*, 3346.
52. N. Shibata, H. Yasui, S. Nakamura, T. Toru, *Synlett* **2007**, 1153.
53. E. W. Dijk, B. L. Feringa, G. Roelfes, *Tetrahedron: Asymmetry* **2008**, *19*, 2374.
54. A. J. Boersma, D. Coquière, D. Geerdink, F. Rosati, B. L. Feringa, G. Roelfes, *Nature Chem.* **2010**, *2*, 991.
55. E. Yashima, K. Maeda, *Macromolecules* **2008**, *41*, 3.
56. M. M. Green, J. - . Park, T. Sato, A. Teramoto, S. Lifson, R. L. B. Selinger, J. V. Selinger, *Angew. Chem. Int. Ed.* **1999**, 38.
57. E. Yashima, T. Matsushima, Y. Okamoto, *J. Am. Chem. Soc.* **1997**, *119*, 6345.
58. Y. Hase, Y. Mitsutsuji, M. Ishikawa, K. Maeda, K. Okoshi, E. Yashima, *Chem. Asian J.* **2007**, *2*, 755.
59. T. Miyabe, Y. Hase, H. Iida, K. Maeda, E. Yashima, *Chirality* **2009**, *21*, 44.
60. T. Yamamoto, T. Yamada, Y. Nagata, M. Sugimoto, *J. Am. Chem. Soc.* **2010**, *132*, 7899.
61. B. M. L. Dooos, I. F. J. Vankelecom, P. A. Jacobs, *Adv. Synth. Catal.* **2006**, *348*, 1413.

## **Chapter 2**

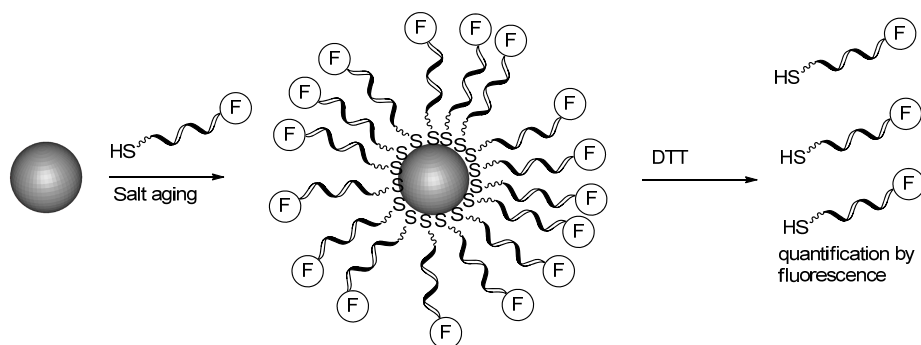
# **DNA-Au-Nanoparticles in Catalysis**

*DNA-based asymmetric catalysis has been used for a variety of reactions in water (chapter 1). Covalently attaching nucleotides to gold nanoparticles represents a potentially attractive method for immobilizing and recycling the catalyst. In this chapter efforts towards the development of DNA-gold nanoparticle catalysts will be discussed.*

## 2.1 Introduction

Nanoparticles represent an interesting solid support for DNA strands: they can be made easily, they are miscible in water and can be isolated after use by simple centrifugation. A variety of particles have been functionalized with DNA like Au,<sup>1</sup> Ag,<sup>2</sup> Fe<sub>3</sub>O<sub>4</sub>,<sup>3</sup> CdSe,<sup>4</sup> silica<sup>5</sup> and polymers.<sup>6,7</sup> All these materials require several steps to functionalize, except for gold nanoparticles (Au np's), which can be functionalized in one single and easy step.

DNA Au np's have interesting properties, they have: 1) higher binding affinity for their complementary DNA strands, compared to "simple" DNA,<sup>8</sup> 2) sharp melting transitions, due to cooperative binding/melting,<sup>9</sup> 3) are resistant to nucleases<sup>10</sup> and 4) can transfect cells without the use of transfection agents.<sup>11</sup> Furthermore, additional functionalities can be introduced via the modification of both the covalently bound oligonucleotide and the complementary strand. For example, by the addition of a fluorescent tag it was possible to establish the average number of strands on a nanoparticle.<sup>12</sup> An average of 80 strands are bound to one single Au np's of 15 nm. However this should be considered an approximation, since the quantification is not straightforward: the Au np's are first functionalized with a fluorophore bound oligonucleotide, washed and then the bound DNA is liberated again by the treatment of DTT, after which the concentration was determined by fluorescence spectroscopy (Figure 2.1).



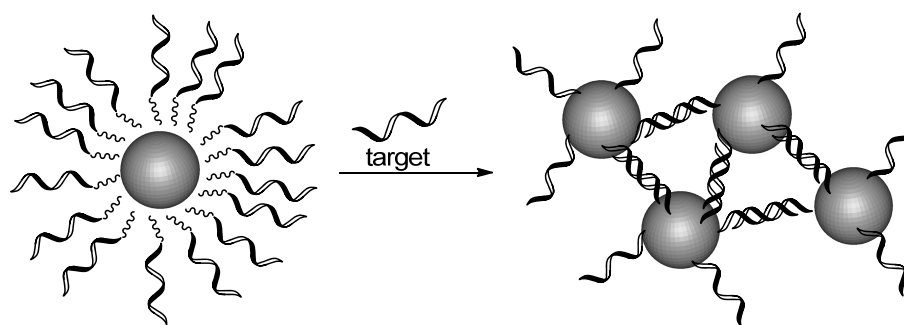
**Figure 2.1.** Quantification method for particle loading by fluorescence spectroscopy.

## 2.2 Applications

DNA functionalized gold nanoparticles (DNA-Au np's) have been used in several applications like selective colorimetric detection of nucleotides,<sup>13-15</sup> programmable nanoparticle crystallization,<sup>16</sup> nanoparticle size separation<sup>17,18</sup> and cellular uptake.<sup>11</sup> These different applications will be discussed briefly.

### 2.2.1 Selective colorimetric detection of nucleotides.

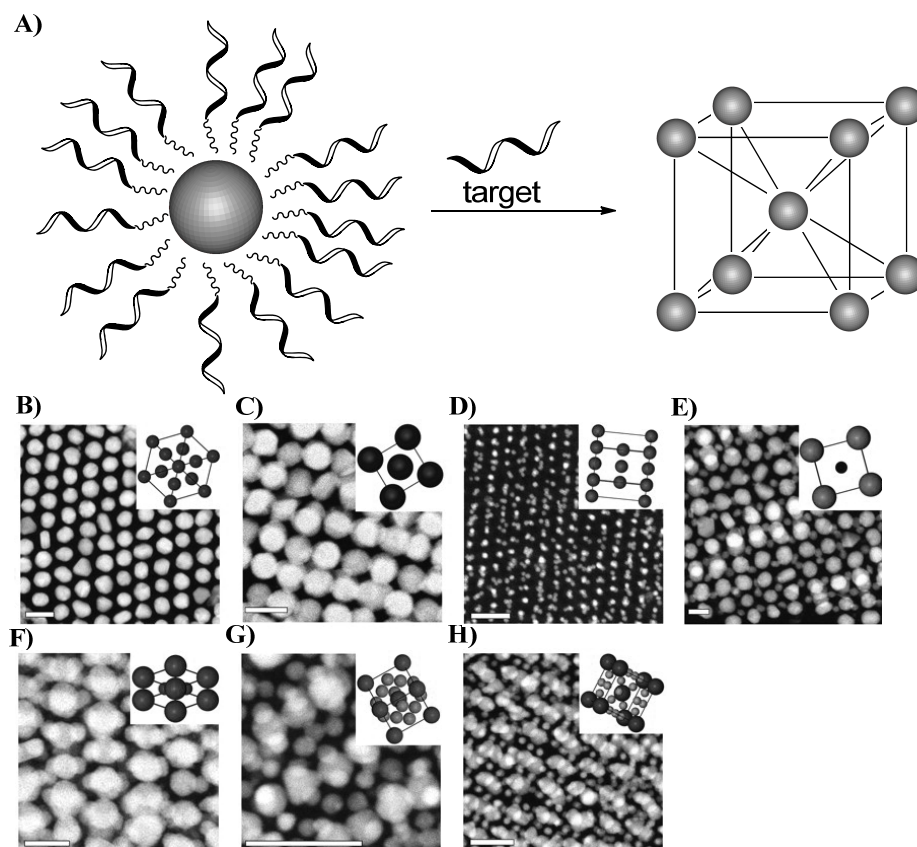
Sequence specific detection of oligonucleotides is important for diagnosis of genetic and pathogenic diseases.<sup>19</sup> Mirkin et al. developed a colorimetric detection method using DNA-Au np's. In this approach the DNA-Au np's are used as a reporter group for the detection of target oligonucleotides. This method relies on the hybridization of the oligonucleotide to the nanoparticle assemblies and formation of an extended polymeric network. This network is formed when the DNA-Au np's are interlocked by multiple short duplex segments (Figure 2.2). The nanoparticle aggregation gives rise to a color change from red to blue. This color change can be attributed to the surface plasmon resonance of the Au nanoparticles.<sup>20</sup> In combination with a temperature dependence assay, a variety of oligonucleotides with different mismatches can be identified, in addition to the complementary oligonucleotide detection. Via this method 10 fmol of an oligonucleotide can be detected.



**Figure 2.2.** Formation of nanoparticle networks by DNA hybridization.

### 2.2.2 Programmable nanoparticle crystallization

Programmable nanoparticle crystallization is based on the same principle as the above described network formation. The DNA-functionalized nanoparticles are viewed as building blocks and the complementary DNA strand can be used as a linkage to bring differently sized nanoparticles together in order to construct higher ordered materials, like colloidal crystals (Figure 2.3A). By choosing the appropriate ratio of linker length to particle core size, the nanoparticles could be crystallized into exclusively face-centered cubic (fcc) or body-centered cubic (bcc) colloidal crystals.<sup>16,21</sup> This provides a method to construct materials with controllable particle to particle distances.<sup>22-24</sup> This method was later extended to the formation of colloidal crystals with hexagonal close-packed (hcp), cesium chloride (CsCl), AB<sub>2</sub>, AB<sub>3</sub> or AB<sub>6</sub> symmetry (Figure 2.3B-H).<sup>23</sup>

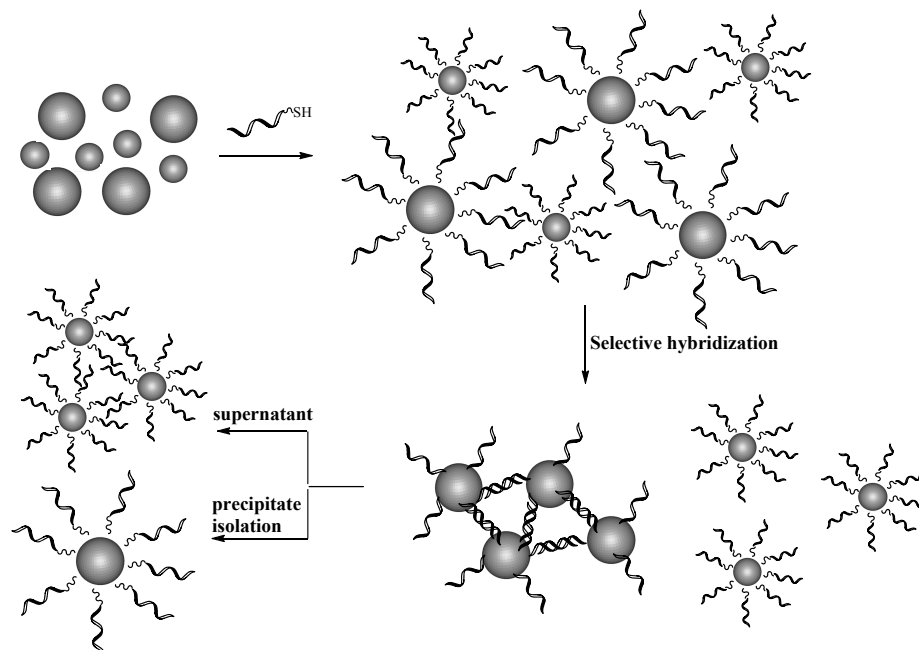


**Figure 2.3.** programmable nanoparticle crystallization. A; Assembly, B; fcc, C; bcc, D; hcp, E; CsCl, F;  $AB_2$ , G;  $AB_3$ , H;  $AB_6$  lattices.

### 2.2.3 Size separation

The DNA-Au np's have also been used to separate nanoparticles of different sizes.<sup>17,18</sup> The separation is possible due to the fact that the melting temperature of the DNA-Au np's is dependent on the particle size and they exhibit a sharp melting transition. This effect is due to the larger contact area between larger particles and therefore the cooperative binding is increased. The procedure involves a mixture of nanoparticles of two different sizes which are subsequently functionalized with DNA. The mixture can be separated by size-selective hybridization at a specific temperature. Under these conditions the large particles are hybridized leaving the small particles in the supernatant. After a simple centrifugation step the particles can be separated (Figure 2.4). This procedure was demonstrated with particle mixtures of 15/40, 30/60, 40/80 and 2/15 nm particles.





**Figure 2.4.** DNA-induced size selective separation of nanoparticle mixtures.

### 2.2.4 Cellular uptake

DNA-Au np's are able to enter a wide variety of cells: over 30 cell lines were reported, to date.<sup>25</sup> This is quite surprising given the fact that the DNA functionalized nanoparticles contain a densely covered shell of polyanionic DNA. Moreover, nucleases cannot cleave the DNA due to fact that the nanoparticle is too densely covered and therefore the nuclease cannot reach the DNA.<sup>10</sup> This advantage has been used in a variety of applications in cells, like gene transfection,<sup>26</sup> antisense gene control,<sup>11,27-31</sup> (intra)cellular detection<sup>32-43</sup> and RNA interference.<sup>44-46</sup> All these applications are based on binding of the DNA functionalized nanoparticles with their complementary strand either to transport it into the cell or blocking the DNA, so it cannot fulfill its original purpose.

## 2.3 DNA-based catalysis with DNA-Au np's

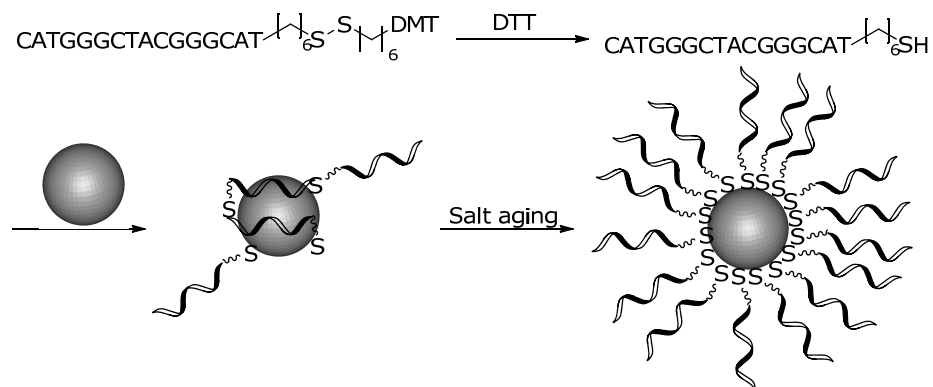
It has been shown that the DNA catalyst can be recycled after the reaction by simply extracting the reaction mixture and adding new reactants to the aqueous phase.<sup>47</sup> However, in many cases, after a couple of cycles all of the DNA has precipitated and the reactivity is lost. Therefore, covalently attaching DNA to a solid support represent an attractive method for recycling the catalyst. Au np's would be an attractive solid support for this purpose due to the ease of synthesis and functionalization. The gold nanoparticles can be functionalized with short

oligonucleotides. This has as an additional advantage that specific DNA sequences can be used. As has been shown before, certain sequences have a beneficial effect on the rate and enantioselectivity of the catalyzed reaction.<sup>48</sup> By functionalizing Au np's with these sequences, the sequence dependence of DNA-based catalysis can be combined with a facile method for recycling the catalyst.

## 2.4 Synthesis of DNA-Au-np's

The nanoparticles were synthesized by reducing chloroauric acid (HAuCl<sub>4</sub>) with the appropriate amount of sodium citrate.<sup>49,50</sup> The size of the gold nanoparticles is dependent on the ratio HAuCl<sub>4</sub> to citrate; a size of 15 nm was chosen, since these particles exhibit a sharp Plasmon absorption band and can be prepared with a narrow size distribution.<sup>50</sup>

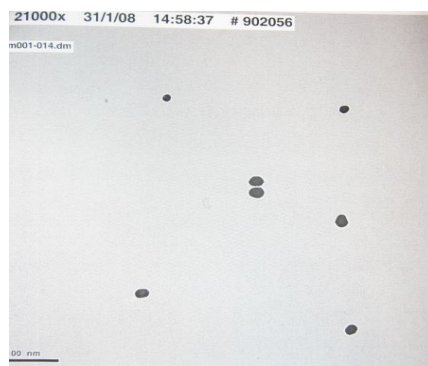
For the functionalization with DNA a commercially available oligonucleotide with a protected thiol was used. The thiol was deprotected with Dithiothreitol (DTT) and purified by size exclusion chromatography prior to use. The Au np's were functionalized according to a literature procedure (Scheme 2.1).<sup>9</sup>



**Scheme 2.1.** Deprotection of thiol modified oligonucleotide and nanoparticle functionalization. DMT= bis-(4-methoxyphenyl)phenylmethyl.

However, these nanoparticles are not fully functionalized, some oligonucleotides are occupying parts of the nanoparticle by laying on the surface. Therefore, a subsequent salt-aging process was required.<sup>13</sup> In this step the oligonucleotides are slowly removed from the surface by the addition of salt, leaving space available for more oligonucleotides to attach to the surface. This step needs to be performed carefully because rapid addition of salt will result in unprotected nanoparticles, which will form aggregates. In this procedure the salt-aging is of utmost importance: without this step the nanoparticles cannot resist the catalytic conditions and will aggregate in time.

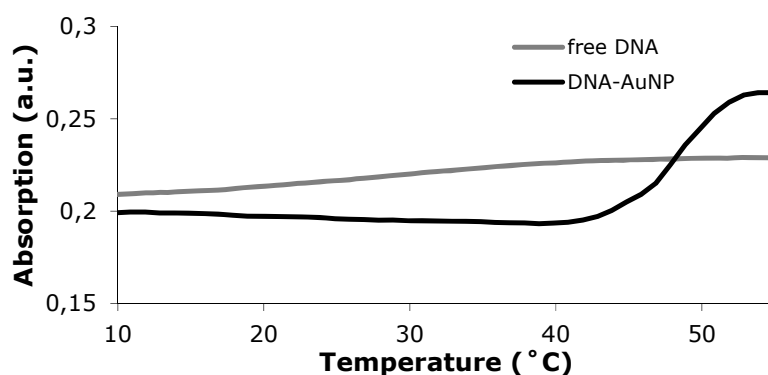
After the salt aging step the salt was removed by washing the nanoparticles with water. The size of the particles was confirmed to be  $15 \pm 2$  nm (50 particles sampled) by TEM (Figure 2.5) and the characteristic absorption maximum at 524 nm.<sup>50</sup>



**Figure 2.5.** TEM picture of Au np's.

The loading of the particles was checked by determining the DNA concentration in the supernatant after centrifugation. It was approximated that the DNA loading was around 70 strands/particle which is comparable to the maximum loading reported in the literature.<sup>12</sup>

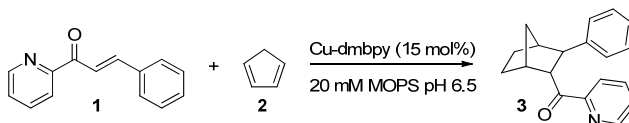
The DNA-Au np's were hybridized in 20 mM MOPS pH 6.5 with the complementary strand. By the attachment to the nanoparticle, the melting temperature was dramatically increased from  $29^\circ\text{C}$  (free DNA) to  $48^\circ\text{C}$  (DNA-Au np's; Figure 2.6) and a sharp transition was observed. This can be attributed to the cooperative binding of the complementary strand as a result of the increase in local salt concentration.<sup>1,9</sup>



**Figure 2.6.** Melting curve of DNA-Au np's and free DNA determined by UV/Vis spectroscopy at 260 nm.

## 2.5 DNA-Au np's based catalysis

The DNA-Au np's were used in the DNA-based catalyzed Diels-Alder reaction of azachalcone (**1**) with cyclopentadiene (**2**; Figure 2.7) using 15 mol% of copper (4,4'-dimethyl-2,2'-bipyridine) (Cu-dmbpy) in 20 mM MOPS buffer (pH 6.5). When unfunctionalized Au np's were used 6% conversion was obtained, which is comparable with the uncatalyzed reaction (Figure 2.7, Entries 1 and 2). It has to be noted that after 1 day, precipitation of the nanoparticles was observed, probably due to aggregation. The DNA-Au np's afforded 80% conversion, however without any enantioselectivity (Entry 3). To rule out the inhibition of the copper catalyzed reaction the Diels-Alder reaction was also carried out with st-DNA in the presence of Au np's. Full conversion and 99% ee were obtained which is similar to the results obtained without the Au np's (Entries 4 and 5).

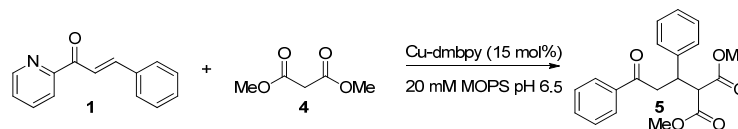


| Entry | Additive                     | Cu(dmbpy) | Conv. | ee  |
|-------|------------------------------|-----------|-------|-----|
| 1     | Au np's <sup>a</sup>         | No        | 6%    | <5% |
| 2     | -                            | No        | 5%    | <5% |
| 3     | DNA-Au np's                  | Yes       | 80%   | <5% |
| 4     | st-DNA+ Au np's <sup>a</sup> | Yes       | Full  | 99% |
| 5     | st-DNA                       | Yes       | Full  | 99% |

General conditions: 0.15 mM Cu(dmbpy), st-DNA or CATGGGCTACGGGCAT-Au np's + complementary strand (1 mM in basepairs (bp)) in 20 mM MOPS (pH 6.5), 1 mM azachalcone (**1**), 15 mM cyclopentadiene (**2**), 3d, 4°C. a; precipitation of Au NP's after 1 day; st-DNA = salmon testes DNA.

**Figure 2.7.** Diels-Alder reaction catalyzed by DNA-Au np's.

The Michael addition of dimethylmalonate (**4**) to azachalcone (**1**) was also performed using the DNA-Au np's (Figure 2.8). Also in this case the reaction with unfunctionalized Au np's resulted in only the uncatalyzed reaction (Figure 2.8, Entries 1 and 2). However, hardly any reaction was observed in the presence of the DNA-Au np's (Entry 3). The st-DNA in combination with unfunctionalized Au np's afforded comparable results to the reaction without Au np's (Entries 4 and 5).

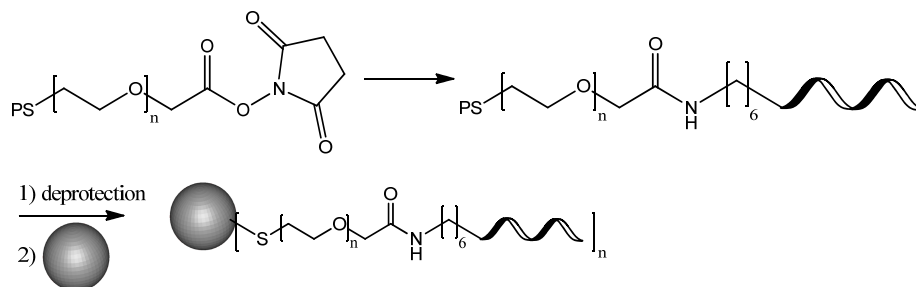


| Entry | Additive                     | Cu(dmbpy) | Conv. | ee  |
|-------|------------------------------|-----------|-------|-----|
| 1     | Au np's <sup>a</sup>         | No        | 4%    | <5% |
| 2     | -                            | No        | 5%    | <5% |
| 3     | DNA-Au np's                  | Yes       | 5%    | <5% |
| 4     | st-DNA+ Au np's <sup>a</sup> | Yes       | 95%   | 96% |
| 5     | st-DNA                       | Yes       | Full  | 96% |

General conditions: 0.15 mM Cu(dmbpy), st-DNA or CATGGGCTACGGGCAT-Au np's + complementary strand (1 mM in bp) in 20 mM MOPS (pH 6.5), 1 mM azachalcone (**1**), 100 mM dimethylmalonate (**4**), 3d, 4°C. a; precipitation of Au np's after 1 day.

**Figure 2.8.** Michael addition catalyzed by DNA-Au np's.

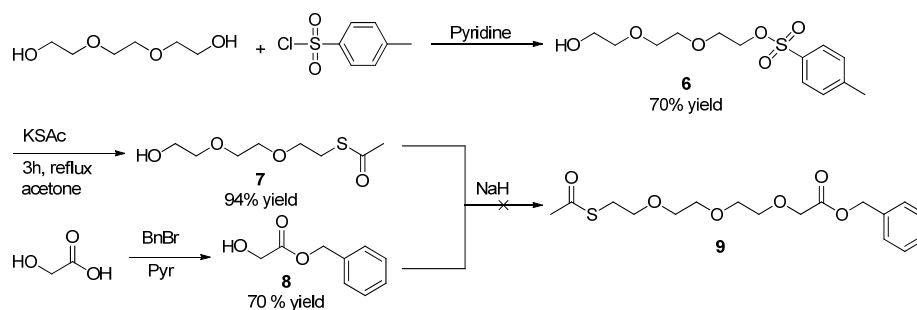
It was hypothesized that no catalysis was achieved because the DNA is too densely packed on the nanoparticle and therefore the copper center can not be reached by the reagents. Two solutions for this problem were envisioned. Firstly, the DNA loading can be lowered. However this would result in DNA-Au conjugates with lower stability. Alternatively, the linker between the thiol moiety and the DNA can be extended. This would position the DNA further away from the gold nanoparticle and therefore the nanoparticle would be less densely packed. As a spacer an oligoethyleneglycol linker would be suitable, because they are known to stabilize gold nanoparticles.<sup>51</sup> It was envisioned that the linker could be prepared by the attachment of a protected thiol at one end of the oligoethyleneglycol linker and this could be attached to an amine modified oligonucleotide by coupling via an activated ester at the other end. After deprotection of the thiol functionality the extended oligonucleotide sequence could be attached to the Au np's.



**Figure 2.9.** General scheme for linker synthesis and attachment to Au np's.

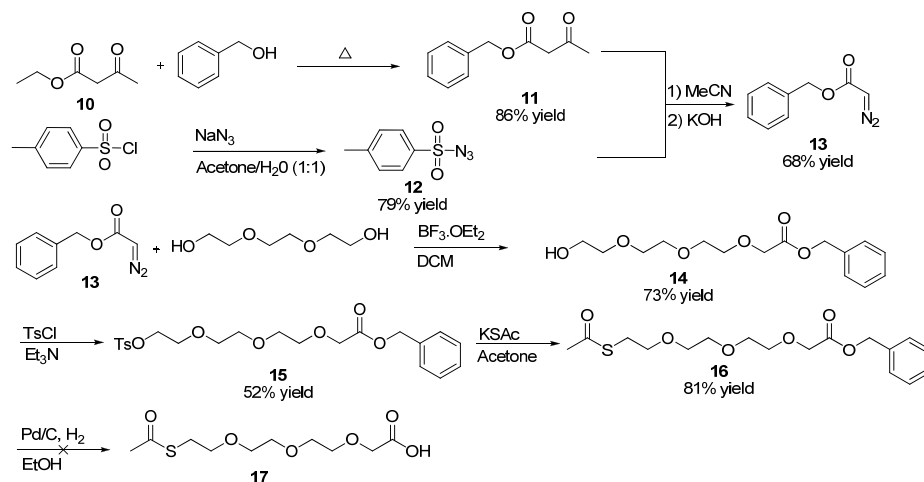
## 2.6 Linker synthesis

The first synthetic strategy involved the mono-tosylation of triethyleneglycol followed by substitution of the tosyl group with thioacetic acid to yield **7** in 70% yield (Scheme 2.2).<sup>52</sup> This was reacted with benzyl glycolic acid (**8**), which was prepared by reacting glycolic acid with benzyl bromide using a catalytic amount of triethylamine.<sup>53</sup> However, instead of forming the desired product (**9**), a mixture of compounds was obtained, mainly due to the reaction of benzyl glycolic acid with itself (Scheme 2.2).



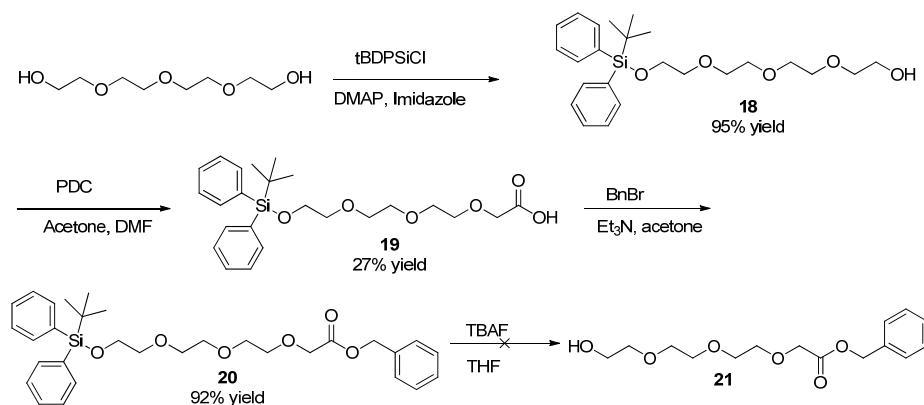
**Scheme 2.2.** Linker synthesis; first strategy.

The synthetic route was changed slightly: now triethyleneglycol was reacted with benzyl 2-diazoacetate (**13**) with a catalytic amount of  $\text{BF}_3 \cdot \text{Et}_2\text{O}$  to form **14** (Scheme 2.3). Benzyl 2-diazoacetate can be prepared by first reacting ethyl acetoacetate (**10**) with benzylalcohol to form benzyl acetoacetate (**11**).<sup>54</sup> Via a diazo transfer from freshly prepared tosyl azide (**12**), benzyl 2-diazoacetate is formed in 68% yield.<sup>55</sup> Tosyl azide should be handled with care since it is potentially explosive and therefore should not be evaporated to complete dryness. The remaining free alcohol moiety of **14** was then reacted with tosylchloride and substituted with thioacetic acid to give **15**. The benzyl protected linker (**16**) was hydrogenated to remove the benzyl protecting group. However, probably due to poisoning of the palladium by the thiol-group, no reaction occurred (Scheme 2.3).



**Scheme 2.3.** Linker synthesis; second strategy.

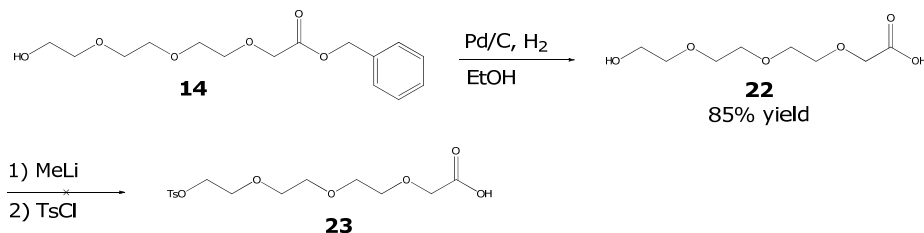
A third strategy was employed in which a silyl protecting group was introduced instead of a thioacetate group (Scheme 2.4). For this purpose tetraethyleneglycol was monoprotected with *t*BDPSiCl to afford **18** in 95% yield.<sup>56</sup> Subsequently, the remaining free alcohol was oxidized to the carboxylic acid by pyridinium dichromate to form **19**. This was reacted with benzyl bromide to form **20** in 92% yield. Unfortunately, deprotection with *t*BAF failed and from NMR it could be concluded that the acetyl moiety was unstable under the acidic conditions. Also using pyridine hydrofluoride did not result in the desired product (Scheme 2.4).



**Scheme 2.4.** Linker synthesis; third strategy.

A fourth and final strategy was developed, in which triethyleneglycol was reacted with benzyl 2-diazoacetate (**13**) to form **14**, as was shown in Scheme 2.2. The benzyl group was removed by hydrogenation to

yield **22** in 85% yield (Scheme 2.5). It was shown in a similar example that the alcohol could be selectively reacted with tosylchloride by deprotonation with 2 equivalents of methyl lithium and subsequent tosylation (Scheme 2.5).<sup>57</sup> However the acetyl moiety was not stable to the basic conditions and a mixture of compounds was obtained instead of the tosylated product (**18**).



**Scheme 2.5.** Linker synthesis; fourth strategy.

Finally, since the linker synthesis was not as straightforward as envisioned, a commercially available decathymine spacer was used to increase the distance between the nanoparticle and the duplex DNA. The DNA functionalized nanoparticle was synthesized using the same procedure as mentioned before. The melting temperature of the extended linker was slightly increased to 51 °C. However, when these nanoparticles were used in DNA-based catalysis again no enantioselectivity was found in both the Diels-Alder reaction and the Michael addition. Probably, the DNA is still too densely packed for the reagents to reach the active copper centre.

**Table 2.1.** Diels-Alder reaction and Michael addition catalyzed by DNA T<sub>10</sub>-AuNP's.

| Reagent  | Cat.                         | Product  | Conv. | ee  |
|----------|------------------------------|----------|-------|-----|
| <b>2</b> | DNA T <sub>10</sub> -Au NP's | <b>3</b> | 75%   | <5% |
| <b>2</b> | st-DNA-                      | <b>3</b> | Full  | 99% |
| <b>4</b> | DNA T <sub>10</sub> -Au NP's | <b>5</b> | -     | nd. |
| <b>4</b> | st-DNA                       | <b>5</b> | Full  | 96% |

General conditions: 0.15 mM Cu(dmbpy), st-DNA or TTTTTTTTTTCATGGGCTACGGGCAT + ATGCCCGTAGCCCATG (1 mM in bp) in 20 mM MOPS (pH 6.5), 1 mM azachalcone (**1**), 15 mM cyclopentadiene (**2**) or 100 mM dimethylmalonate (**4**), 3d, 4 °C.

## 2.7 Conclusions

DNA-Au np's were prepared and tested in combination with Cu(dmbpy) in DNA-based catalysis. Although unfunctionalized nanoparticles do not affect the catalysis itself, the DNA-Au np's did not show any enantioselective catalysis. Probably the catalytically active sites are not accessible because the DNA on the nanoparticles is too densely packed. Future research could include mixed monolayers to



decrease DNA loading or the use of different solid supports, such as glass, which can be functionalized less densely.

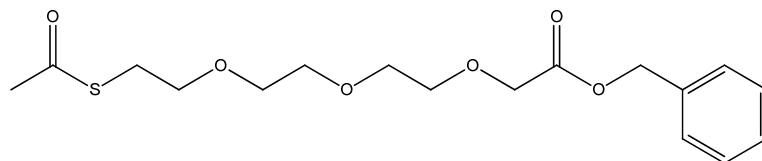
## 2.8 Experimental section

### General remarks

Salmon testes DNA was obtained from Sigma. Copper complexes<sup>58</sup>, Azachalcone (**1**),<sup>59</sup> Au NP's,<sup>49,50</sup> **6**,<sup>60</sup> **7**,<sup>60</sup> **8**,<sup>53</sup> **11**,<sup>61</sup> **12**,<sup>62</sup> **13**,<sup>63</sup> **14**,<sup>63</sup> **15**,<sup>63</sup> **18**,<sup>64</sup> were synthesized according to literature procedures. Tosyl azide is potentially explosive and therefore should not be evaporated to complete dryness. Cyclopentadiene was prepared freshly from its dimer. <sup>1</sup>H-NMR and <sup>13</sup>C-NMR were recorded on a Varian 400 (400 MHz and 100 MHz, respectively). Chemical shifts ( $\delta$ ) are quoted in ppm using residual solvent as internal standard ( $\delta_H$  7.26 and  $\delta_C$  77.0 for CDCl<sub>3</sub>). The melting curve was measured on a JASCO v-560 with a Peltier temperature control attachment. Enantiomeric excess determination was performed by HPLC analysis on a Shimadzu 10AD-VP system as described before.<sup>47,65</sup>

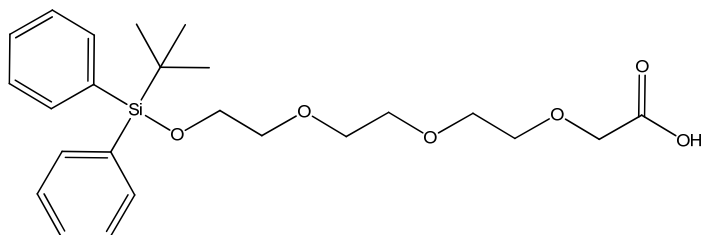
### DNA-based catalysis, representative procedure<sup>47,58,65</sup>

A buffered solution (40 mM Mops, pH 6.5) of DNA-AuNP's (1 mM DNA in basepairs) and 0.15 mM [Cu(dmbipy)(NO<sub>3</sub>)<sub>2</sub>] was prepared by mixing a solution of prehybridized DNA-AuNP's (500  $\mu$ l of a 2 mM (in bp) solution in water, prepared 24 h in advance) with 500  $\mu$ l of an buffered solution of Cu(dmbipy) (0.30 mM solution of [Cu(dmbipy)(NO<sub>3</sub>)<sub>2</sub>] in 40 mM MOPS pH 6.5). 1  $\mu$ mol of substrate in 10  $\mu$ l MeCN was added and the mixture was cooled to <5 °C. The reaction was started by addition of the appropriate amount of reactant (Diels-Alder 15 eq. **2**; Michael addition 100 eq. **4**; and mixed by continuous inversion for 3d, followed by extraction of the product with Et<sub>2</sub>O, drying (Na<sub>2</sub>SO<sub>4</sub>) and removal of the solvent. The crude product was analyzed by <sup>1</sup>H-NMR and HPLC.



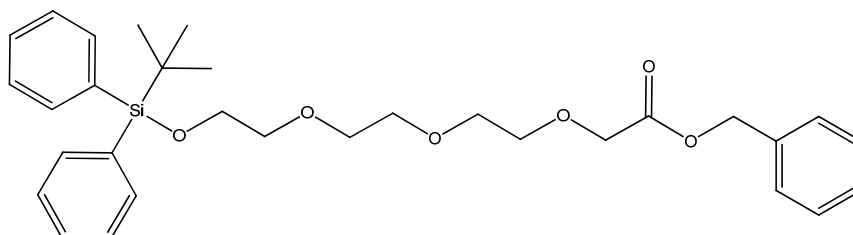
### benzyl 2-(2-(2-(2-(thioacetate)ethoxy)ethoxy)ethoxy)acetate (**16**)

To a solution of 1.26 g of benzyl ester **15** (2.8 mmol) in 40 ml acetone was added 0.64 g potassium thioacetate (3.6 mmol) and the mixture was heated under reflux for 3 h. The mixture was cooled to RT and filtered over a glass filter. the solvent was removed and the product was further purified by column chromatography (SiO<sub>2</sub>, EtOAc/pentane 4:1). 0.81 g of a slightly brown oil (2.3 mmol; 81%) was obtained. <sup>1</sup>H NMR (400 MHz, CDCl<sub>3</sub>)  $\delta$  7.41 (m, 5H), 5.19 (s, 2H), 4.21 (s, 2H), 3.66 (m, 10H), 3.08 (t, *J* = 6.4 Hz, 2H), 2.33 (s, 3H). <sup>13</sup>C NMR (50 MHz, CDCl<sub>3</sub>)  $\delta$  188.3, 163.0, 128.1, 121.3, 121.1, 121.0, 63.6, 63.4, 63.2 (2C), 63.0, 62.4, 61.4, 59.2, 23.2, 21.5.



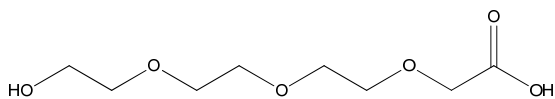
**2-(2-(2-(2-O-*tert* butyldiphenylsilylethoxy)ethoxy)ethoxy)acetic acid (19).**

4.03 g of **18** (10 mmol), powdered molecular sieves (4 Å, 1 g) and pyridinium dichromate (19.2 g; 50 mmol) were suspended in 75 ml of dry DMF, and the mixture was stirred for 3h. 200 ml of water was added to quench the reaction followed by 50 ml Et<sub>2</sub>O. The aqueous layer was extracted 4 times with 50 ml Et<sub>2</sub>O. The combined organic layers were dried over MgSO<sub>4</sub>, filtered and the solvent was removed. The green oil was further purified by column chromatography (SiO<sub>2</sub>, EtOAc/Pentane; 3/2) to yield 1.12 g of a slightly yellow oil (2.66 mmol; 27%). <sup>1</sup>H NMR (400 MHz, CDCl<sub>3</sub>) δ 7.68 (m, 4H), 7.44 (m, 6H), 4.13 (s, 2H), 3.63 (m, 12H), 1.05 (s, 9H). <sup>13</sup>C NMR (50 MHz, CDCl<sub>3</sub>) δ 173.5, 134.6, 130.1, 129.2, 128.7, 73.6, 70.5, 70.4 (2C), 70.2, 67.9, 63.5, 26.5, 19.3.



**benzyl 2-(2-(2-(2-O-*tert*-butylsilylethoxy)ethoxy)ethoxy)acetate (20)**

1.0 g of **19** (2.4 mmol) was added to 5 ml of dry acetone on N<sub>2</sub> atmosphere. 0.4 ml of triethylamine and 0.32 ml benzylbromide were added. The mixture was heated under reflux overnight. A white precipitate was filtered off and the solvent was removed. The yellow oil was taken up in 50 ml EtOAc and washed with 50 ml water, dried over Na<sub>2</sub>SO<sub>4</sub> and the solvent was removed. The product was obtained as a yellow oil (1.12g; 2.19 mmol; 92%). <sup>1</sup>H NMR (400 MHz, CDCl<sub>3</sub>) δ 7.68 (d, J = 6.0 Hz, 4H), 7.38 (m, 11H), 5.18 (s, 2H), 4.19 (s, 2H), 3.80 (t, J = 5.4 Hz, 2H), 3.66 (m, 10H), 1.05 (s, 9H). <sup>13</sup>C NMR (50 MHz, CDCl<sub>3</sub>) δ 163.0, 137.6, 134.6, 130.1, 129.1, 128.8, 128.2, 121.4, 121.0, 73.6, 66.5, 64.2, 63.8, 63.6, 63.2, 62.8, 26.4, 19.6.



**2-(2-(2-(2-hydroxyethoxy)ethoxy)ethoxy)acetic acid (22)**

2.93 g of **14** (9.8 mmol) was dissolved in 30 ml EtOH. 52.3 mg of Pd/C (10 %) was added. The mixture was placed under a H<sub>2</sub> atmosphere and stirred for 5 h. The mixture was filtered over celite, washed with 50 ml EtOH and the solvent was evaporated. The product was obtained as a colorless oil (1.73g; 0.83 mmol; 85%). <sup>1</sup>H NMR (400 MHz, CDCl<sub>3</sub>) δ 6.21 (br, 2H), 4.19 (m, 2H), 3.65 (m, 10H). <sup>13</sup>C NMR (101 MHz, CDCl<sub>3</sub>) δ 172.4, 72.7, 71.0, 70.9, 70.4, 70.3, 69.3, 61.8.

## 2.9 References

1. C. A. Mirkin, R. L. Letsinger, R. C. Mucic, J. J. Storhoff, *Nature* **1996**, *382*, 607.
2. J. S. Lee, A. K. Lytton-Jean, S. J. Hurst, C. A. Mirkin, *Nano Lett.* **2007**, *7*, 2112.
3. J. I. Cutler, D. Zheng, X. Xu, D. A. Giljohann, C. A. Mirkin, *Nano Lett.* **2010**, *10*, 1477.
4. G. Mitchell, C. Mirkin, R. Letsinger, *J. Am. Chem. Soc.* **1999**, *121*, 8122.
5. C. Xue, X. Chen, S. J. Hurst, C. A. Mirkin, *Adv. Mater.* **2007**, *19*, 4071.
6. Z. Li, Y. Zhang, P. Fullhart, C. A. Mirkin, *Nano Lett.* **2004**, *4*, 1055.
7. H. Liu, Z. Zhu, H. Kang, Y. Wu, K. Sefan, W. Tan, *Chem. Eur. J.* **2010**, *16*, 3791.
8. A. K. Lytton-Jean, C. A. Mirkin, *J. Am. Chem. Soc.* **2005**, *127*, 12754.
9. R. Jin, G. Wu, Z. Li, C. A. Mirkin, G. C. Schatz, *J. Am. Chem. Soc.* **2003**, *125*, 1643.
10. D. S. Seferos, A. E. Prigodich, D. A. Giljohann, P. C. Patel, C. A. Mirkin, *Nano Lett.* **2009**, *9*, 308.
11. N. L. Rosi, D. A. Giljohann, C. S. Thaxton, A. K. Lytton-Jean, M. S. Han, C. A. Mirkin, *Science* **2006**, *312*, 1027.
12. S. J. Hurst, A. K. R. Lytton-Jean, C. A. Mirkin, *Anal. Chem.* **2006**, *78*, 8313.
13. R. Elghanian, J. J. Storhoff, R. C. Mucic, R. L. Letsinger, C. A. Mirkin, *Science* **1997**, *277*, 1078.
14. B. D. Smith, J. Liu, *J. Am. Chem. Soc.* **2010**, *132*, 6300.
15. R. Reynolds, C. Mirkin, R. Letsinger, *J. Am. Chem. Soc.* **2000**, *122*, 3795.
16. S. Y. Park, A. K. Lytton-Jean, B. Lee, S. Weigand, G. C. Schatz, C. A. Mirkin, *Nature* **2008**, *451*, 553.
17. J. Lee, D. S. Seferos, D. A. Giljohann, C. A. Mirkin, *J. Am. Chem. Soc.* **2008**, *130*, 5430.
18. J. Lee, S. I. Stoeva, C. A. Mirkin, *J. Am. Chem. Soc.* **2006**, *128*, 8899.
19. S. Razin, *Mol. Cell. Probes* **1994**, *8*, 497.
20. U. Kreibitz, L. Genzel, *Surf. Sci.* **1985**, *156*, 678.
21. D. Nykypanchuk, M. M. Maye, D. van der Lelie, O. Gang, *Nature* **2008**, *451*, 549.
22. R. J. Macfarlane, M. R. Jones, A. J. Senesi, K. L. Young, B. Lee, J. Wu, C. A. Mirkin, *Angew. Chem. Int. Ed.* **2010**, *49*, 4589.
23. R. J. Macfarlane, B. Lee, M. R. Jones, N. Harris, G. C. Schatz, C. A. Mirkin, *Science* **2011**, *334*, 204.
24. H. D. Hill, R. J. Macfarlane, A. J. Senesi, B. Lee, S. Y. Park, C. A. Mirkin, *Nano Lett.* **2008**, *8*, 2341.
25. D. A. Giljohann, D. S. Seferos, P. C. Patel, J. E. Millstone, N. L. Rosi, C. A. Mirkin, *Nano Lett.* **2007**, *7*, 3818.
26. G. Han, C. C. You, B. J. Kim, R. S. Turingan, N. S. Forbes, C. T. Martin, V. M. Rotello, *Angew. Chem. Int. Ed.* **2006**, *45*, 3165.
27. T. Kubo, Z. Zhelev, H. Ohba, R. Bakalova, *Biochem. Biophys. Res. Commun.* **2008**, *365*, 54.
28. D. S. Seferos, D. A. Giljohann, N. L. Rosi, C. A. Mirkin, *ChemBioChem* **2007**, *8*, 1230.

29. S. Singh, P. Nielsen, A. Koshkin, J. Wengel, *Chem. Commun.* **1998**, 455.
30. F. McKenzie, K. Faulds, D. Graham, *Small* **2007**, *3*, 1866.
31. A. Koshkin, P. Nielsen, M. Meldgaard, V. Rajwanshi, S. Singh, J. Wengel, *J. Am. Chem. Soc.* **1998**, *120*, 13252.
32. A. M. Femino, F. S. Fay, K. Fogarty, R. H. Singer, *Science* **1998**, *280*, 585.
33. W. P. Kloosterman, E. Wienholds, E. de Bruijn, S. Kauppinen, R. H. Plasterk, *Nat. Methods* **2006**, *3*, 27.
34. S. Tyagi, F. R. Kramer, *Nat. Biotechnol.* **1996**, *14*, 303.
35. D. L. Sokol, X. Zhang, P. Lu, A. M. Gewirtz, *Proc. Natl. Acad. Sci. U.S.A.* **1998**, *95*, 11538.
36. S. Sando, E. T. Kool, *J. Am. Chem. Soc.* **2002**, *124*, 9686.
37. P. J. Santangelo, B. Nix, A. Tsourkas, G. Bao, *Nucleic Acids Res.* **2004**, *32*, 57.
38. L. Wang, C. Yang, C. Medley, S. Benner, W. Tan, *J. Am. Chem. Soc.* **2005**, *127*, 15664.
39. N. Nitin, P. Santangelo, G. Kim, S. Nie, G. Bao, *Nucleic Acids Res.* **2004**, *32*, 58.
40. D. S. Seferos, D. A. Giljohann, H. D. Hill, A. E. Prigodich, C. A. Mirkin, *J. Am. Chem. Soc.* **2007**, *129*, 15477.
41. A. E. Prigodich, D. S. Seferos, M. D. Massich, D. A. Giljohann, B. C. Lane, C. A. Mirkin, *ACS Nano* **2009**, *3*, 2147.
42. D. Zheng, D. S. Seferos, D. A. Giljohann, P. C. Patel, C. A. Mirkin, *Nano Lett.* **2009**, *9*, 3258.
43. C. D. Medley, J. E. Smith, Z. Tang, Y. Wu, S. Bamrungsap, W. Tan, *Anal. Chem.* **2008**, *80*, 1067.
44. D. A. Giljohann, D. S. Seferos, A. E. Prigodich, P. C. Patel, C. A. Mirkin, *J. Am. Chem. Soc.* **2009**, *131*, 2072.
45. Y. Chiu, T. Rana, *RNA-a Publication of the RNA Society* **2003**, *9*, 1034.
46. J. Soutschek, A. Akinc, B. Bramlage, K. Charisse, R. Constien, M. Donoghue, S. Elbashir, A. Geick, P. Hadwiger, J. Harborth, M. John, V. Kesavan, G. Lavine, R. Pandey, T. Racie, K. Rajeev, I. Rohl, I. Toudjarska, G. Wang, S. Wuschko, D. Bumcrot, V. Kotliansky, S. Limmer, M. Manoharan, H. Vornlocher, *Nature* **2004**, *432*, 173.
47. A. J. Boersma, B. L. Feringa, G. Roelfes, *Angew. Chem. Int. Ed.* **2009**, *48*, 3346.
48. A. J. Boersma, J. E. Klijn, B. L. Feringa, G. Roelfes, *J. Am. Chem. Soc.* **2008**, *130*, 11783.
49. M. C. Daniel, D. Astruc, *Chem. Rev.* **2004**, *104*, 293.
50. K. C. Grabar, R. G. Freeman, M. B. Hommer, M. J. Natan, *Anal. Chem.* **1995**, *67*, 735.
51. J. Gao, X. Huang, H. Liu, F. Zan, J. Ren, *Langmuir* **2012**, *28*, 4464.
52. M. J. Stefanko, Y. K. Gun'ko, D. K. Rai, P. Evans, *Tetrahedron* **2008**, *64*, 10132.
53. J. C. Barrish, H. L. Lee, T. Mitt, G. Pizzolato, E. G. Baggiolini, M. R. Uskokovic, *J. Org. Chem.* **1988**, *53*, 4282.
54. J. Canceill, L. Jullien, L. Lacombe, J. M. Lehn, *Helv. Chim. Acta* **1992**, *75*, 791.
55. X. Qi, J. Ready, *Angew. Chem. Int. Ed.* **2007**, *46*, 3242.
56. C. W. Dicus, M. H. Nantz, *Synlett* **2006**, 2821.

57. Y. Wu, Y. Sun, *Chem. Commun.* **2005**, 1906.
58. G. Roelfes, A. J. Boersma, B. L. Feringa, *Chem. Commun.* **2006**, 635.
59. S. Otto, J. Engberts, *J. Am. Chem. Soc.* **1999**, *121*, 6798.
60. W. H. A. Kuijpers, C. A. A. van Boeckel, *Tetrahedron* **1993**, *49*, 10931.
61. X. Qi, J. M. Ready, *Angew. Chem. Int. Ed.* **2007**, *46*, 3242.
62. A. Pollex, M. Hiersemann, *Org. Lett.* **2005**, *7*, 5705.
63. J. Canceill, L. Jullien, L. Lacombe, J. M. Lehn, *Helv. Chim. Acta* **1992**, *75*, 791.
64. Z. Jiang, Y. B. Yu, *Tetrahedron* **2007**, *63*, 3982.
65. D. Coquière, B. L. Feringa, G. Roelfes, *Angew. Chem. Int. Ed.* **2007**, *46*, 9308.



## Chapter 3

# Organic Co-Solvents in Aqueous DNA-Based Asymmetric Catalysis

*DNA-based asymmetric catalysis has been used for a wide variety of reactions in water (chapter 1). However in most cases the solubility of the reactants in water remains a challenge. This could possibly be solved by the addition of organic co-solvents. In this chapter the addition of co-solvents will be discussed. Water-miscible organic co-solvents can be used in DNA-based catalytic asymmetric reactions at appreciable concentration without having a negative effect on enantioselectivity. While the rate of the copper(II) Diels-Alder reaction is affected negatively by the presence of organic co-solvents, the copper(II) catalyzed Michael addition and Friedel-Crafts alkylation reaction are significantly faster. Additionally, the presence of organic co-solvents allows for reaction temperatures  $< 0^{\circ}\text{C}$ , resulting in higher ee's. This is used to perform enantioselective Michael additions and Friedel-Crafts alkylations at gram scale, with lower catalyst loadings.*

Parts of this chapter have been published: R.P. Megens, G. Roelfes *Org. Biomol. Chem.* **2010**, 1387

### 3.1 Introduction

A common feature in DNA-based catalysis approaches is that they inherently require water as the reaction medium. Aqueous phase catalysis is an area of considerable interest due to the potential advantages of replacing organic solvents with water and the special properties of water as a reaction medium.<sup>1-3</sup> For example, water has been shown to be beneficial for the rate and enantioselectivity of catalyzed reactions.<sup>3</sup> An obvious complication is the limited solubility in water of many organic substrates and reagents, which may hamper applications of this concept in organic synthesis. However, this does not necessarily pose a problem as is illustrated by the recently developed on water protocols,<sup>4,5</sup> which involve insoluble reagents. Efficient conversions can sometimes also be obtained in partially heterogeneous reaction mixtures.<sup>6</sup> Nevertheless, for many DNA-based catalytic reactions organic co-solvents will be required to achieve chemical transformations at synthetically relevant scales. The challenge herein lies in the presence of DNA, which might precipitate and/or undergo a structural change.<sup>7</sup>

Previously, it has been shown by Liu *et al.* that up to 99% organic solvents can be used in DNA-templated synthesis.<sup>8,9</sup> Furthermore, the use of organic solvents in combination with DNA has also been demonstrated in the DNA-mediated aldol and Henry reactions. These reactions were performed using DNA far above its solubility range in combination with organic solvents in which DNA is not soluble at all. Additionally, the addition of organic solvents had a negative effect on the yields of the Henry reaction.<sup>10,11</sup>

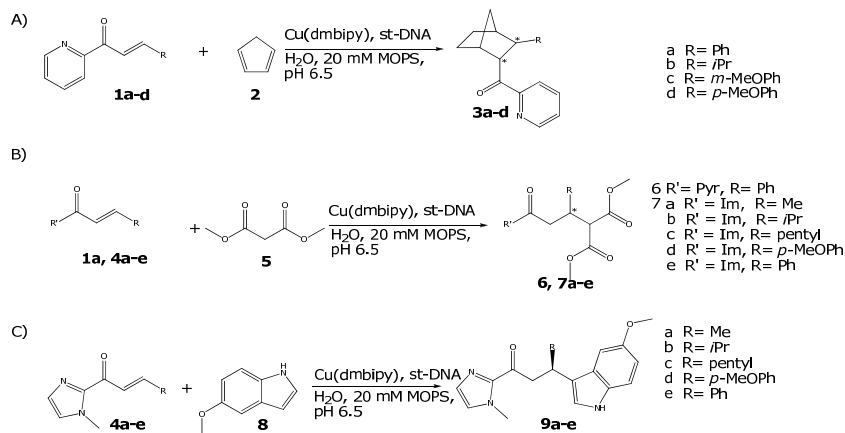
In this chapter we discuss the results of a study on the effect of organic co-solvents on DNA-based asymmetric catalysis. The goal of this study was twofold: first of all to establish the effect that organic co-solvents have on the rate and enantioselectivity of DNA-based catalytic reactions and secondly, to enable the application of the DNA-based asymmetric catalysis concept in organic synthesis.

### 3.2 Solvent scope

#### 3.2.1 Studied reactions

We have focused on the Diels-Alder reaction, the Michael addition and the Friedel-Crafts alkylation (Scheme 3.1), catalyzed by a [Cu<sup>II</sup>(4,4'-dimethyl-2,2'-bipyridine)(NO<sub>3</sub>)<sub>2</sub> (Cu-dmbipy)/salmon testes-DNA (st-DNA) (15 mol% in copper), which is the most enantioselective catalyst to date for these reactions.<sup>6,12,13</sup> As the benchmark substrates azachalcone (**1a**) and the  $\alpha,\beta$ -unsaturated 2-acyl imidazole **4a** were used, which provide a bidentate coordination. This is generally required in copper(II)-catalyzed reactions of this type.<sup>14</sup>





**Scheme 3.1.** Cu-dmbipy/DNA-catalyzed Diels-Alder reaction (A), Michael reaction (B) and Friedel-Crafts alkylation (C). General conditions: 0.15 mM Cu-dmbipy, 1 mM st-DNA in in basepairs, 1 mM enone substrate, 20 mM MOPS pH 6.5. Pyr = 2-pyridyl, Im. = 1-methylimidazol-2-yl.

### 3.2.2 Diels-Alder reaction

Initially the effect of organic solvents on enantioselectivity and conversion in the Diels-Alder reaction of azachalcone (**1a**) with cyclopentadiene (**2**) after a fixed reaction time was investigated.

A wide variety of organic solvents was screened. Water-miscible solvents such as MeCN, alcohols, DMSO and DMF were tolerated well in the Diels-Alder reaction (Table 3.1). However when either THF or CH<sub>2</sub>Cl<sub>2</sub>, which are not or only partially water-miscible, was used, a strong decrease in conversion and enantioselectivity was observed. This can be ascribed to the partial DNA precipitation that was observed. The tolerance towards organic solvents in the Diels-Alder reaction was up to 33% v/v of water-miscible organic co-solvent: no decrease in ee was observed compared to the reactions in water. Further increase of the amount of organic co-solvent gave rise to a loss of reactivity and enantioselectivity, which is most likely the result of precipitation of DNA.

### 3.2.3 Michael addition and Friedel-Crafts alkylation

The solvent scope for the Michael addition was studied for the addition of dimethyl malonate (**5**) to azachalcone (**1a**) and the Friedel-Crafts alkylation by the alkylation of 5-methoxyindole (**8**) with  $\alpha,\beta$ -unsaturated 2-acylimidazole (**4a**) (Scheme 3.1), after a fixed reaction time. For the solvent scope of the Michael addition and the Friedel-Crafts alkylation a similar trend was observed; with up to 10% v/v of co-solvent the same ee's were obtained compared to water alone. Further increase of the fraction of organic solvents led to a slow decrease in enantioselectivity (Table 3.2, 3.3). Also the Michael addition of nitromethane to **1a** was performed however no reaction was observed upon using a water-miscible co-solvent.

**Table 3.1.** Solvent scope of the Diels-Alder reaction of azachalcone (**1a**) with cyclopentadiene (**2**).

| Fraction (v/v%) | MeCN Conv. (ee)        | MeOH Conv. (ee)        | EtOH Conv. (ee)        | <i>i</i> PrOH Conv. (ee) | DMF Conv. (ee)         | DMSO Conv. (ee)        | 1,4-dioxane Conv. (ee)  | DCM Conv. (ee) | THF Conv. (ee)         |
|-----------------|------------------------|------------------------|------------------------|--------------------------|------------------------|------------------------|-------------------------|----------------|------------------------|
| 30%             | Full (99%)             | Full (99%)             | Full (99%)             | Full (99%)               | Full (99%)             | Full (99%)             | Full (99%)              | - <sup>a</sup> | 50% (99%) <sup>a</sup> |
| 33%             | Full (99%)             | Full (99%)             | Full (99%)             | Full (99%)               | Full (99%)             | Full (99%)             | Full (99%)              | - <sup>a</sup> | 34% (99%) <sup>a</sup> |
| 35%             | Full (98%)             | Full (98%)             | Full (98%)             | Full (97%)               | Full (98%)             | Full (98%)             | Full (93%)              | - <sup>a</sup> | - <sup>a</sup>         |
| 40%             | 60% (80%) <sup>a</sup> | 49% (81%) <sup>a</sup> | 43% (79%) <sup>a</sup> | 40% (75%) <sup>a</sup>   | 52% (80%) <sup>a</sup> | 39% (74%) <sup>a</sup> | Full (82%) <sup>a</sup> | - <sup>a</sup> | - <sup>a</sup>         |

General conditions: 0.15 mM Cu(dmbipy), 0.67 mg/ml st-DNA, 1 mM 2-acyl imidazole **4a**, 5 mM 5-methoxyindole (**8**), 1d. <sup>a</sup> DNA precipitation observed.

**Table 3.2.** Solvent scope of the Michael Addition of azachalcone (**1a**) with dimethyl malonate (**5**).

| Fraction (v/v%) | MeCN Conv. (ee) | MeOH Conv. (ee) | EtOH Conv. (ee) | <i>i</i> PrOH Conv. (ee) | DMF Conv. (ee) | DMSO Conv. (ee) | 1,4-dioxane Conv. (ee) | DCM Conv. (ee)         | THF Conv. (ee)          |
|-----------------|-----------------|-----------------|-----------------|--------------------------|----------------|-----------------|------------------------|------------------------|-------------------------|
| 5%              | Full (96%)      | Full (96%)      | Full (96%)      | Full (96%)               | Full (95%)     | Full (96%)      | Full (94%)             | 15% (96%) <sup>a</sup> | Full (92%)              |
| 10%             | Full (96%)      | Full (96%)      | Full (96%)      | Full (96%)               | Full (95%)     | Full (95%)      | Full (93%)             | 8% (94%) <sup>a</sup>  | Full (90%) <sup>a</sup> |
| 15%             | Full (95%)      | Full (95%)      | Full (96%)      | Full (96%)               | Full (94%)     | Full (93%)      | Full (92%)             | 5% (96%) <sup>a</sup>  | 90% (87%) <sup>a</sup>  |
| 20%             | Full (94%)      | Full (95%)      | Full (95%)      | Full (95%)               | Full (92%)     | Full (93%)      | Full (90%)             | 4% (61%) <sup>a</sup>  | 60% (81%) <sup>a</sup>  |

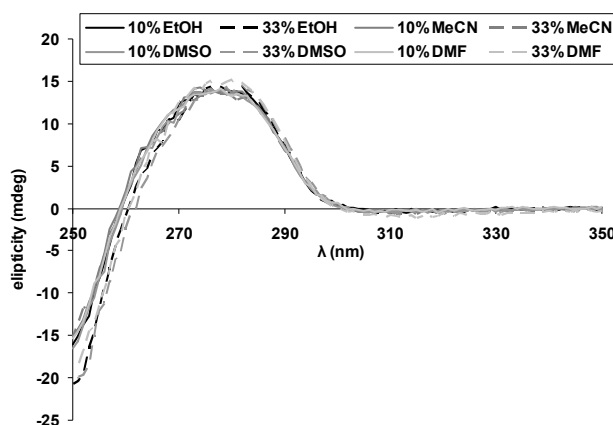
General conditions: 0.15 mM Cu(dmbipy), 0.67 mg/ml st-DNA, 1 mM azachalcone (**1a**), 100 mM dimethyl malonate (**5**), 1d. <sup>a</sup> DNA precipitation observed

**Table 3.3.** Solvent scope of the Friedel-Crafts alkylation of  $\alpha,\beta$ -unsaturated 2-acylimidazole (**4a**) with 5-methoxyindole (**8**).

| Fraction (v/v%) | MeCN Conv. (ee) | MeOH Conv. (ee) | EtOH Conv. (ee) | <i>i</i> PrOH Conv. (ee) | DMF Conv. (ee) | DMSO Conv. (ee) | 1,4-dioxane Conv. (ee) | DCM Conv. (ee)          | THF Conv. (ee)          |
|-----------------|-----------------|-----------------|-----------------|--------------------------|----------------|-----------------|------------------------|-------------------------|-------------------------|
| 5%              | Full (83%)      | Full (83%)      | Full (83%)      | Full (83%)               | Full (83%)     | Full (82%)      | Full (83%)             | Full (81%) <sup>a</sup> | Full (81%)              |
| 10%             | Full (83%)      | Full (83%)      | Full (82%)      | Full (83%)               | Full (82%)     | Full (83%)      | Full (83%)             | 78% (75%) <sup>a</sup>  | Full (81%) <sup>a</sup> |
| 15%             | Full (81%)      | Full (83%)      | Full (82%)      | Full (82%)               | Full (83%)     | Full (82%)      | Full (83%)             | 55% (64%) <sup>a</sup>  | Full (71%) <sup>a</sup> |
| 20%             | Full (81%)      | Full (82%)      | Full (82%)      | Full (81%)               | Full (82%)     | Full (82%)      | Full (82%)             | 23% (60%) <sup>a</sup>  | Full (61%) <sup>a</sup> |

General conditions: 0.15 mM Cu(dmbipy), 0.67 mg/ml st-DNA, 1 mM azachalcone (**1a**), 3d, 15 mM cyclopentadiene (**2**). <sup>a</sup> DNA precipitation observed

The decrease in enantioselectivity at higher fractions of organic co-solvents could theoretically be related to a change in DNA structure; it has been reported that the rate acceleration and enantioselectivity in DNA-based catalysis are DNA sequence, and hence, structure dependent.<sup>13,15,16</sup> However, no differences were observed in the circular dichroism spectra upon addition of organic solvents to a DNA solution (Figure 3.1), suggesting that structural changes in the DNA do not play a role.



**Figure 3.1.** CD-spectra of st-DNA in the presence of organic solvents.

Alternatively, the decrease in enantioselectivity at higher organic solvent content could be the result of a decrease in binding affinity of the copper complex to the DNA, perhaps as result of a weakening of the interactions between the catalyst and the DNA. This would result in more unbound copper complex being present, which will catalyze the reaction in a racemic fashion. Indeed, the binding constant ( $K_b$ ) of the copper complex to DNA for different solvents decreased when >10% v/v of organic co-solvent was employed, albeit that this decrease was only up to 3-fold (Table 3.4).

**Table 3.4.** Binding constant of  $\text{Cu}(\text{dmbipy})(\text{NO}_3)_2$  to DNA.

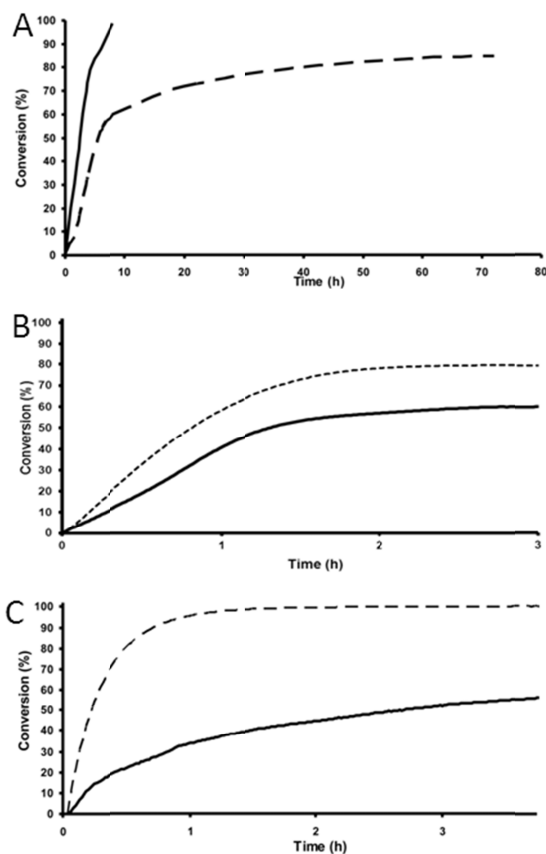
|                      | $K_b$ ( $10^4 \text{ M}^{-1}$ ) |
|----------------------|---------------------------------|
| $\text{H}_2\text{O}$ | $1.18 \pm 0.01$                 |
| 10% v/v MeCN         | $1.18 \pm 0.01$                 |
| 25% v/v MeCN         | $0.55 \pm 0.06$                 |
| 10% v/v DMSO         | $1.08 \pm 0.02$                 |
| 10% v/v EtOH         | -                               |
| 25% v/v EtOH         | $0.31 \pm 0.02$                 |

Yet, this implies that the fraction of copper complexes bound to DNA decreases from 92% to 84% and 75% for 25% v/v MeCN and EtOH, respectively. The fact that this significant decrease in fraction of complexes bound to DNA is not translated into a similar drop in ee is the result of the significant rate acceleration induced by DNA in these

reactions.<sup>13,16</sup> In the presence of 10% v/v of EtOH no reliable data could be obtained. The reason for this is not yet understood. Possibly, it relates to a change in binding geometry of the copper complex at this solvent composition.

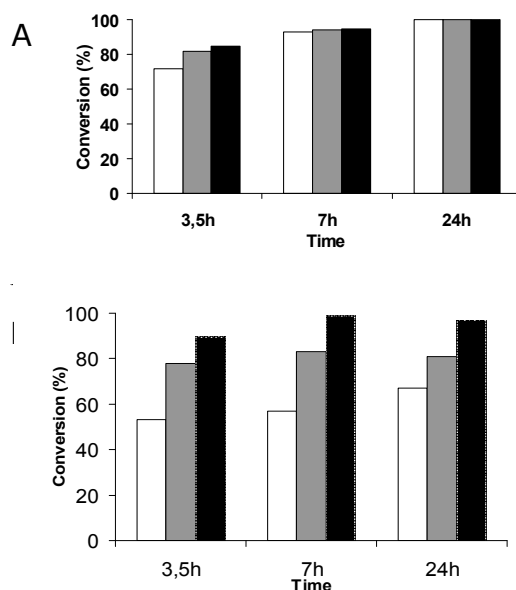
### 3.3 Influence on reaction rate

The effect of organic solvents on the reaction rate was studied using MeCN as benchmark solvent. The reactions were monitored by UV/Vis spectroscopy, following the decrease of the absorption of the enone substrate. In the case of the Diels-Alder reaction a significant deceleration was observed (Figure 3.2A). This is not surprising since it is well-established that the reaction is water accelerated,<sup>17,18</sup> which is due to the hydrophobic effect;<sup>19</sup> addition of MeCN disrupts these favourable interactions.<sup>20</sup>



**Figure 3.2.** A; Temporal conversion curve of the Cu(dmbipy)/DNA catalyzed Diels-Alder reaction of **1a** with **2**: 0.15 mM Cu(dmbipy), 1 mM st-DNA in basepairs, 1 mM **1a**, 15 mM **2**, 20 mM MOPS pH 6.5, 5 °C; — 0%, - - 33% MeCN, B; Temporal conversion curve of the Cu(dmbipy)/DNA catalyzed Michael addition of **1a** with **5**: 0.15 mM Cu(dmbipy), 0.67 mg/ml st-DNA, 1 mM **1a**, 100 eq. **5**, 20 mM MOPS pH 6.5, 5 °C; — 0%, - - 10% v/v MeCN, C; Temporal conversion curve of the Friedel-Crafts alkylation of **4a** with **8**: 0.15 mM Cu(dmbipy), 1 mM st-DNA in basepairs, 1 mM **4a**, 5 mM **8**, 20 mM MOPS pH 6.5, 5 °C; — 0%, - - 10% v/v MeCN.

In contrast, in the Friedel-Crafts alkylation and Michael reaction, both conjugate additions, the reaction is significantly faster when the content of MeCN is increased. (Figure 3.2 B,C). These data were verified by HPLC analysis of samples taken from the reaction at different time intervals (Figure 3.3). For example, the conversion after 3.5 h with 10% v/v MeCN increased from 53% to 90% and 72% to 85% in the Friedel-Crafts alkylation and Michael addition, respectively.

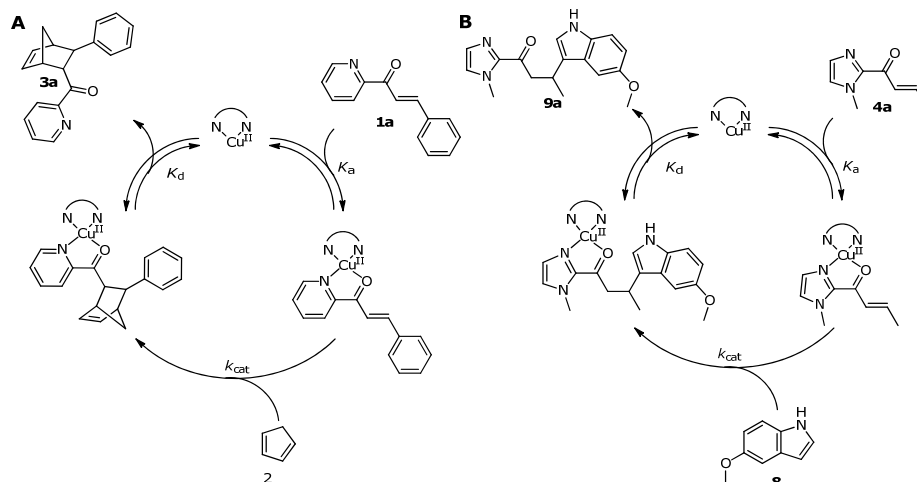


**Figure 3.3.** A; Temporal conversion of the Michael addition of azachalcone (**1a**) and dimethyl malonate (**5**): 0.15 mM Cu(dmbipy), 0.67 mg/ml st-DNA, 1 mM **1a**, 100 eq. **5**, 20 mM MOPS pH 6.5, 5 °C, analyzed with NMR and HPLC; □ = Water = 5% MeCN ■ = 10% MeCN, B; Temporal conversion of the Friedel-Crafts alkylation reaction of 5-methoxyindole (**8**) with  $\alpha,\beta$ -unsaturated 2-acylimidazole (**4a**): 0.15 mM Cu(dmbipy), 0.67 mg/ml st-DNA, 1 mM (**4a**), 5 eq. **8**, 20 mM MOPS pH 6.5, 5 °C, analyzed with NMR and HPLC; □ = Water = 5% MeCN ■ = 10% MeCN.

The apparent second-order rate constant ( $k_{app}$ ) for the Diels-Alder and Friedel-Crafts alkylation were determined using the methods developed by Engberts *et al.* in order to verify these results.<sup>15,16,21, 5</sup> In this model, the overall rate is determined by the equilibrium constant for the reversible binding ( $K_a$ ) of the enone substrate to the Cu<sup>II</sup> complex, the rate of the reaction of the reactant, that is, cyclopentadiene or

<sup>5</sup> Determination of the kinetic parameters for the Michael addition is complicated by the additional enolisation equilibrium of dimethyl malonate that is involved.<sup>22</sup>

methoxyindole, with the  $\text{Cu}^{\text{II}}$  bound enone substrate ( $k_{\text{cat}}$ ) and the reversible dissociation of the product from the  $\text{Cu}^{\text{II}}$  complex ( $K_{\text{d}}$ ). In accordance with the generally accepted approach, the kinetic experiments were performed using a large excess of  $\text{Cu}(\text{dmbipy})$  with respect to the substrates, thus assuming that the contribution of the  $K_{\text{d}}$  to the overall rate ( $k_{\text{app}}$ ) is negligible (Scheme 3.2).<sup>21</sup>



**Scheme 3.2.** A; Proposed catalytic cycle of the  $\text{Cu}^{\text{II}}$ -catalyzed Diels-Alder reaction of azachalcone (**1a**) with cyclopentadiene (**2**) and B; the  $\text{Cu}^{\text{II}}$ -catalyzed Friedel-Crafts alkylation reaction of  $\alpha,\beta$ -unsaturated 2-acylimidazole (**4a**) with 5-methoxyindole (**8**).

In the case of the Diels-Alder reaction, comparison of the  $k_{\text{app}}$  values showed the same trend as could be seen in the temporal conversion curve (Table 3.5). A decrease in the  $k_{\text{app}}$  of 2 orders of magnitude was found upon increasing the MeCN content to 30% v/v.

**Table 3.5**  $k_{\text{app}}$  of the Diels-Alder reaction and Friedel-Crafts alkylation catalyzed by  $\text{Cu}(\text{dmbipy})$  with DNA in various mixtures  $\text{H}_2\text{O}/\text{MeCN}$ .

| Diels-Alder reaction <sup>a</sup> |   | Friedel-Crafts alkylation <sup>b</sup> |   |
|-----------------------------------|---|--|---|
| % v/v MeCN                        | $k_{\text{app}} (\times 10^{-2} \text{ M}^{-1} \text{ s}^{-1})$ | % v/v MeCN                             | $k_{\text{app}} (\times 10^{-2} \text{ M}^{-1} \text{ s}^{-1})$ |
| 0                                 | 39.0 ± 0.6  | 0                                      | 52.6 ± 2.5  |
| 10                                | 15.6 ± 2.1  | 10                                     | 31.6 ± 4.3  |
| 20                                | 2.18 ± 0.17   | 20                                     | 20.1 ± 1.4  |
| 30                                | 0.81 ± 0.01   | 30                                     | 6.31 ± 1.0  |

<sup>a</sup>  $k_{\text{app}}$  determined for reaction of **1a** (6  $\mu\text{M}$ ) with **2** (0.5–2.0 mM) with 0.15 mM  $\text{Cu}(\text{dmbipy})$  and 1 mM DNA in basepairs in 20 mM MOPS pH 6.5 at 18 °C, 226 nm; <sup>b</sup>  $k_{\text{app}}$  determined for reaction of **4a** (14  $\mu\text{M}$ ) with **8** (0.5–2.0 mM) with 0.15 mM  $\text{Cu}(\text{dmbipy})$  and 1 mM DNA in basepairs in 20 mM MOPS pH 6.5 at 18 °C, 265 nm.

Surprisingly, in the Friedel-Crafts alkylation an almost 10-fold decrease in  $k_{\text{app}}$  was found in the presence of 30% v/v MeCN. This represents the opposite trend as observed in the experiments under turnover conditions, that is, with an excess of enone substrate with respect to the catalyst. This suggests that in these reactions the

dissociation step, and not the actual conjugate addition reaction, is rate limiting, and that it is this step in which the favourable effect of organic co-solvents is found. This proposed acceleration of the dissociation step is only to a minor extent reflected in the position of the dissociation equilibrium. The  $K_d$  of **9a** was determined to be  $2.8 \pm 0.1 \times 10^{-4}$  M in water, while the  $K_d$  was  $5.55 \pm 0.04 \times 10^{-4}$  M in 10% v/v MeCN.

The observations presented here show that, although the kinetic model provides valuable information about the initial steps of the catalytic reaction, care should be exercised in extrapolating this data to the overall reaction. The assumptions underlying this kinetic model, that is the negligibility of the dissociation step, should always be verified by experiments under turnover conditions.

### 3.4 Substrate scope

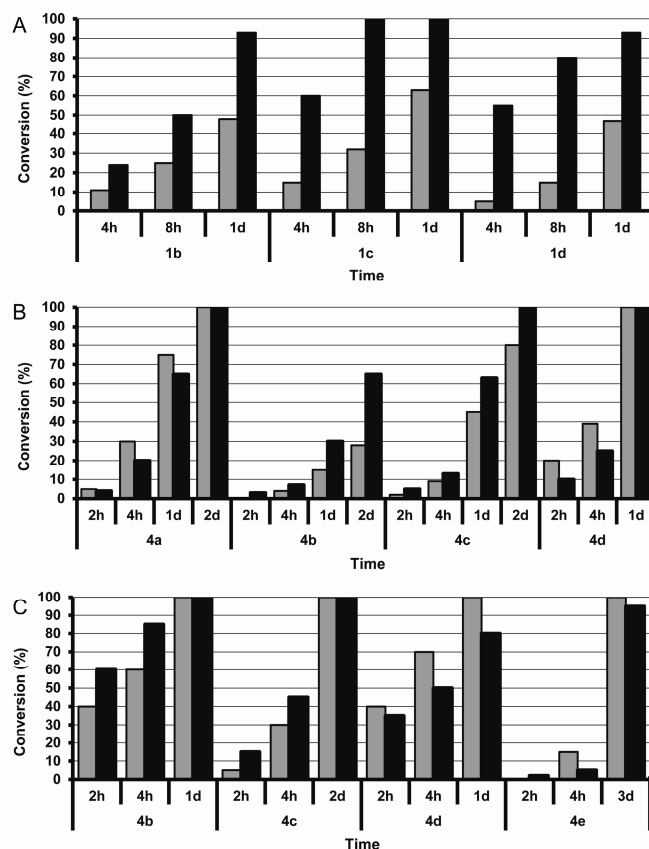
Using MeCN as benchmark solvent, the substrate scope of the DNA-based catalytic reactions was explored. In all cases the ee found in the presence of 10% v/v MeCN was similar to that obtained in water (Table 3.6) Unsurprisingly, in the Diels-Alder reaction, always higher conversions were observed in water compared to 10% v/v MeCN, even though with enones **1c** and **1d** the reaction was partly heterogeneous due to precipitation of these substrates (Figure 3.4A).

**Table 3.6.** Substrate scope of DNA-based catalytic Diels-Alder, Michael addition and Friedel-Crafts alkylation reactions with and without organic co-solvent

| Enone     | Reactant | ee (H <sub>2</sub> O) | ee (10% v/v MeCN) |
|-----------|----------|-----------------------|-------------------|
| <b>1b</b> | <b>2</b> | 96                    | 94                |
| <b>1c</b> | <b>2</b> | 99                    | 99                |
| <b>1d</b> | <b>2</b> | 99                    | 93                |
| <b>4a</b> | <b>5</b> | 56                    | 56                |
| <b>4b</b> | <b>5</b> | 8                     | 10                |
| <b>4c</b> | <b>5</b> | 13                    | 15                |
| <b>4d</b> | <b>5</b> | 93                    | 94                |
| <b>4b</b> | <b>8</b> | 70                    | 70                |
| <b>4c</b> | <b>8</b> | 57                    | 56                |
| <b>4d</b> | <b>8</b> | 77                    | 78                |
| <b>4e</b> | <b>8</b> | 69                    | 69                |

General conditions: 0.15 mM Cu(dmbipy), 1 mM st-DNA in basepairs, 1 mM enone, 20 mM MOPS pH 6.5.

For the Michael addition higher conversions were observed when the substituent at the enone [R] was Me (**4a**) and *p*-methoxyphenyl (**4d**). However, enones **4b** and **4c**, which contain a large alkyl substituent at the enone, surprisingly gave rise to lower conversions in 10% v/v MeCN compared to the reaction in water (Figure 3.4B).



**Figure 3.4.** Temporal conversion of the Diels-Alder reaction (A), the Michael addition (B) and the Friedel-Crafts alkylation (C). 0.15 mM Cu-dmbipy, 1 mM st-DNA in basepairs, 1 mM enone substrate, 20 mM MOPS pH 6.5,  $\text{H}_2\text{O} = 10\%$  MeCN

A similar trend was observed for the Friedel-Crafts alkylation; in case of [R] being an aryl group, that is, with substrates **4d** and **4e**, higher conversions were obtained in the presence of 10% v/v MeCN. But also here, the reactions with **4b** and **4c**, were more efficient in water alone. The reason why **4b** and **4c** undergo conjugate addition more efficiently in water compared to 10% v/v MeCN is at present unknown. It can be speculated that for these substrates, which carry large alkyl substituents at the enone moiety, hydrophobic effects contribute favorably to the reaction in water. Analogous to the Diels-Alder reaction, this favorable interaction is disturbed by the presence of an organic co-solvent, resulting in lower conversion.



### 3.5 Lower temperature

Lowering of the reaction temperature is an often used approach to increase the enantioselectivity of catalytic asymmetric reactions. When using water as the solvent, obviously the temperature cannot be lowered much below 0 °C. However, in the presence of organic co-solvents the freezing temperature is decreased significantly and this allows for DNA-based asymmetric catalysis at temperatures below 0 °C. The Friedel-Crafts reaction was investigated at -18 °C. At least 25% v/v of co-solvent was required to keep the solutions liquid. At this temperatures the enantioselectivity increased from 82% to 90% using MeOH and EtOH, with 90% conversion after 1.5h (Table 3.7). Using DMSO a comparable reactivity was found, albeit that the enantioselectivity was slightly lower. DMF and 1,4-dioxane however, did not improve the efficiency of the reaction and full conversion was not reached within 3 days.

**Table 3.7.** Friedel-Crafts alkylation of **8** with **4a** at 4 °C and -18 °C

| co-Solvent  | % v/v | 4 °C     |        | -18 °C          |        |
|-------------|-------|----------|--------|-----------------|--------|
|             |       | conv (%) | ee (%) | conv (%)        | ee (%) |
| MeOH        | 25    | Full     | 82     | 90              | 90     |
|             | 30    | Full     | 82     | 90              | 90     |
| EtOH        | 25    | Full     | 82     | - <sup>a</sup>  | -      |
|             | 30    | Full     | 82     | 90              | 90     |
| DMSO        | 25    | Full     | 83     | 90              | 89     |
|             | 30    | Full     | 82     | 75              | 89     |
| DMF         | 25    | Full     | 83     | 90 <sup>b</sup> | 84     |
|             | 30    | Full     | 81     | 70 <sup>b</sup> | 83     |
| 1,4-dioxane | 25    | Full     | 80     | - <sup>a</sup>  | -      |
|             | 30    | Full     | 78     | 73 <sup>b</sup> | 76     |

General conditions: 0.15 mM Cu(dmbipy), 0.67 mg/ml st-DNA, 1 mM **6**, 5 mM **7**, 20 mM MOPS pH 6.5, 1.5h; <sup>a</sup> reaction mixture freezes; <sup>b</sup> after 3d.

### 3.6 Larger scale

The effect of increasing substrate concentration in the presence of organic co-solvents was investigated and the results were compared to those obtained with water alone. The azachalcone (**1a**) concentration could be increased to 5 mM in 33% v/v MeCN for the Diels-Alder reaction (71% conversion; 99% ee). However, in water full conversion was found in the same time (Table 3.8). This was expected in view of the well-established acceleration of the the Diels-Alder reaction in water and the results presented above.<sup>17,18</sup> It has to be noted that in the latter case the concentrations used are above the solubility limit and, hence, the reaction mixture is partly heterogeneous. Still the reaction is more efficient than in the presence of MeCN, even though the reaction mixture is homogeneous in this case.

**Table 3.8.** Increasing substrate concentration in the Diels-Alder reaction

| Conc. <b>1a</b> | Water      | 33% MeCN   |
|-----------------|------------|------------|
|                 | Conv. (ee) | Conv. (ee) |
| 1 mM            | Full (99%) | Full (99%) |
| 2 mM            | Full (99%) | Full (99%) |
| 5 mM            | Full (99%) | 71% (99%)  |
| 10 mM           | 84% (96%)  | 50% (93%)  |

General conditions: 0.15 mM Cu(dmbipy), 0.67 mg/ml st-DNA, 15 eq **2**

Since both the Michael addition and the Friedel-Crafts alkylation are, in some cases, accelerated in the presence of organic co-solvents, these reactions were performed on a synthetically relevant scale.

The Michael addition of dimethyl malonate (**5**) to the  $\alpha,\beta$ -unsaturated 2-acylimidazole (**4e**) was investigated since the N-methylimidazole auxiliary can be displaced readily afterwards.<sup>23-25</sup> Using a final concentration of 14.5 mM of **4e**, full conversion was obtained in 3d using only 1 mol% of catalyst. A slightly higher isolated yield (85%) was obtained from the reaction in 10% v/v MeCN compared to water (72%) (Table 3.9), whereas the ee's were 94 and 95 %, respectively.

The Friedel-Crafts alkylation of indole **8** with **4a** and **4d** was carried out at an enone concentration of 20 mM on 1.0 g scale and 300 mg scale, respectively. Both in water and water/10% v/v MeCN, at a reaction temperature of 4 °C, full conversion was reached overnight in the case of **4a**, while 6 days were needed for the reaction of **4d** to reach full conversion in 10% v/v MeCN. In this latter case only 40% conversion was reached in water in the same time. It should be noted that the catalyst loading was reduced to 0.75 mol% compared to 15 mol% in the small scale experiments.

**Table 3.9.** Large scale Michael addition and Friedel-Crafts alkylation reaction

|                     | Michael addition <sup>a</sup> |         | Friedel-Crafts alkylation |                 |                    |                 |
|---------------------|-------------------------------|---------|---------------------------|-----------------|--------------------|-----------------|
|                     | Yield                         | ee      | <b>4a</b>                 |                 | <b>4d</b>          |                 |
|                     |                               |         | Yield <sup>b</sup>        | ee <sup>b</sup> | Yield <sup>c</sup> | ee <sup>c</sup> |
| Water, 4 °C         | 1.06g<br>(72%)                | 94% (R) | 1.21g<br>(66%)            | 81% (+)         | 0.153g<br>(32%)    | 57% (+)         |
| 10% MeCN,<br>4 °C   | 1.25g<br>(85%)                | 95% (R) | 1.45g<br>(79%)            | 82% (+)         | 0.401g<br>(83%)    | 68% (+)         |
| 30% MeOH,<br>-18 °C | -                             | -       | 1.56g<br>(85%)            | 93% (+)         | -                  | -               |

Conditions: 0.15 mM Cu(dmbipy), 1 mM st-DNA in basepairs, 20 mM MOPS pH 6.5, 3d, 333 ml; <sup>a</sup> 40 eq. **5**, 1g **4d**, 1d; <sup>b</sup> 5 eq 5-methoxyindole, 1g **4a**, 1d; <sup>c</sup> 5 eq **8**, 300 mg **4d** in total volume of 100ml, 6d.

The yields were higher when organic co-solvents were used, albeit that in these cases slightly lower ee were observed compared to the reactions at small scale. When this reaction was carried out with 30% v/v MeOH at -18 °C, **9a** was obtained in an excellent isolated yield of 85% with 93% ee, which is significantly higher than what was obtained for this reaction with Cu(dmbipy)/st-DNA in water alone to date.<sup>13</sup>

### 3.7 Conclusions

Water-miscible organic co-solvents can be used in DNA-based asymmetric catalytic Diels-Alder, Michael addition and Friedel-Crafts alkylation reactions at appreciable concentrations without negatively affecting the ee. Whereas in the Diels-Alder reaction organic co-solvents are tolerated, but at the expense of the reaction rate, in the Michael addition and Friedel-Crafts alkylation in some cases a positive effect on reactivity was observed. It was found that this is not the result of the actual conjugate addition reaction going faster, but is most likely the result of a faster dissociation of the product. An exception was found for enones containing a large alkyl moiety. In these cases higher conversions were obtained in the absence of co-solvents.

Furthermore, by using organic co-solvents these DNA-based catalytic reactions can be performed at synthetically relevant scales, that is, gram scale in 333 ml solvent and also at lower temperatures and low catalysts loadings, resulting in the products being obtained in good isolated yields and excellent ee's. Considering the fact that the costs of salmon testes DNA used in these experiments are comparable to that of commonly used chiral ligands and that protective atmospheres are not required, a bright future for application of the DNA-based asymmetric catalysis concept in organic synthesis is envisioned.

### 3.8 Experimental section

#### General remarks

Salmon testes DNA was obtained from Sigma. Indoles were obtained from Aldrich. Copper complexes<sup>12</sup>, Azachalcone (**1a-d**)<sup>3</sup>, 2-acyl imidazole **4a-d**<sup>24</sup> and **4e**<sup>26</sup> were synthesized according to literature procedures. Cyclopentadiene was prepared freshly from its dimer. <sup>1</sup>H-NMR and <sup>13</sup>C-NMR were recorded on a Varian 400 (400 MHz and 100 MHz, respectively). Chemical shifts ( $\delta$ ) are quoted in ppm using residual solvent as internal standard ( $\delta_{\text{H}}$  7.26 and  $\delta_{\text{C}}$  77.0 for CDCl<sub>3</sub>). CD-spectra were measured on a JASCO J-715 spectropolarimeter, with a temperature control attachment. The UV-VIS spectra were measured on a JASCO v-560 or a JASCO v-570 with a temperature control attachment. Enantiomeric excess determination was performed by HPLC analysis using a chiral stationary phase on a Shimadzu 10AD-VP system.

#### DNA-based catalysis, representative procedure<sup>6,12,13</sup>

A buffered solution (20 mM MOPS, pH 6.5) of DNA bound catalyst (1 mM salmon testes DNA in basepairs and 0.15 mM [Cu(dmbipy)(NO<sub>3</sub>)<sub>2</sub>]) was prepared by mixing a solution of salmon testes DNA (5 ml of a 2 mg/ml solution in 30 mM MOPS, prepared 24 h in advance) with an aqueous solution of catalyst (5 ml of a 0.45 mM solution of [Cu(dmbipy)(NO<sub>3</sub>)<sub>2</sub>] in 30 mM MOPS pH 6.5) and adding water and/or organic solvent to a total volume of 15 ml. 15  $\mu$ mol of substrate in 10  $\mu$ L MeCN was added and the mixture was cooled to <5 °C. The reaction was started by addition of the appropriate amount of reactant (Diels-Alder 15 eq. **2**; Michael addition 100 eq. **5**; Friedel-Crafts reaction 5 eq. **8**) and mixed by continuous inversion for the indicated time, followed by extraction of the product with Et<sub>2</sub>O, drying (Na<sub>2</sub>SO<sub>4</sub>) and removal of the solvent. The crude product was analyzed by <sup>1</sup>H-NMR and HPLC.

### Large scale reaction, representative procedure

A buffered solution (20 mM MOPS, pH 6.5) of DNA bound catalyst (1 mM st-DNA salmon testes DNA in basepairs and 0.15 mM [Cu(dmbipy)(NO<sub>3</sub>)<sub>2</sub>]) was prepared by mixing a solution of salmon testes DNA (111 ml of a 2 mg/ml solution in 30 mM MOPS pH 6.5, prepared 48 h in advance) with an aqueous solution of catalyst (111 ml of a 0.45 mM solution of [Cu(dmbipy)(NO<sub>3</sub>)<sub>2</sub>] in 30 mM MOPS) and adding water and/or organic solvent up to a total volume of 333 ml. To this was added 1 g of enone (**4a** or **e**). After addition of reactant (40 eq. **5** for Michael addition; 5 eq. **8** for Friedel-Crafts alkylation) at <5°C, the reaction was mixed for 1 days by continuous inversion at 4°C. The product was isolated by extraction with Et<sub>2</sub>O. After drying (Na<sub>2</sub>SO<sub>4</sub>) and removal of the solvent the crude product was further purified by column chromatography (SiO<sub>2</sub>, EtOAc/pentane 2:3) and analyzed by NMR and HPLC.

HPLC conditions (Michael addition): Daicel chiralcel-AD, heptane/iPrOH 90:10, 0.5 ml/min. Retention times: 29.8 and 34.1 min. (**7e**), 24.0 and 29.3 min. (**9**)

HPLC conditions (Friedel-Crafts alkylation): Daicel chiralcel-AD, heptane/iPrOH 90:10, 0.5 ml/min. Retention times: 32.8 and 39.4 min.

### Determination of binding constant (K<sub>b</sub>)

Equilibrium binding constants to salmon testes DNA were determined by UV/Vis titration, following the procedure of Meehan.<sup>26</sup> After dissolution of salmon testes DNA (2 mg/ml), the stock solution was dialyzed extensively against Mops buffer (20 mM pH 6.5) prior to use. The concentration in base pairs was determined spectrophotometrically, using ε<sub>260</sub> = 12800 M<sup>-1</sup> cm<sup>-1</sup>. The absorbance ratio of λ<sub>260</sub>/λ<sub>280</sub> was 1.8-1.9, indicating the DNA was sufficiently free of protein. The K<sub>b</sub> was determined by titration of DNA to a solution of copper complex in buffered solution. Concentrations of copper complex was 30 μM. Under conditions where the ratio of bound complex : DNA base pairs approaches zero, the K<sub>b</sub> can be determined using :

$$\frac{D}{\Delta\epsilon_{ap}} = \frac{1}{\Delta\epsilon} D + \frac{1}{\Delta\epsilon K_b}$$

where Δε<sub>ap</sub> = |ε<sub>a</sub> - ε<sub>f</sub>|, Δε = |ε<sub>b</sub> - ε<sub>f</sub>|, ε<sub>a</sub>, ε<sub>f</sub> and ε<sub>b</sub> are the apparent, free and bound extinction coefficients for the complex, respectively, and D is the DNA concentration in base pairs. In a plot of D/Δε<sub>ap</sub> vs. D, K<sub>b</sub> is given by the ratio of the slope to the y intercept.

### Determination of k<sub>app</sub> (Diels-Alder reaction)

The procedures to determine k<sub>app</sub> were adapted from Engberts et al.<sup>21</sup> A 2.0 μL portion of a fresh solution of azachalcone **1a** (1.0 mg/mL in MeCN) was added to a 0.15 mM [Cu(dmbipy)(NO<sub>3</sub>)<sub>2</sub>], 1.0 mM of salmon testes DNA in base pairs in buffer (20 mM MOPS, pH 6.5) in a quartz cuvette. After the absorption stabilized, 1-10 μL of a freshly prepared cyclopentadiene solution in MeCN was added, resulting in a final concentration of 0.5-2.0 mM. The cuvette was closed immediately and sealed tightly to prevent evaporation of cyclopentadiene. The reaction was monitored at 326 nm, at the appropriate temperature, on a JASCO V-560 or a JASCO V-570 spectrophotometer. The decrease in absorption of **1a** was followed for the first 15% of the reaction, and the following expression was used to calculate k<sub>app</sub>:

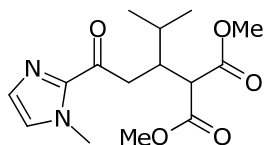
$$k_{app} = \frac{dA_1}{dt} \cdot \frac{1}{d \cdot (\epsilon_1 - \epsilon_3) \cdot [1]_0 \cdot [2]_0}$$

in which ε<sub>1</sub> and ε<sub>3</sub> are the extinction coefficients of **1a** and **3a**, respectively, and d is the path length of the cuvette. The observed rate constants were determined at different concentrations of **2**, after which the k<sub>app</sub> was extracted from the slope of the resulting plot. Thus, reactions other than the reaction of **1a** with **2** were excluded.

### Determination of k<sub>app</sub> (Friedel-Crafts reaction)

The measurements were performed as described earlier.<sup>16</sup> The samples contained 0.15 mM of [Cu(dmbipy)(NO<sub>3</sub>)<sub>2</sub>], 1.0 mM of salmon testes DNA in base pairs, 14 μM of **4a**, and 0.5 - 2.0 mM of 5-methoxy indole, with a total volume of 1.0 mL in 20 mM MOPS-buffered

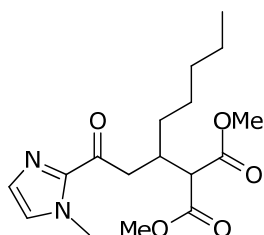
water at pH 6.5. The decrease of absorption at 265 nm was followed in time until the reaction was complete. Pseudo-first-order rate constants were obtained using a fitting program. The rate constants were plotted versus the concentration indole, and the  $k_{app}$  was subsequently determined from the slope of this graph.



**Dimethyl 2-(4-methyl-1-(1-methyl-1H-imidazol-2-yl)-1-oxopentan-3-yl)malonate (7b)**

A colorless oil was obtained after column chromatography ( $\text{SiO}_2$ , EtOAc/Heptane 4:6).  $^1\text{H}$  NMR (400 MHz,  $\text{CDCl}_3$ )  $\delta$  7.16 (d,  $J = 5.0$  Hz, 1H), 7.02 (d,  $J = 14.5$  Hz, 1H), 3.75 (s, 3H), 3.74, (s, 3H), 3.73 (m, 4H), 3.65 (d,  $J = 42.2$ , 1H), 3.40 (dd,  $J = 10.2$ , 1.7 Hz, 2H), 3.24 – 3.14 (m, 1H), 0.90 (m, 6H).  $^{13}\text{C}$  (101 MHz,  $\text{CDCl}_3$ ) 192.6, 168.7, 168.0, 143.3, 129.2, 128.7, 54.5, 53.8, 44.6, 37.9, 36.1, 33.9, 30.3, 21.0, 18.6. HRMS:  $m/z$ : 310.1525 (Calcd. 310.1529).

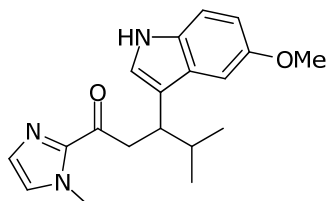
Ee's were determined by HPLC analysis (Chiralcel-AD, heptane/*i*PrOH 98:2, 0.5 mL/min). Retention times: 44.9 and 55.0 mins.



**Dimethyl 2-(1-(1-methyl-1H-imidazol-2-yl)-1-oxooctan-3-yl)malonate (7c)**

A slightly yellow oil was obtained after column chromatography ( $\text{SiO}_2$ , EtOAc/Heptane 4:6).  $^1\text{H}$  NMR (300 MHz,  $\text{CDCl}_3$ )  $\delta$  7.12 (m, 1H), 7.02 (m, 1H), 4.13 – 3.88 (m, 6H), 3.88 – 3.54 (m, 5H), 3.40 – 3.01 (m, 4H), 1.90 – 1.01 (m, 6H), 1.01 – 0.52 (m, 3H).  $^{13}\text{C}$  (101 MHz,  $\text{CDCl}_3$ ) 192.7, 167.1, 167.0, 129.2, 127.4, 60.5, 52.7, 52.6, 47.3, 41.3, 40.7, 37.3, 32.0, 25.4, 22.8, 14.2. HRMS:  $m/z$ : 338.1835 (Calcd. 338.1842).

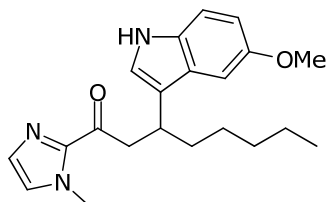
Ee's were determined by HPLC analysis (Chiralcel-ODH, heptane/*i*PrOH 90:10, 0.5mL/min). Retention times: 23.9 and 26.0 mins.



**3-(5-methoxy-1H-indol-3-yl)-4-methyl-1-(1-methyl-1H-imidazol-2-yl)pentan-1-one (9b)**

A yellow oil was obtained after column chromatography ( $\text{SiO}_2$ , EtOAc/Heptane 1:1).  $^1\text{H}$  NMR (400 MHz,  $\text{CDCl}_3$ )  $\delta$  8.02 (s, 1H), 7.16 (d,  $J = 8.7$  Hz, 1H), 7.13 (s, 1H), 7.02 (d,  $J = 13.3$  Hz, 2H), 6.93 (s, 1H), 6.79 (d,  $J = 8.8$  Hz, 1H), 3.84 (s, 3H), 3.76 (s, 3H), 3.63 (dd,  $J = 25.2$ , 11.2 Hz, 2H), 3.44 (dd,  $J = 14.4$ , 3.8 Hz, 1H), 2.09 (dt,  $J = 12.8$ , 6.3 Hz, 1H), 1.74 (s, 1H), 0.94 (t,  $J = 7.4$  Hz, 6H).  $^{13}\text{C}$  (101 MHz,  $\text{CDCl}_3$ )  $\delta$  192.8, 153.9, 131.4, 129.0, 128.9, 126.9, 122.8, 118.1, 112.0, 111.7, 101.6, 56.2, 56.1, 42.1, 38.6, 33.1, 20.7, 20.5. HRMS:  $m/z$ : 325.1782 (Calcd. 325.1790).

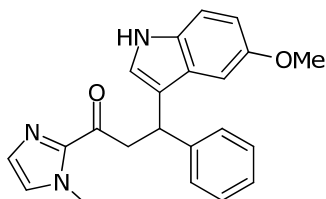
Ee's were determined by HPLC analysis (Chiralcel-AD, heptane/*i*PrOH 98:2, 0.5 mL/min). Retention times: 26.6 and 34.0 mins.



**3-(5-methoxy-1H-indol-3-yl)-1-(1-methyl-1H-imidazol-2-yl)octan-1-one (9c)**

A colorless oil was obtained after column chromatography ( $\text{SiO}_2$ , EtOAc/Heptane 1:1).  $^1\text{H}$  NMR (400 MHz,  $\text{CDCl}_3$ )  $\delta$  7.88 (br, 1H), 7.20 (d,  $J = 7.7$  Hz, 1H), 7.12 (s, 1H), 7.05 (d,  $J = 18.9$  Hz, 2H), 6.96 (s, 1H), 6.81 (d,  $J = 8.7$  Hz, 1H), 3.86 (s, 3H), 3.85 (s, 3H), 3.72 – 3.61 (m, 2H), 3.57 – 3.44 (m, 1H), 1.86 – 1.68 (m, 2H), 1.45 – 1.06 (m, 6H), 1.04 – 0.65 (m, 3H).  $^{13}\text{C}$  (50 MHz,  $\text{CDCl}_3$ ) 192.4, 153.7, 131.3, 128.8, 127.4, 126.7, 121.8, 111.9, 111.6, 105.0, 101.2, 55.9, 45.5, 36.1, 36.0, 32.4, 31.9, 27.2, 22.6, 14.1. HRMS:  $m/z$ : 353.4983 (Calcd. 353.4580).

Ee's were determined by HPLC analysis (Chiralcel-ODH, heptane/*i*PrOH 90:10, 0.5 mL/min). Retention times: 26.6 and 34.5 mins.



**3-(5-methoxy-1H-indol-3-yl)-1-(1-methyl-1H-imidazol-2-yl)-3-phenylpropan-1-one (9e)**

A brownish oil was obtained after column chromatography (SiO<sub>2</sub>, EtOAc/Heptane 1:1). <sup>1</sup>H NMR (400 MHz, CDCl<sub>3</sub>) δ 8.09 (s, 1H), 7.83 (d, J = 16.2 Hz, 1H), 7.70 (s, 2H), 7.40 – 7.01 (m, 5H), 6.87 (d, J = 8.5 Hz, 1H), 6.49 (s, 1H), 4.11 (s, 3H), 3.92–3.85 (m, 2H), 3.86 (s, 3H), 3.76 (m, 1H). <sup>13</sup>C (50 MHz, CDCl<sub>3</sub>) 192.6, 142.5, 129.2, 128.2, 127.8, 127.7, 127.1, 126.2, 123.8, 121.5, 111.3, 110.6, 103.6, 101.3, 59.5, 54.8, 37.9, 28.6. HRMS: m/z: 359.1639 (Calcd. 359.1634).

Ee's were determined by HPLC analysis (Chiralcel-AD, heptane/iPrOH 80:20, 0.5 mL/min). Retention times: 19.0 and 26.8 mins.

### 3.9 References

1. U. M. Lindstrom, *Organic reactions in Water: Principles, Strategies and Applications*, Blackwell, Oxford, **2007**.
2. B. Cornils, W. A. Herrmann, *Aqueous-Phase Organometallic Catalysis*, Wiley-VCH, Weinheim, **1998**.
3. S. Otto, J. Engberts, *J. Am. Chem. Soc.* **1999**, *121*, 6798.
4. S. Narayan, J. Muldoon, M. G. Finn, V. V. Fokin, H. C. Kolb, K. B. Sharpless, *Angew. Chem. Int. Ed.* **2005**, *44*, 3275.
5. A. Chanda, V. V. Fokin, *Chem. Rev.* **2009**, *109*, 725.
6. D. Coquière, B. L. Feringa, G. Roelfes, *Angew. Chem. Int. Ed.* **2007**, *46*, 9308.
7. D. Glick, *Methods of Biochemical Analysis*, Wiley-Liss **1985**, 61.
8. M. M. Rozenman, M. W. Kanan, D. R. Liu, *J. Am. Chem. Soc.* **2007**, *129*, 14933.
9. M. M. Rozenman, D. R. Liu, *ChemBiochem* **2006**, *7*, 253.
10. G. J. Sun, J. M. Fan, Z. Y. Wang, Y. F. Li, *Synlett* **2008**, 2491.
11. J. M. Fan, G. J. Sun, C. F. Wan, Z. Y. Wang, Y. F. Li, *Chem. Commun.* **2008**, 3792.
12. G. Roelfes, A. J. Boersma, B. L. Feringa, *Chem. Commun.* **2006**, 635.
13. A. J. Boersma, B. L. Feringa, G. Roelfes, *Angew. Chem. Int. Ed.* **2009**, *48*, 3346.
14. T. Rovis, D. A. Evans, *Progress in Inorganic Chemistry*, Vol. 50 **2001**, *50*, 1.
15. F. Rosati, A. J. Boersma, J. E. Klijn, A. Meetsma, B. L. Feringa, G. Roelfes, *Chem. Eur. J.* **2009**, *15*, 9596.
16. A. J. Boersma, J. E. Klijn, B. L. Feringa, G. Roelfes, *J. Am. Chem. Soc.* **2008**, *130*, 11783.
17. T. A. Eggelte, H. D. Koning, H. O. Huisman, *Tetrahedron* **1973**, *29*, 2491.
18. D. C. Rideout, R. Breslow, *J. Am. Chem. Soc.* **1980**, *102*, 7816.
19. W. Blokzijl, M. J. Blandamer, J. B. F. N. Engberts, *J. Am. Chem. Soc.* **1991**, *113*, 4241.
20. T. Rispens, J. Engberts, *J. Phys. Org. Chem.* **2005**, *18*, 725.
21. S. Otto, F. Bertoncin, J. B. F. N. Engberts, *J. Am. Chem. Soc.* **1996**, *118*, 7702.
22. E. W. Dijk, A. J. Boersma, B. L. Feringa, G. Roelfes, *Org. Biomol. Chem.* **2010**, *17*, 3868.

23. D. H. Davies, J. Hall, E. H. Smith, *J. Chem. Soc. Perkin Trans. 1* **1991**, 2691.
24. D. A. Evans, K. R. Fandrick, H. J. Song, *J. Am. Chem. Soc.* **2005**, 127, 8942.
25. M. C. Myers, A. R. Bharadwaj, B. C. Milgram, K. A. Scheidt, *J. Am. Chem. Soc.* **2005**, 127, 14675.
26. A. Wolfe, G. H. Shimer, T. Meehan, *Biochemistry* **1987**, 26, 6392.





# Chapter 4

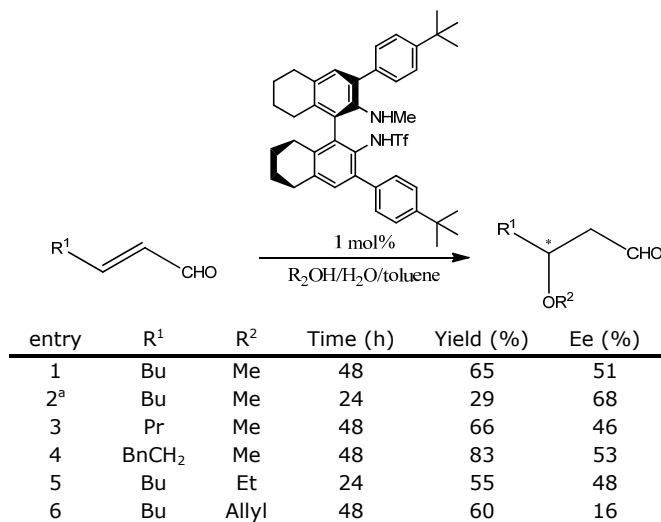
## DNA-Based Catalytic Enantioselective Intermolecular Oxa-Michael Addition Reactions

*DNA-based asymmetric catalysis has been used for a wide variety of reactions in water (chapter 1); furthermore, it has been described in chapter 3 that organic co-solvents can be used in combination with DNA-based catalysis. However some of these co-solvents can also be used as reactant. In this chapter a novel Cu(II)-catalyzed enantioselective oxa-Michael addition of alcohols to enones using the DNA-based catalysis concept is described. Enantioselectivities of up to 86% can be obtained. The presence of water proved to be important for the reactivity, possibly by reverting unwanted side reactions such as 1,2-additions.*

Parts of this chapter have been published: R.P. Megens, G. Roelfes, *Chem. Commun.*, **2012**, 48, 6366.

## 4.1 Introduction

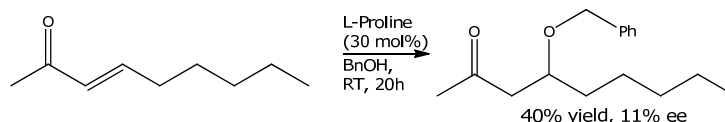
The catalytic enantioselective conjugate addition of alcohols, also known as the oxa-Michael reaction, is a reaction of great potential in organic synthesis.<sup>1,2</sup> Yet, the development of this reaction, and in particular the intermolecular variant, has been complicated by the inherently low reactivity of most alcohols in such reactions and the fact that the conjugate addition step is generally reversible. As a result, reports about catalytic enantioselective intermolecular oxa-Michael reactions of simple achiral alcohols to enones, are scarce.<sup>1,2</sup> Most examples either involve intramolecular oxa-Michael additions,<sup>3-7</sup> or make use of alcohol analogues.<sup>8-11</sup> One of the few examples of such reactions is the organocatalytic oxa-Michael addition developed by Maruoka (Scheme 4.1).<sup>12</sup> A chiral octahydrobinol based diamine is used to catalyze the asymmetric addition of alcohols to  $\alpha,\beta$ -unsaturated aldehydes. The reaction required water, probably for the hydrolysis of the intermediate iminium species, in the absence of water the reaction was significantly slower. By the addition of toluene, which was added to solubilize the catalyst, the yield of the reaction was significantly improved, however at the expense of the enantioselectivity (Entry 1 and 2). A variety of substrates and alcohols were used giving the product with moderate enantioselectivities (Entry 3-6).



Conditions:  $\alpha,\beta$ -unsaturated aldehydes 0.25 mmol, 1 mol% catalyst in MeOH (950  $\mu$ l), H<sub>2</sub>O (50  $\mu$ l) and toluene (100  $\mu$ l). a; without toluene.

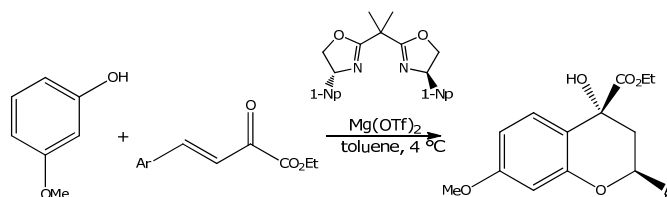
**Scheme 4.1.** Organocatalytic oxa-Michael addition of alcohols to  $\alpha,\beta$ -unsaturated aldehydes.

The only other example is an isolated case of a proline catalyzed oxa-Michael addition of benzylalcohol to an  $\alpha,\beta$ -unsaturated ketone.<sup>13</sup> The oxa-Michael addition product was obtained in 40% yield and only 11% ee (Scheme 4.2).



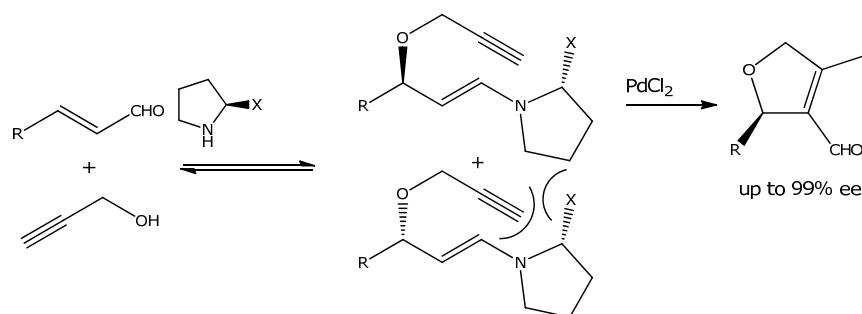
**Scheme 4.2.** Proline catalyzed oxa-Michael addition of benzylalcohol to an  $\alpha,\beta$ -unsaturated ketone.

The intermolecular oxa-Michael addition has also been reported as the first step of an enantioselective tandem reaction. In both published cases a subsequent reaction was used to push the unfavorable equilibrium of the C-O bond formation by a follow up reaction of the product.<sup>14,15</sup> The first example is an oxa-Michael addition of phenol to an  $\beta,\gamma$ -unsaturated  $\alpha$ -ketoester followed by a Friedel-Crafts alkylation catalyzed by a bisoxazoline-Mg(OTf)<sub>2</sub> complex. After optimization of the reaction conditions diastereometrically pure chromans could be obtained with reasonable yields and up to 81% ee (Scheme 4.3).<sup>15</sup>



**Scheme 4.3.** Oxa-Michael addition followed by Friedel-Crafts alkylation of phenol to  $\beta,\gamma$ -unsaturated  $\alpha$ -ketoesters.

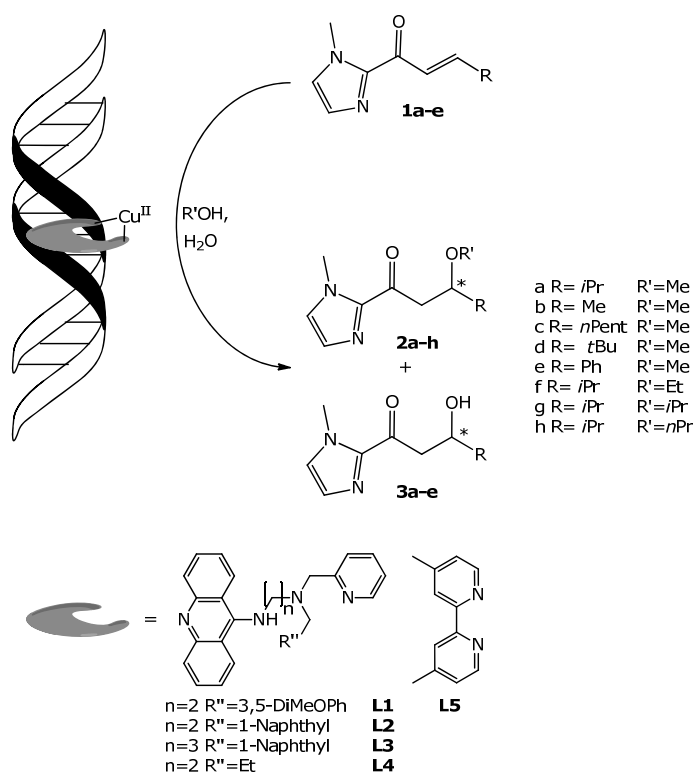
The second and last example comes from the group of Córdova, who developed a dynamic kinetic asymmetric domino oxa-Michael/carbocyclization catalyzed by a combination of a transition-metal and a proline derivative (Scheme 4.4).<sup>14</sup> By combining these catalysts substituted furans could be synthesized with excellent enantioselectivities. It is thought that the enantioselectivity in this domino reaction originates from the carbocyclization since one of the enantiomers would react faster. However, the enantioselectivity of the oxa-Michael reaction itself has not been determined because the reaction without palladium gave only trace amounts of the oxa-Michael product.



**Scheme 4.4.** Dynamic kinetic asymmetric domino oxa-Michael/carbocyclization cascade reaction.

## 4.2 DNA-based catalytic enantioselective intermolecular oxa-Michael addition reactions

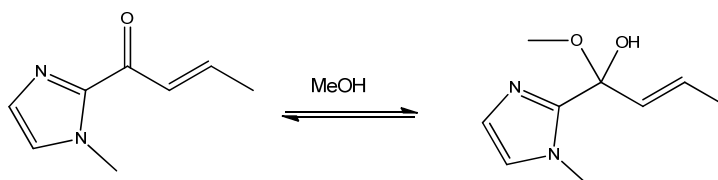
Recently, DNA-based catalysis was used to achieve the first catalytic enantioselective *syn*-hydration of enones.<sup>16</sup> This remarkable reaction, which has no equivalent in homogeneous catalysis, demonstrated the power of the DNA-based catalysis concept and suggested the possibility of achieving enantioselective intermolecular oxa-Michael addition reaction of alcohols to enones. In this study, as a benchmark reaction the addition of methanol to  $\alpha,\beta$ -unsaturated 2-acyl imidazole **1a** was investigated (Figure 4.1).



**Figure 4.1.** DNA-based catalytic enantioselective intermolecular oxa-Michael addition reaction in water.

Since the DNA-based catalyst requires aqueous conditions, first the optimal water/methanol mixture was investigated in the reaction catalyzed by  $\text{Cu}(\text{NO}_3)_2$  in the absence of DNA. Interestingly, it was observed that the highest yield of the methanol addition product **2a** was obtained when the catalyzed reaction was performed in a 50:50 water/methanol mixture; further increasing the fraction of methanol led to a lower yield of **2a** (Figure 4.2). This surprising observation suggests that water plays an important role in the reaction, possibly by reverting unwanted side reactions such as 1,2-additions of the alcohol, which

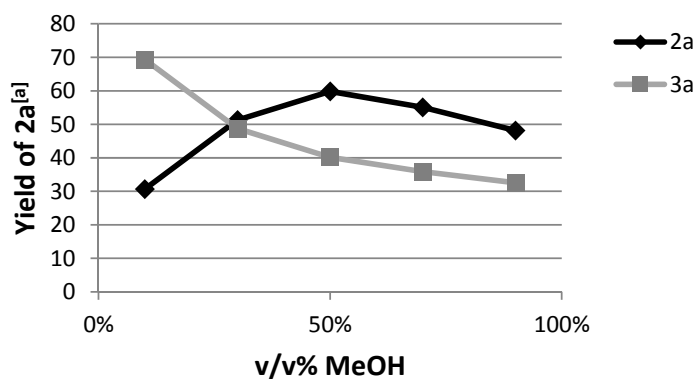
would give rise to (hemi-)acetals (Scheme 4.5). For the DNA-based reactions 40% v/v methanol was selected, since it was found before that this methanol content can be used without causing precipitation of DNA (chapter 3).



**Scheme 4.5.** 1,2-addition of alcohol.

#### 4.2.1 Optimization of conditions of DNA-based catalysis

The pH and MeOH contents were varied in order to find the best conditions for the enantioselectivity and conversion (Table 4.1). In the optimization pH 6.5 was found to be the pH at which the highest ee's could be obtained with high yields.



**Figure 4.2.** Conversion towards oxa-Michael product as function of methanol content. a; Determined by  $^1\text{H-NMR}$ . Conditions: 0.15 mM  $[\text{Cu}(\text{NO}_3)_2 \cdot 3 \text{H}_2\text{O}]$ , 20 mM MOPS pH 6.5, 1 mM **1a**, RT, 1d.

Next, bidentate nitrogen ligands **L1-L5** were evaluated in the catalytic reaction in the presence of salmon testes DNA (st-DNA) at pH 6.5. In addition to the methanol addition product **2a**, ~30 % of the hydration product **3a** was obtained as a side-product, with ee's similar to the methanol addition product. The highest enantioselectivities for the methanol addition product **2a** were achieved with the ligands **L1** and **L2**: 64 and 57 % ee, respectively (Table 4.2). This trend is consistent with what was observed before in the catalytic hydration reaction.<sup>16</sup> Since also the highest conversions of **1a** were obtained with **L1**, this ligand was selected for further study.

**Table 4.1.** Screening of reaction conditions.

| 20 mM MES pH 5.5  |       |                  |              |              |
|-------------------|-------|------------------|--------------|--------------|
| MeOH (v/v%)       | Conv. | Ratio <b>2/3</b> | ee <b>2a</b> | ee <b>3a</b> |
| 10%               | Full  | 24/76            | 55%          | 57%          |
| 20%               | Full  | 41/59            | 56%          | 58%          |
| 30%               | Full  | 43/57            | 49%          | 54%          |
| 40%               | Full  | 45/55            | 49%          | 53%          |
| 20 mM MOPS pH 6.5 |       |                  |              |              |
| MeOH (v/v%)       | Conv. | Ratio <b>2/3</b> | ee <b>2a</b> | ee <b>3a</b> |
| 10%               | 80%   | 26/74            | 49%          | 53%          |
| 20%               | 86%   | 41/59            | 50%          | 55%          |
| 30%               | 83%   | 50/50            | 53%          | 57%          |
| 40%               | 83%   | 59/41            | 64%          | 66%          |
| 20 mM MOPS pH 7.5 |       |                  |              |              |
| MeOH (v/v%)       | Conv. | Ratio <b>2/3</b> | ee <b>2a</b> | ee <b>3a</b> |
| 10%               | 50%   | 40/60            | 27%          | 43%          |
| 20%               | 52%   | 60/40            | 42%          | 52%          |
| 30%               | 55%   | 64/36            | 42%          | 52%          |
| 40%               | 61%   | 60/40            | 42%          | 52%          |

General conditions: 0.66 mg/ml st-DNA, 1 mM **1a**, 0.15 mM Cu(NO<sub>3</sub>)<sub>2</sub>, 0.165 mM **L1**, 4 °C, 1d.

**Table 4.2.** Screening of ligands.

| Entry | Ligand    | Time | Conv. | Ratio <b>2/3</b> | Ee <b>2</b> | Ee <b>3</b> |
|-------|-----------|------|-------|------------------|-------------|-------------|
| 1     | <b>L1</b> | 4h   | 82%   | 59/41            | 64%         | 66%         |
| 2     | <b>L2</b> | 1d   | 69%   | 70/30            | 57%         | 59%         |
| 3     | <b>L3</b> | 1d   | 34%   | 58/42            | 4%          | 21%         |
| 4     | <b>L4</b> | 1d   | 26%   | 62/38            | 13%         | 46%         |
| 5a    | <b>L5</b> | 1d   | 28%   | 54/46            | -5%         | 5%          |

Conditions: 0.66 mg/ml st-DNA, 20 mM MOPS pH 6.5, 0.165 mM **L**, 0.15 mM Cu(NO<sub>3</sub>)<sub>2</sub>, 1 mM **1a**, 40 v/v% MeOH, 4 °C. a; 0.15 mM Cu(dmbipy)(NO<sub>3</sub>)<sub>2</sub>. All conversions and enantioselectivities are the average of triplicate experiments; all values are reproducible within +/- 2%.

#### 4.2.2 Substrate scope

Using Cu-**L1**/st-DNA and the optimized conditions, the substrate scope of the reaction was investigated. It was found that the maximum conversion of the enone and the ratio of **2/3** decreased with increasing

steric bulk of the substituent R at the  $\beta$  position (Table 4.3). The opposite trend was observed for the ee of **2**, namely, an increase in enantioselectivity upon going from R= methyl (24% ee, Entry 3) to R= *t*-butyl (81% ee; Entry 7). In case of R= phenyl, no conversion was observed. Most likely, the addition to this highly conjugated substrate is thermodynamically unfavorable.

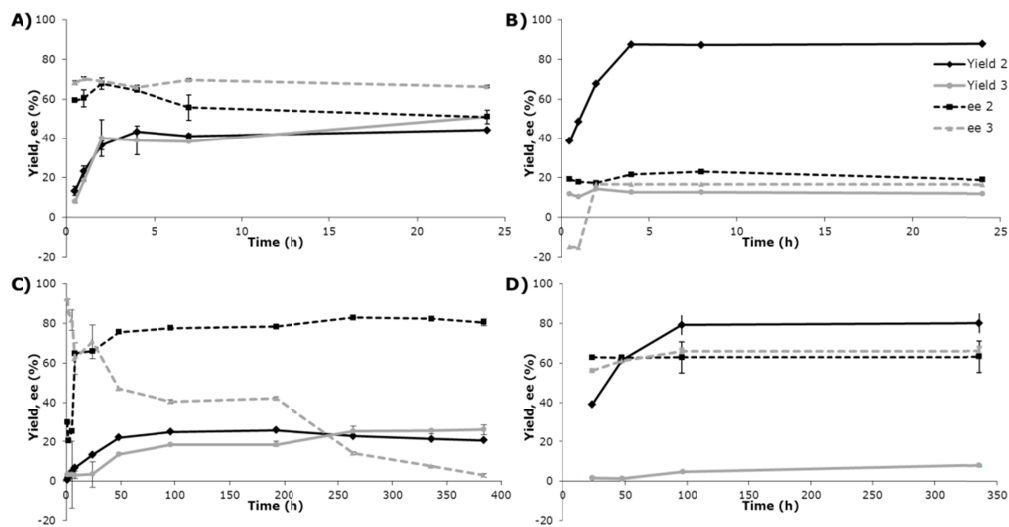
**Table 4.3.** Substrate scope.

| Entry          | Substrate | Time | Conv. | Product   | Ratio <b>2/3</b> | ee <b>2</b> | ee <b>3</b> |
|----------------|-----------|------|-------|-----------|------------------|-------------|-------------|
| 1              | <b>1a</b> | 4h   | 82%   | <b>2a</b> | 59/41            | 64%         | 66%         |
| 2 <sup>a</sup> | <b>1a</b> | 4d   | 85%   | <b>2a</b> | 94/6             | 63%         | 66%         |
| 3              | <b>1b</b> | 4h   | Full  | <b>2b</b> | 87/13            | 24%         | 17%         |
| 4 <sup>a</sup> | <b>1b</b> | 1d   | Full  | <b>2b</b> | 99/1             | 25%         | n.d.        |
| 5              | <b>1c</b> | 1d   | 76%   | <b>2c</b> | 76/24            | 35%         | 51%         |
| 6 <sup>a</sup> | <b>1c</b> | 1d   | 70%   | <b>2c</b> | 93/7             | 58%         | 82%         |
| 7              | <b>1d</b> | 4d   | 43%   | <b>2d</b> | 58/42            | 81%         | 40% (R)     |
| 8 <sup>a</sup> | <b>1d</b> | 7d   | 21%   | <b>2d</b> | 63/37            | 83%         | 85%         |
| 9              | <b>1e</b> | 1d   | -     | <b>2e</b> | -                | nd.         | nd.         |

Conditions: 0.66 mg/ml st-DNA, 20 mM MOPS pH 6.5, 0.165 mM **L1**, 0.15 mM Cu(NO<sub>3</sub>)<sub>2</sub>, 1 mM substrate, 40 v/v% MeOH, 4 °C. a; Reaction performed at -18 °C. All conversions, product **2/3** ratios and enantioselectivities are the average of at least duplicate experiments; all values are reproducible within  $\pm 2\%$ .

The reaction of **1a–d** with methanol was also performed at -18 °C, which is possible due to the high methanol content in the reaction mixture (Chapter 3). This resulted in a similar ee of the alcohol addition products, with exception of **2c** for which the ee increased from 35% to 58%. Interestingly, at -18 °C, the hydration side reaction was suppressed. The ratio **2/3** was increased moderately in the case of **1d** (Entry 8), but almost complete selectivity towards the alcohol addition product **2** was found for **1a–c** (Entries **2**, **4**, and **6**). Apparently, the rate of the hydration reaction depends much stronger on temperature than the alcohol addition reaction. Hence, even though the requirement for aqueous conditions causes the formation of a side product resulting from hydration of the enone, the reaction can be made chemoselective by lowering the reaction temperature.

Several of these reactions were followed in time (Figure 4.3). In contrast to the hydration product **3**, which in several cases racemizes in time,<sup>16</sup> the ee of the alcohol addition product **2** was found to be constant over time; no significant racemization occurred in the time investigated.<sup>17</sup>



**Figure 4.3.** Time profile for the reaction of A; **1a**, B; **1b**, C; **1d**, D; **1a** at  $-18^{\circ}\text{C}$ .

#### 4.2.3 Nucleophile scope.

The nucleophile scope was examined by using various alcohols. (Table 4.4). It was found that the reaction rate decreased dramatically with increasing steric bulk of the alcohol. As a consequence also the ratio of **2/3** decreased. A clear illustration for this are the results obtained for the addition of *i*PrOH to **1a**: after 16 days 60% of conversion of **1a** was achieved, of which only a minor fraction, i.e. 7%, was towards the alcohol addition product **2g** (Entry 3). This indicates that *i*-propanol is too large to attack the  $\beta$  position of the enone and the hydration reaction becomes dominant. The highest ee for the alcohol addition was obtained using *n*-propanol, that is, 86% (Entry 4).

**Table 4.4.** Nucleophile scope.

| Entry    | R'OH          | Time | Conv. | Product   | Ratio <b>2/3</b> | Ee <b>2</b> | Ee <b>3</b> |
|----------|---------------|------|-------|-----------|------------------|-------------|-------------|
| <b>1</b> | MeOH          | 4h   | 82%   | <b>2a</b> | 59/41            | 64%         | 66%         |
| <b>2</b> | EtOH          | 11d  | 74%   | <b>2f</b> | 51/49            | 52%         | 28%         |
| <b>3</b> | <i>i</i> PrOH | 16d  | 60%   | <b>2g</b> | 7/93             | 57%         | 36%         |
| <b>4</b> | <i>n</i> PrOH | 11d  | 65%   | <b>2h</b> | 32/68            | 86%         | 36%         |

Conditions: 0.66 mg/ml st-DNA, 20 mM MOPS pH 6.5, 0.165 mM **L1**, 0.15 mM  $\text{Cu}(\text{NO}_3)_2$ , 1 mM **1a**, 40% v/v R'OH,  $4^{\circ}\text{C}$ . All conversions and enantioselectivities are the average of triplicate experiments; all values are reproducible within  $\pm 2\%$ .

A preliminary study of the DNA sequence dependence of the oxa-Michael addition, using self-complementary oligonucleotides as catalyst scaffold, showed that sequences containing a central AT segment give



rise to higher ee's than GC rich sequences (Table 4.5), a pattern that was also observed for the hydration reaction. However, the ee's obtained are lower than what is obtained with salmon testes DNA. This indicates that the optimal DNA sequence has most likely not been found to date. However, it can also not be excluded that the high methanol content of the reaction mixture affects the structure of small duplex DNAs and, hence, the enantioselectivity of the catalyzed reaction.<sup>18</sup> The decrease of stability of the duplexes in the presence of MeOH is obvious from the lowering of the melting temperature ( $T_m$ ).

**Table 4.5.** DNA-sequence dependence.

| Sequence     | $T_m$<br>(water) | $T_m$<br>(40 v/v% MeOH) | Conv. | Ratio<br><b>2/3</b> | ee<br><b>2a</b> | ee<br><b>3a</b> |
|--------------|------------------|-------------------------|-------|---------------------|-----------------|-----------------|
| TCAGGGCCCTGA | 41 °C            | 31 °C                   | 68%   | 50/50               | 19%             | 25%             |
| GCGCGCGCGCGC | 50 °C            | 33 °C                   | 71%   | 58/42               | 14%             | 31%             |
| GCGCTATAGCGC | 32 °C            | 21 °C                   | 85%   | 53/47               | 36%             | 40%             |
| CAAAAATTTTGG | 21 °C            | 13 °C                   | 82%   | 40/60               | 43%             | 39%             |

Conditions: DNA (1 mM in bp), 20 mM MOPS pH 6.5, 0.165 mM **L1**, 0.15 mM Cu(NO<sub>3</sub>)<sub>2</sub>, 1 mM **1a**, 40% v/v MeOH, 4 °C, 1d.

### 4.3 Conclusions

In conclusion, using the DNA-based catalysis concept, we have achieved the catalytic enantioselective intermolecular oxa-Michael addition reactions of simple achiral alcohols to enones mediated by a transition metal complex. Up to 81% ee was achieved for the addition of methanol to enones and up to 86% ee could be obtained when using *n*-propanol as nucleophile. These ee values represent the highest enantioselectivities achieved for the catalytic asymmetric intermolecular oxa-Michael addition reaction to date.

### 4.4 Experimental section

#### General remarks

Salmon testes DNA was obtained from Sigma. Ligands **L1-4** and 2-acyl imidazole substrates were synthesized according to published procedures<sup>16,19</sup> Enantiomeric excess determination was performed by HPLC analysis on a Shimadzu 10AD-VP system. <sup>1</sup>H-NMR and <sup>13</sup>C-NMR were recorded on a Varian 400, at 400 MHz and 100 MHz, respectively. Chemical shifts ( $\delta$ ) are quoted in ppm using residual solvent as internal standard ( $\delta$ H 7.26 and  $\delta$ C 77.0 for CDCl<sub>3</sub>). Mass spectra were recorded on a LTQ ORBITRAP XL.

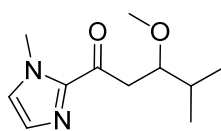
#### Catalytic Oxa-Michael addition, representative procedure

A buffered solution (20 mM Mops, pH 6.5) of DNA bound catalyst (0.67 mg/ml salmon testes DNA, 0.165 mM **L1** and 0.15 mM Cu(NO<sub>3</sub>)<sub>2</sub>) was prepared by mixing a solution of salmon testes DNA (5 ml of a 2 mg/ml solution in 60 mM MOPS, prepared 24 h in advance) with an aqueous solution of catalyst (2.5 ml of a 0.90 mM solution of Cu(NO<sub>3</sub>)<sub>2</sub> and 0.99 mM **L1** in water) and adding water and alcohol to a total volume of 15 ml. The mixture was cooled to 4 °C and 15  $\mu$ mol of enone dissolved in 10  $\mu$ L MeCN was added. The

reaction was mixed by continuous inversion at 4 °C, followed by extraction of the product with Et<sub>2</sub>O. After drying (Na<sub>2</sub>SO<sub>4</sub>) and removal of the solvent the crude product was analyzed by <sup>1</sup>H-NMR and HPLC using a chiral stationary phase. Reaction was followed in time by taking samples at specific time points and analyzing them by NMR and HPLC

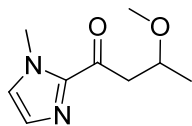
#### Oxa-Michael addition general synthesis of racemates

A buffered solution (20 mM MOPS, pH 6.5) containing 40% alcohol and 0.15 mM [Cu(NO<sub>3</sub>)<sub>2</sub>]<sub>3</sub> H<sub>2</sub>O was prepared. To this mixture 15 μmol of enone dissolved in 10 μL MeCN was added. The reaction was mixed by continuous inversion at RT, followed by extraction of the product with Et<sub>2</sub>O. After drying (Na<sub>2</sub>SO<sub>4</sub>) and removal of the solvent the crude product was purified by column chromatography (EtOAc/heptanes 1:4).



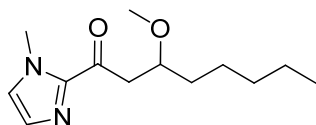
#### 3-Methoxy-4-methyl-1-(1-methyl-1H-imidazol-2-yl)pentan-1-one (2a)

After column chromatography the product was obtained as a slightly yellow oil. <sup>1</sup>H NMR (400 MHz, CDCl<sub>3</sub>) δ 7.14 (s, 1H), 7.02 (s, 1H), 3.99 (s, 3H), 3.70 (dt, *J* = 8.4, 4.2, 1H), 3.41 (dd, *J* = 16.4, 8.4, 1H), 3.32 (s, 3H), 3.07 (dd, *J* = 16.3, 3.7, 1H), 1.95 (dq, *J* = 6.7, 1.9, 1H), 0.93 (dd, *J* = 6.8, 1.7, 6H). <sup>13</sup>C NMR (101 MHz, CDCl<sub>3</sub>) δ 191.52, 143.10, 128.74, 126.90, 81.82, 57.59, 40.48, 36.27, 30.71, 18.08, 17.54. HRMS: *m/z*: 211.14377 (M+1), (Calcd. 211.14410; M+1)



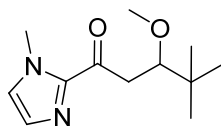
#### 3-Methoxy-1-(1-methyl-1H-imidazol-2-yl)butan-1-one (2b)

After column chromatography the product was obtained as a slightly yellow oil. <sup>1</sup>H -NMR (400 MHz, CDCl<sub>3</sub>) δ 7.12 (d, *J* = 0.8, 1H), 7.01 (s, 1H), 3.99 (s, 3H), 3.99 (dd, *J* = 18.0, 5.3, 1H), 3.48 (dd, *J* = 15.7, 7.5, 1H), 3.32 (s, 3H), 3.05 (dd, *J* = 15.7, 5.3, 1H), 1.24 (d, *J* = 6.2, 3H). <sup>13</sup>C- NMR (75 MHz, CDCl<sub>3</sub>) 191.17, 143.87, 129.28, 127.21, 73.60, 56.35, 46.07, 36.38, 19.63. HRMS: *m/z*: 183.11288 (M+1), (Calcd. 183.11280; M+1)



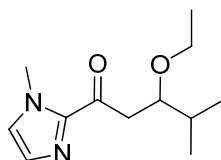
#### 3-Methoxy-1-(1-methyl-1H-imidazol-2-yl)octan-1-one (2c)

After column chromatography the product was obtained as a slightly yellow oil. <sup>1</sup>H NMR (400 MHz, CDCl<sub>3</sub>) δ 7.13 (s, 1H), 7.01 (s, 1H), 4.00 (s, 3H), 3.85 (tt, *J* = 9.8, 4.8, 1H), 3.46 (dd, *J* = 16.0, 7.5, 1H), 3.33 (s, 3H), 3.10 (dd, *J* = 16.0, 4.9, 1H), 1.68 - 1.47 (m, 2H), 1.46 - 1.32 (m, 2H), 1.47 - 1.20 (m, 6H), 0.87 (t, *J* = 6.9, 1H). <sup>13</sup>C NMR (101 MHz, CDCl<sub>3</sub>) δ 191.27, 143.24, 129.03, 126.92, 77.29, 56.61, 43.60, 36.15, 33.94, 31.90, 24.82, 22.58, 14.00. HRMS: *m/z*: 239.17589 (M+1), (Calcd. 239.17540; M+1)



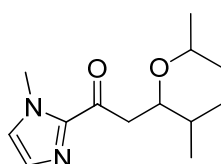
#### 3-Methoxy-4,4-dimethyl-1-(1-methyl-1H-imidazol-2-yl)pentan-1-one (2d)

After column chromatography the product was obtained as a slightly yellow oil. <sup>1</sup>H NMR (400 MHz, CDCl<sub>3</sub>) δ 7.14 (s, 1H), 7.02 (s, 1H), 4.00 (s, 3H), 3.56 (dd, *J* = 8.1, 3.3, 1H), 3.37 (dd, *J* = 16.8, 8.1, 1H), 3.35 (s, 3H), 3.18 (dd, *J* = 16.8, 3.3, 1H), 0.94 (s, 9H). <sup>13</sup>C NMR (101 MHz, CDCl<sub>3</sub>) δ 192.10, 143.29, 129.07, 126.89, 85.17, 59.93, 40.81, 36.20, 35.70, 26.04. HRMS: *m/z*: 225.15983 (M+1), (Calcd. 225.15975; M+1)



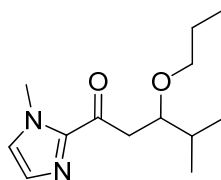
### 3-Ethoxy-4-methyl-1-(1-methyl-1H-imidazol-2-yl)pentan-1-one (2f)

After column chromatography the product was obtained as a slightly yellow oil.  $^1\text{H}$  NMR (400 MHz,  $\text{CDCl}_3$ )  $\delta$  7.13 (s, 1H), 7.01 (s, 1H), 3.99 (s, 3H), 3.78 (dt,  $J = 8.0, 4.6$ , 1H), 3.50 (q,  $J = 7.0$ , 2H), 3.37 (dd,  $J = 16.1, 7.8$ , 1H), 3.12 (dd,  $J = 16.1, 4.1$ , 1H), 1.91 (h,  $J = 6.5$ , 1H), 1.09 (t,  $J = 7.0$ , 3H), 0.95 (d,  $J = 6.8$ , 6H).  $^{13}\text{C}$  NMR (101 MHz,  $\text{CDCl}_3$ )  $\delta = 191.84, 143.12, 129.00, 126.76, 80.31, 65.22, 41.21, 36.14, 31.60, 18.14, 17.98, 15.52$ . HRMS:  $m/z$ : 183.11288 (M+1), (Calcd. 183.11280; M+1)



### 3-Isopropoxy-4-methyl-1-(1-methyl-1H-imidazol-2-yl)pentan-1-one (2g)

After column chromatography the product was obtained as a slightly yellow oil.  $^1\text{H}$  NMR (400 MHz,  $\text{CDCl}_3$ )  $\delta$  7.13 (d,  $J = 4.9$  Hz, 1H), 7.00 (d,  $J = 6.7$  Hz, 1H), 3.99 (s, 3H), 3.93 (t,  $J = 5.9$  Hz, 1H), 3.80 (m, 1H), 3.67 (m, 1H), 3.55 (dd,  $J = 15.5, 5.9$  Hz, 1H), 3.06 (dd,  $J = 15.4, 6.0$  Hz, 1H), 1.12 (d,  $J = 6.1$  Hz, 3H), 1.03 (d,  $J = 6.1$  Hz, 3H), 0.99 (d,  $J = 6.1$  Hz, 3H), 0.81 (d,  $J = 6.1$  Hz, 3H).  $^{13}\text{C}$  NMR (101 MHz,  $\text{CDCl}_3$ )  $\delta$  192.1, 128.8, 126.4, 80.0, 71.0, 63.4, 40.8, 36.1, 24.1, 23.1, 22.2, 20.1. C2-imidazole signal is missing. HRMS:  $m/z$ : 239.17602 (M+1), (Calcd. 239.17531; M+1)




### 4-Methyl-1-(1-methyl-1H-imidazol-2-yl)-3-propoxy-pentan-1-one (2h)

After column chromatography the product was obtained as a slightly yellow oil.  $^1\text{H}$  NMR (400 MHz,  $\text{CDCl}_3$ )  $\delta$  7.13 (d,  $J = 0.8$  Hz, 1H), 7.00 (s, 1H), 3.99 (s, 3H), 3.85 – 3.69 (m, 1H), 3.42 – 3.33 (m, 3H), 3.09 (dd,  $J = 16.0, 4.2$  Hz, 1H), 1.92 (dtd,  $J = 13.6, 6.8$  Hz, 5.0, 1H), 1.47 (q,  $J = 6.8$  Hz, 2H), 0.94 (d,  $J = 6.9$  Hz, 6H), 0.82 (t,  $J = 7.4$  Hz, 3H).  $^{13}\text{C}$  NMR (101 MHz,  $\text{CDCl}_3$ )  $\delta$  191.8, 143.4, 129.0, 126.8, 80.3, 65.2, 41.2, 36.2, 31.60, 18.1, 18.0, 15.5. HRMS:  $m/z$ : 239.17602 (M+1), (Calcd. 239.17595; M+1)

## 4.5 References

1. C. F. Nising, S. Bräse, *Chem. Soc. Rev.* **2012**, *41*, 988.
2. C. F. Nising, S. Bräse, *Chem. Soc. Rev.* **2008**, *37*, 1218.
3. L. Wang, X. Liu, Z. Dong, X. Fu, X. Feng, *Angew. Chem. Int. Ed.* **2008**, *47*, 8670.
4. M. M. Biddle, M. Lin, K. A. Scheidt, *J. Am. Chem. Soc.* **2007**, *129*, 3830.
5. C. Dittmer, G. Raabe, L. Hintermann, *Eur. J. Org. Chem.* **2007**, *35*, 5886.
6. E. Sekino, T. Kumamoto, T. Tanaka, T. Ikeda, T. Ishikawa, *J. Org. Chem.* **2004**, *69*, 2760.
7. Q. Gu, Z. Q. Rong, C. Zheng, S. L. You, *J. Am. Chem. Soc.* **2010**, *132*, 4056.
8. C. D. Vanderwal, E. N. Jacobsen, *J. Am. Chem. Soc.* **2004**, *126*, 14724.
9. X. Zhang, S. Zhang, W. Wang, *Angew. Chem. Int. Ed.* **2010**, *49*, 1481.
10. S. Bertelsen, P. Diner, R. L. Johansen, K. A. Jørgensen, *J. Am. Chem. Soc.* **2007**, *129*, 1536.

11. C. M. Reisinger, X. Wang, B. List, *Angew. Chem. Int. Ed.* **2008**, *47*, 8112.
12. T. Kano, Y. Tanaka, K. Maruoka, *Tetrahedron* **2007**, *63*, 8658.
13. D. B. Ramachary, R. Mondal, *Tetrahedron Lett.* **2006**, *47*, 7689.
14. S. Lin, G. L. Zhao, L. Deiana, J. Sun, Q. Zhang, H. Leijonmarck, A. Córdova, *Chem. Eur. J.* **2010**, *16*, 13930.
15. H.L. van Lingen, W. Zhuang, T. Hansen, F.P.J.T. Rutjes, K. Jørgensen, *Org. Biomol. Chem.* **2003**, *1*, 1953.
16. A. J. Boersma, D. Coquière, D. Geerdink, F. Rosati, B. L. Feringa, G. Roelfes, *Nature Chem.* **2010**, *2*, 991.
17. In the early stage of the reaction the ee sometimes deviates significantly from the final ee. The reason for this is at present not understood.
18. A. J. Boersma, J. E. Klijn, B. L. Feringa, G. Roelfes, *J. Am. Chem. Soc.* **2008**, *130*, 11783.
19. D. A. Evans, K. R. Fandrick, H. J. Song, *J. Am. Chem. Soc.* **2005**, *127*, 8942.



# **Chapter 5**

## **DNA-Based Catalytic Enantioselective Protonation in Water**

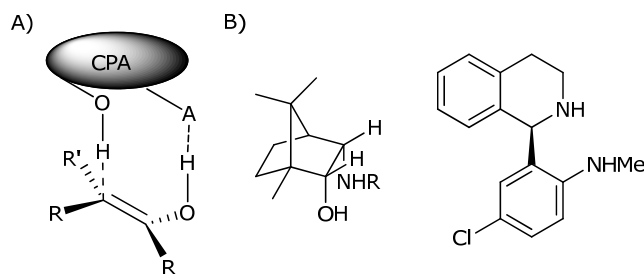
*Enantioselective protonation is an elegant method for introducing chirality in a molecule. In this chapter a new method for enantioselective protonation in water using DNA-based catalysis is described.*

## 5.1 Introduction

Tertiary carbon stereocenters are common in natural products. Therefore, useful and easy methods for the enantioselective synthesis of these compounds are of utmost importance. One of the conceptually most straightforward methods for the selective preparation of compounds with a chiral tertiary carbon is the enantioselective introduction of a proton to a carbanion. However, protonation is difficult to control due to the small size of the proton. Furthermore, protonations are among the most rapid reactions and are often diffusion controlled.<sup>1</sup> Most examples of the enantioselective protonation in the literature involve the asymmetric protonation of metal enolates with chiral protonating agents (CPA's).<sup>1-5</sup> The choice of CPA, acidity of the CPA, E/Z ratio of the substrate and temperature need to be optimized in order to achieve enantioselective protonation with high selectivities. Here, these parameters will be discussed separately and illustrated with examples.

### 5.1.1 Chiral protonating agent

A variety of chiral protonating agents have been reported to induce high enantioselectivities in the asymmetric protonation of a variety of substrates. Especially CPA's consisting of a proton donor combined with a proton acceptor group in a *syn* arrangement have been shown to afford good enantioselectivities.<sup>6</sup> The proton acceptor group can coordinate via hydrogen bonding to the enol and thereby lock the position of the proton donor over the prochiral center (Figure 5.1). This approach can also be applied to a metal-enolate, however, in that case the proton acceptor group should be replaced by a metal binding moiety.



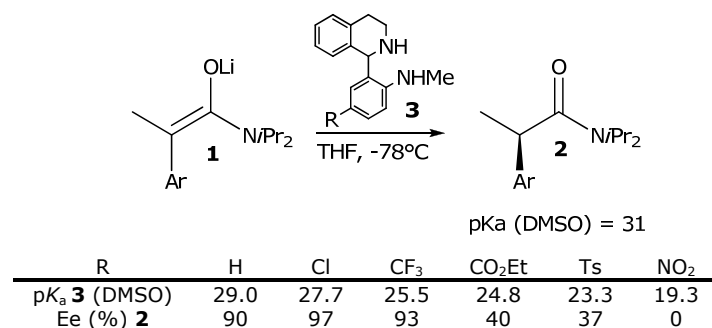
**Figure 5.1.** A; Induction of selectivity in enantioselective protonation, B; examples of CPA's with *syn* oriented donor and acceptor groups.

### 5.1.2 Acidity of the chiral protonating agent

The acidity of the protonating agent should be matched to the product: the protonating agent should be weakly acidic compared to the product. The reason for this is twofold, first of all when the difference of in  $pK_a$  is too large the protonation will proceed fast and the reaction proceeds *a*-selective. Therefore, in order to perform the reaction under kinetic control the  $\Delta pK_a$  needs to be small. On the other hand, the

protonation needs to be as complete as possible, since otherwise it will result in an  $\alpha$ -selective protonation during work-up. In practice, the best enantioselectivities and complete protonation are obtained when  $2 < \Delta pK_a < 4$ .<sup>5</sup>

This has been nicely demonstrated by Vedejs *et al.*,<sup>7</sup> who have investigated the selective protonation of lithium enolate **1** with a series of anilines (**3**) (Scheme 5.1). The best result (ee = 97%) was obtained when  $\Delta pK_a = 3$ , illustrating the importance of the choice of protonating agent.



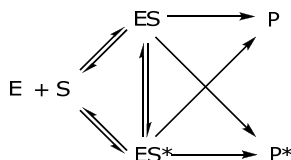
**Scheme 5.1.** Selective protonation of **1** by a series of anilines.

### 5.1.3 Temperature

Most enantioselective protonation reactions occur at low temperatures due to instability of the metal enolate and because in most cases then the enantioselectivity is higher. However, there are a few examples where the enantioselectivity goes through a maximum with increasing temperature. There are two possible explanations for this behavior. Firstly, it can be explained by C- versus O-protonation.<sup>5</sup> This means that at lower temperature the enolate is preferentially protonated on the oxygen. Then the enol is preferentially obtained, which will tautomerize during work-up and thereby cause formation of the racemic product.

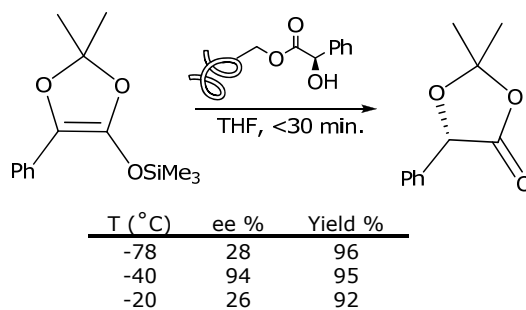
Secondly, it can be explained by the isoinversion principle proposed by Scharf and co-workers.<sup>8</sup> The isoinversion principle is a theoretical model that is designed to explain the selectivity of reactions containing two or more stages. It is a dynamic model, which takes all the reaction components and the optimization into consideration. The general kinetic scheme, which resembles enzyme kinetics, for this model involves a prochiral starting material which can react with a chiral substrate or catalyst to afford two diastereomeric intermediates (ES + ES\*). These intermediates are in equilibrium with each other. These intermediates can then either react further to form P and P\*, or revert back to the starting materials (Scheme 5.2). Since the selectivity is induced in two steps and each step has its own kinetic parameters, inversion points are

expected in the temperature dependent kinetics measurement. The inversion point is called the isoinversion temperature.



**Scheme 5.2.** General kinetics scheme for the isoinversion principle.

This type of kinetics was found in the enantioselective protonation of a silyl enol ether by a polymer supported CPA.<sup>9</sup> The maximum ee was obtained at -40 °C while lower selectivities were found at both higher and lower temperatures. (Scheme 5.3).



**Scheme 5.3.** Selective protonation of **4** by a polymer supported CPA.

## 5.2 Catalytic enantioselective protonation

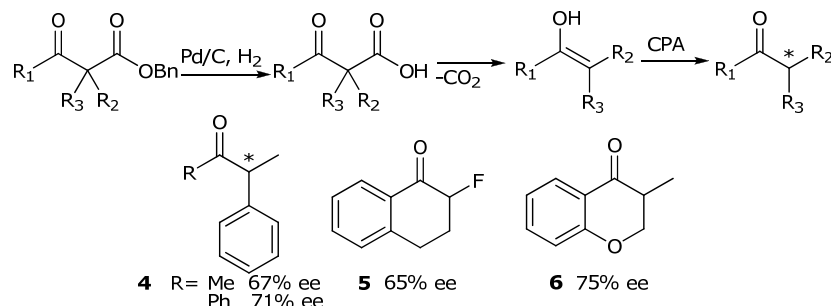
Enantioselective protonation can be performed catalytically via two different routes. First of all, via the regeneration of the chiral protonating agent and secondly, by forming the enolate catalytically.

The chiral protonating agent can be regenerated via different routes. Most examples make use of a preformed silyl enol ether in combination with a chiral Brønsted acid catalyst. After protonation of the silyl enol ether by the chiral Brønsted acid, the Brønsted acid can be regenerated by a proton donor, typically an alcohol.<sup>7,10-15</sup> For the catalytic formation of the enolate various approaches have been followed.

### 5.2.1 Enantioselective protonation via catalytic enolate formation.

Hénin *et al.* performed a catalytic enantioselective protonation via a reaction cascade of deprotection/decarboxylation followed by asymmetric protonation (Scheme 5.4).<sup>16-18</sup>

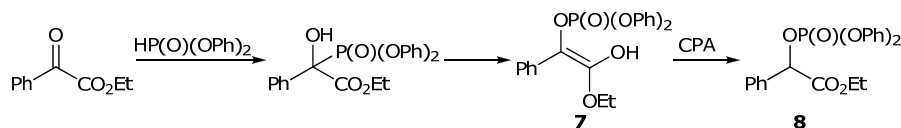




**Scheme 5.4.** Deprotection/decarboxylation enantioselective protonation cascade.

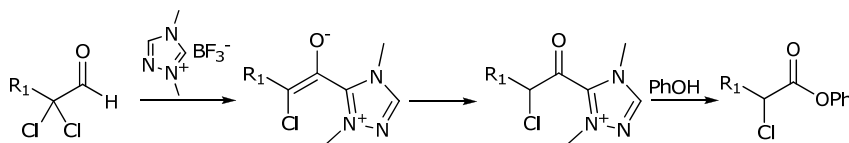
This methodology still requires the use of a chiral protonating agent, for example chiral amino alcohols such as cinchonidine and aminoborneol. However the CPA is regenerated in the course of the reaction by the enol intermediate. The cascade was used to form  $\alpha$ -arylpropanones (**4**)<sup>17</sup>, 2-fluorotetralones (**5**)<sup>18</sup> and 3-methylchromanones (**6**)<sup>16</sup>. It is thought that either the chiral protonating agent coordinates to proton on the enolate or a palladium enolate is formed, which is protonated by the CPA.<sup>17</sup>

An alternative method makes use of a rearrangement reaction to form an enol, the phospho-Brook rearrangement. In this cascade an  $\alpha$ -ketoester is phosphonated which is followed by the rearrangement to form an  $\alpha$ -phosphonyloxy enolate (**7**).<sup>19</sup> This is finally protonated by the chiral protonating agent to form  $\alpha$ -phosphonyloxy ester (**8**) with up to 92% ee (Scheme 5.5).



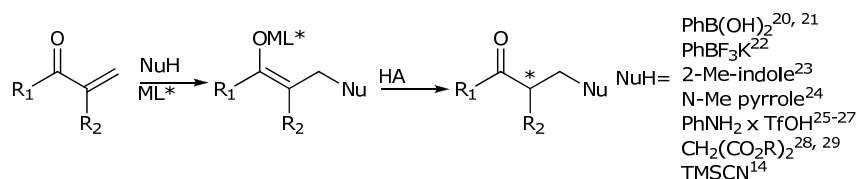
**Scheme 5.5.** Phosphonylation/phospha-Brook rearrangement/ enantioselective protonation cascade.

An alternative method for the formation of the enolate is via the formation of an azolium salt/elimination of HCl followed by selective protonation and substitution of the azolium salt by phenol (Scheme 5.6).<sup>20</sup> By using a chiral azolium salt it was possible to form the  $\alpha$ -chloroester with up to 93% ee, in cases that  $R_1$  is a benzyl- or alkyl group.



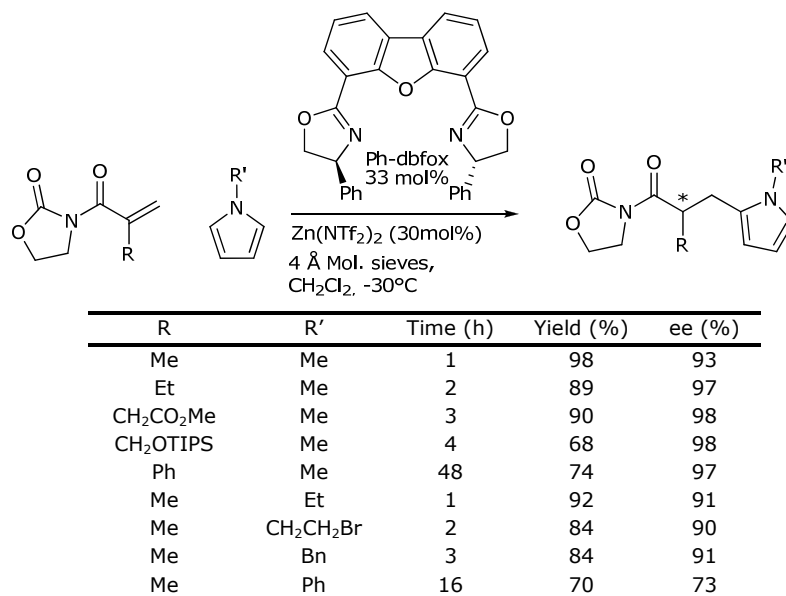
**Scheme 5.6.** Formation of an azolium salt/elimination of HCl followed by selective protonation and acylation with phenol.

Finally, the most often used strategy is formation of the enolate via conjugate additions. Various conjugate addition reactions have been performed in such a cascade process like rhodium catalyzed conjugate addition of organoboron reagents<sup>21-23</sup>, conjugate additions of neutral  $\pi$ -nucleophiles<sup>24,25</sup>, (aza)<sup>26-28</sup> Michael additions<sup>29,30</sup> or cyanation<sup>15</sup> (Scheme 5.7). In all these cases a chiral metal-ligand complex or organocatalyst is used for the induction of the chirality in the enantioselective protonation step. Furthermore, in most cases a proton source is used in stoichiometric amounts to obtain enantioselectivity.



**Scheme 5.7.** Conjugate addition-enantioselective protonation to  $\alpha$ -substituted enones.

One of the key examples involves the Friedel-Crafts alkylation of N-methyl pyrrole with  $\alpha$ -substituted oxazolidinone acrylates, followed by enantioselective protonation of the formed enolate, catalyzed by a chiral Lewis acid complex (Scheme 5.8).<sup>24</sup> Using a combination of a Ph-dbfox ligand in combination with zinc(II) salts at  $-30^\circ\text{C}$  was found to give the product in good yield and excellent enantioselectivity. A wide range of  $\alpha$ -substituents and N-alkyl pyrrole could be used with up to 98% ee.



**Scheme 5.8.** Friedel-Crafts alkylation of  $\alpha$ -substituted oxazolidinone acrylates with N-substituted pyrrole followed by enantioselective protonation of the enolate.

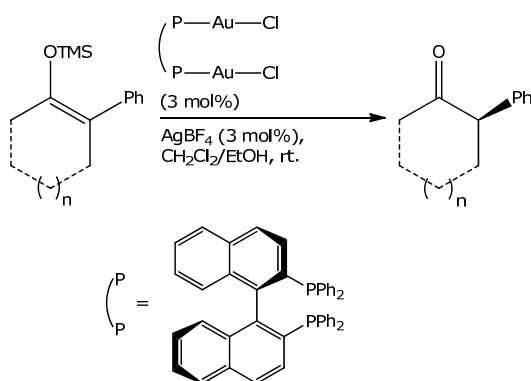
### 5.3 Enantioselective catalytic protonations in protic solvents

One of the major challenges in enantioselective catalytic protonations is the necessity to use stoichiometric amounts of proton donor. The reaction would be facilitated substantially if it could be carried out in a protic solvent, which also acts as the proton donor. However, the use of large amounts of proton donor will result in fast protonation of the enolate and therefore it will be difficult to achieve enantioselectivity.

#### 5.3.1 Transition metal- or organocatalyzed enantioselective protonation in protic solvents

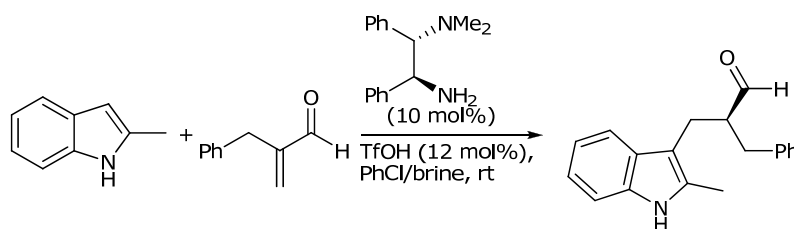
Examples of transition metal- or organocatalyzed enantioselective protonation in pure protic solvents are not known to date. However two examples are known, which use an excess of protic solvent. These strategies make use of positioning of the proton source above the face of the enolate.

The first example is a chiral Brønsted acid derived from a cationic gold(I) complex that is able to catalyze the enantioselective protonation of a silyl enol ether of ketones in a 1:1 mixture of dichloromethane and EtOH.<sup>12</sup> Generation of a cationic gold(I) catalyst with AgBF<sub>4</sub> proved essential, as no reaction was observed without AgBF<sub>4</sub>. Cyclic and acyclic silyl enol ethers were converted with up to 95% ee. Moreover, different mixtures of E/Z isomers afforded the same enantioselectivity. It is thought that the gold derived Lewis acid-activated Brønsted acid (LBA)<sup>12</sup> discriminates between the two isomers and approaches both silyl ethers from the same prochiral face, which results in the high enantioselectivity regardless of the E/Z ratio. However, due to the high substrate content this 1:1 mixture of DCM/EtOH still resembles only 13.7 equivalents of protonating agent. Additionally, this approach requires the generation of the silyl enol ether prior to use.



**Scheme 5.9.** Catalytic enantioselective protonation of silyl enol ethers with a chiral Brønsted acid derived from a cationic gold(I) complex.

The second example involves a Friedel-Crafts alkylation/enantioselective protonation catalyzed by a chiral primary amine (Scheme 5.10).<sup>24</sup> Using a 2:1 mixture of chlorobenzene and brine (50 eq. compared to substrate) resulted in 74% yield and 93% ee. The reaction could also be performed in brine alone, however, in that case the yield dropped to 34% with a small decrease in enantioselectivity. The reaction shows a wide substrate and nucleophile scope, although in many cases only 5 eq. of brine was used in order to obtain good yield and enantioselectivity. Mechanistic studies showed that water most likely is the proton donor in this reaction.

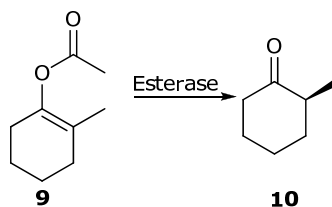


**Scheme 5.10.** Chiral primary amine catalyzed Friedel-Crafts alkylation/enantioselective protonation.

### 5.3.2 Enzymatic enantioselective protonation in protic solvents

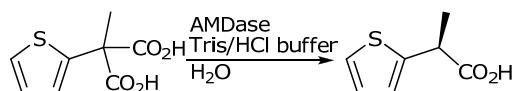
Enzymes are most likely by far the best catalysts for the enantioselective protonation in a protic solvent. Generally, an enzyme contains a hydrophobic and well-defined catalytic pocket in which the proton can be directed via an amino acid or an isolated hydrogen bonded solvent molecule. Several enzymes are able to catalyze the enantioselective protonation reaction in protic solvents. These enzymes can be divided in two general classes, namely, esterases and decarboxylases.

Esterases catalyze the enantioselective protonation reaction from enol acetates via an enolate to yield enantioenriched ketones. Live *Pichia miao* IAM 4682 yeast cells,<sup>31</sup> liverwort *Marchantia polymorpha* esterase I<sup>32</sup> and Lipase PS-C II<sup>33</sup> are able to convert enol acetate **9** into ketone (*S*)-**10** with 99%, 99% and -77% ee, respectively (Scheme 5.11). The yeast cells can also catalyze the enantioselective protonation of larger ring systems, up to 12-membered rings, with high enantioselectivities. The liverwort *Marchantia polymorpha* esterase I can use several different alkyl substituted enol acetates to produce the corresponding ketone with up to 99% ee. However in both cases the facial preference for proton delivery and, hence, which enantiomer is formed in excess, varied for different ring sizes and alkyl substitutions. In the case of Lipase PS-C II the enantioselectivity was highly dependent on the reaction temperature and proton source. The best results were obtained using a solid supported enzyme at 0 °C and EtOH as proton source.



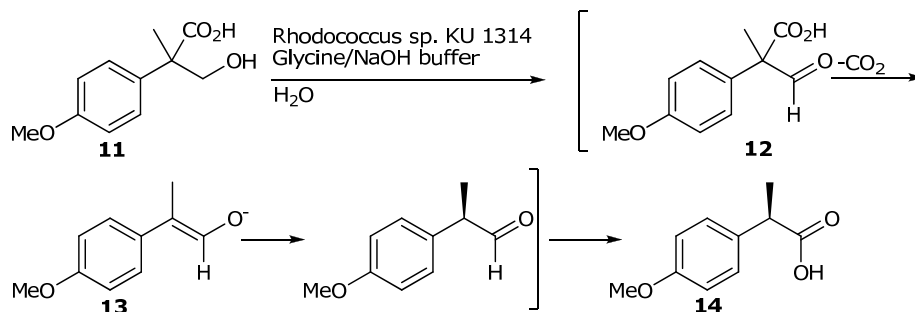
**Scheme 5.11.** Enzymatic hydrolysis followed by enantioselective protonation of enol acetates.

Decarboxylases generate enolates *in situ* by decarboxylation of malonic acid derivatives, which are subsequently protonated to form enantioenriched carboxylic acids. Ohta and co-workers have isolated arylmalonate decarboxylase (AMDase), which catalyzes the decarboxylation of  $\alpha$ -methyl- $\alpha$ -thiophen-2-yl-malonates followed by enantioselective protonation to form  $\alpha$ -thiophen-2-ylpropionic acid in 99% (Scheme 5.12).<sup>34,35</sup> The cysteine residue on position 188 was essential for activity as it is active in the decarboxylation and protonation step. By preparation of the double mutant AMDase G74C/C188S, the opposite enantiomer was obtained. These mutations remove the active site cysteine and place it at the opposite side of the catalytic pocket. Although the opposite enantiomer was obtained in 97% ee, the activity of the enzyme was several orders of magnitude lower.<sup>36,37</sup>



**Scheme 5.12.** Enzymatic decarboxylative protonation with AMDase.

Another example is the conversion of a  $\beta$ -hydroxyacid to  $\alpha$ -arylpropionic acid by *Rhodococcus sp.* KU1314 via an oxidation/decarboxylation/protonation/oxidation cascade.<sup>38</sup> In the proposed metabolic cycle the alcohol **11** is oxidized to the corresponding aldehyde (**12**), which is subsequently decarboxylated to form an enolate (**13**). After enantioselective protonation and oxidation,  $\alpha$ -arylpropionic acid (**14**) was obtained in 74% ee. A variety of larger alkyl substituents could be used, giving rise to moderate enantioselectivities. However, in these cases the activity dropped significantly, indicating that the enzyme is sensitive to steric hindrance.



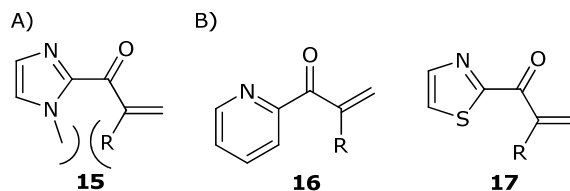
**Scheme 5.13.** Enzymatic oxidation/decarboxylation/protonation/oxidation cascade.

In summary, a few examples of enantioselective protonation in protic solvent are known. However, in the enzymatic protonation the substrate scope is limited due to the tight enzymatic pocket. Moreover, for the transition metal catalyzed protonations a co-solvent is required in order to limit the amount of proton donor. Therefore, a more general method for the enantioselective protonation in protic solvents with a wide substrate scope is desirable. Here, the aim was the development of an enantioselective protonation reaction by using the DNA-based catalysis concept. This would combine the hydrophobic environment, created by the DNA, with a broad substrate scope by using transition metal catalysis.

## 5.4 DNA-based catalytic enantioselective protonation in water

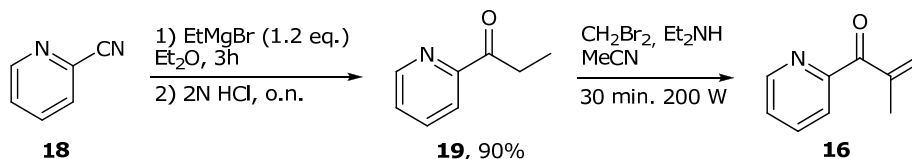
### 5.4.1 Substrate synthesis

$\alpha,\beta$ -Unsaturated 2-acyl imidazoles have been widely used for DNA-based asymmetric catalysis. To date, attention has been focused on the use of  $\beta$ -substituted substrates. However, in order to perform the enantioselective protonation reaction, an  $\alpha$ -substituent is required. It has been shown that  $\alpha$ -substituted  $\alpha,\beta$ -unsaturated 2-acyl imidazoles (**15**) are not reactive in  $\text{Cu}^{\text{II}}$ -catalyzed conjugate additions.<sup>39</sup> This is probably due to steric hindrance between the  $\alpha$ -substituent and the methyl group of the imidazole-moiety (Scheme 5.14A). As a result, the carbonyl group and the olefin are prevented from being co-planar and, therefore, the substrate cannot bind to the  $\text{Cu}^{\text{II}}$ -center in a bidentate fashion and thus the substrate is not activated. For this reason, two new types of substrates were designed. In these substrates, the imidazole moiety is replaced by either a 2-pyridinyl (**16**) or a 2-thiazolyl (**17**) moiety (Scheme 5.14B). These substrates can still coordinate in a bidentate fashion to the  $\text{Cu}^{\text{II}}$  catalyst but the steric hindrance is removed.



**Scheme 5.14.** A;  $\alpha$ -substituted  $\alpha,\beta$ -unsaturated 2-acyl imidazole, B; new  $\alpha$ -substituted  $\alpha,\beta$ -unsaturated substrates.

The  $\alpha$ -substituted  $\alpha,\beta$ -unsaturated 2-acylpyridine (**16**) was synthesized in a two step process starting from 2-cyano pyridine (**18**). The 2-cyano pyridine was reacted with EtMgBr followed by acidic workup to form **19** (Scheme 5.15).<sup>40</sup> This was then  $\alpha$ -methenylated with bromoform in a closed vessel in the microwave to form the  $\alpha,\beta$ -unsaturated substrate (**16**).<sup>41</sup> However, the conditions of the last step gave some problems. First of all, the reaction can only be performed in small scale (up to 100 mg) and, secondly, the reaction is exothermic and difficult to control. Therefore this class of enones was abandoned as substrates.

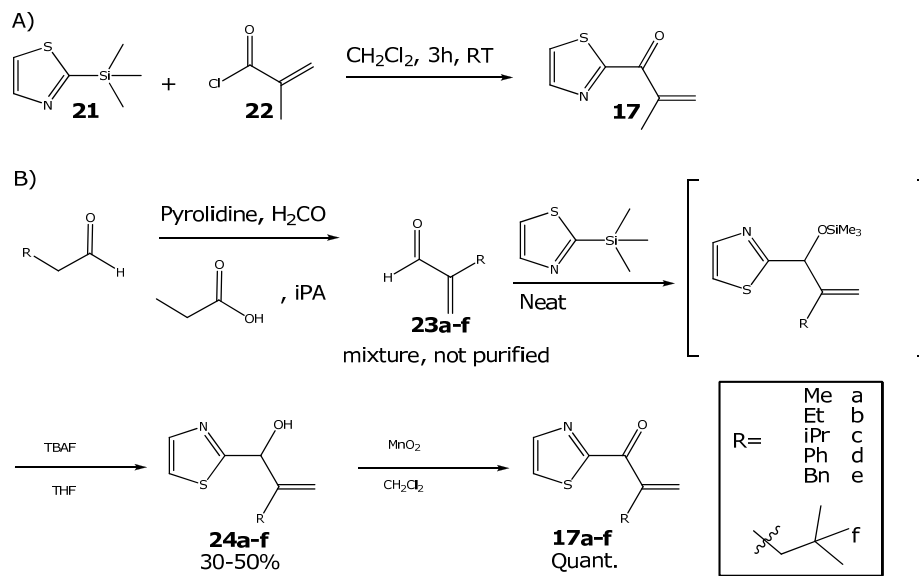


**Scheme 5.15.** Synthesis of  $\alpha,\beta$ -unsaturated pyridine substrate.

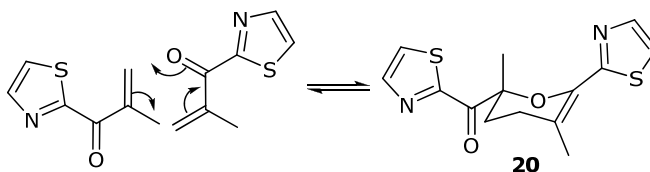
$\alpha,\beta$ -unsaturated acyl 2-thiazole substrate (**17**) was synthesized by the addition of the corresponding  $\alpha,\beta$ -unsaturated acid chloride (**22**) to 2-trimethylsilyl thiazole, the so called Dondoni reagent (**21**; Scheme 5.16A).<sup>42</sup> However, the substrates bearing a terminal alkene are unstable and slowly form dimers (Scheme 5.17), which are the result of an intermolecular Diels-Alder reaction. The structure of the dimer has been confirmed by mass spectrometry, <sup>1</sup>H, <sup>13</sup>C, COSY and HSQC NMR.

The dimer is formed upon storing the enone over an extended period. The problem of dimerization could be overcome by preparation of the enone just before use in catalysis. For that purpose an  $\alpha,\beta$ -unsaturated aldehyde was reacted with the Dondoni reagent (**21**) followed by deprotection of the formed silyl ether with tetrabutylammonium fluoride to yield the allylic alcohol **24** (Scheme 5.16B).<sup>42</sup> This was oxidized with MnO<sub>2</sub>, after which the substrate was used immediately without extensive purifications. Not all  $\alpha$ -substituted  $\alpha,\beta$ -unsaturated aldehydes were commercially available. These were prepared from the corresponding aldehyde and  $\alpha$ -methenylated using formaldehyde with a catalytic amount of propionic acid and pyrrolidine and used without further purification.<sup>43</sup> The exception was 4,4-dimethyl-2-methylenepentanal (**23f**) which was prepared via an iridium-catalyzed

hydroformylation of 3,3-dimethylbutene,<sup>44</sup> followed by the  $\alpha$ -methenylation with formaldehyde



**Scheme 5.16.** Synthesis of  $\alpha,\beta$ -unsaturated 2-thiazole substrates.

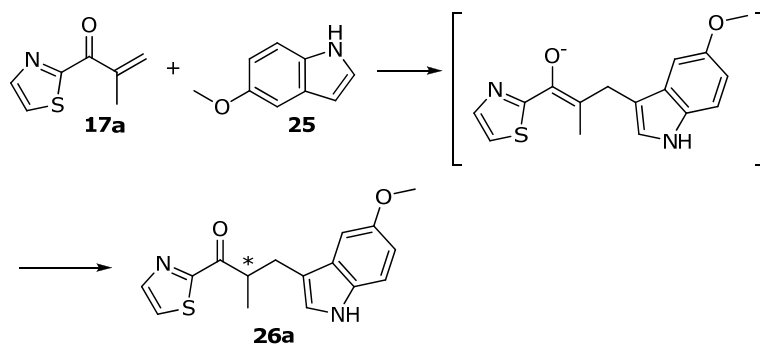


**Scheme 5.17.** Intermolecular Diels-Alder reaction of substrate.

#### 5.4.2 Reaction optimization

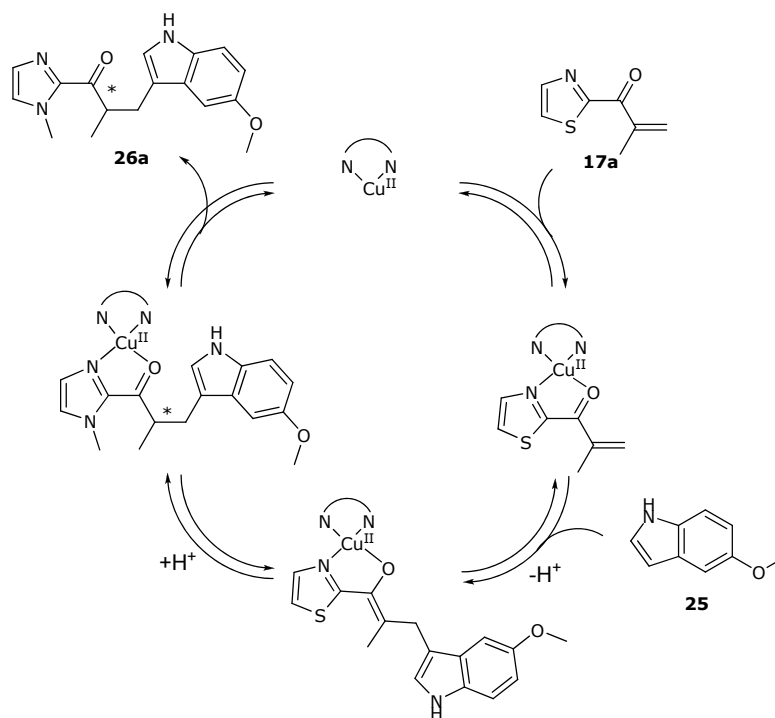
For the selective protonation of  $\alpha$ -substituted  $\alpha,\beta$ -unsaturated thiazoles, the Friedel-Crafts alkylation was chosen, which has been developed in our group.<sup>24,25</sup> This reaction proved to be strongly DNA accelerated. As model reaction for the optimization of the reaction conditions the Friedel-Crafts alkylation of 5-methoxyindole (**25**) with **17a**, followed by the enantioselective protonation of the formed enolate was selected (Scheme 5.18).





**Scheme 5.18.** Friedel-Crafts alkylation followed by selective protonation.

There are several challenges associated with this reaction when using DNA-based catalysis. Firstly, the reaction is performed in water. This implies that the concentration of the protonating agent, *q.* water, is very high. Therefore, a major challenge is to control the protonation step. Secondly, in order to obtain enantioselectivity the protonation needs to be the rate determining step. Therefore, the conjugate addition step needs to be very fast, since protonations are in general quite rapid, especially in water (Scheme 5.19). Additionally, the reaction can also be Brønsted acid catalyzed which will result in a racemate.



**Scheme 5.19.** General reaction mechanism for the Friedel-Crafts alkylation followed by enantioselective protonation.

It was hypothesized that the enantioselective protonation in water using DNA-based catalysis might work because the copper catalyzed reaction takes place in the DNA-environment and since the DNA interior is relatively hydrophobic,<sup>45,46</sup> it provides a hydrophobic environment around the catalyst, thereby reducing the effective concentration of protonating agent. Furthermore, as was mentioned before, the DNA accelerates the Friedel-Crafts alkylation considerably which raised the prospect that the alkylation can be faster than the protonation.

First, the reaction in presence of st-DNA with different indole and catalyst loading was investigated. To our surprise we found reasonable conversion and enantioselectivities in the first attempts. It was found that a ratio of 1:1 of substrate to indole with 15 mol% of Cu-dimethylbipyridine (Cu-dmbipy) gave the best results in terms of enantioselectivity (Table 5.1).

**Table 5.1.** Optimization of reaction conditions.

| ratio<br><b>17a: 25</b> | 15 mol% cat |     | 30 mol% cat |     | 30 mol% cat, no DNA |    |
|-------------------------|-------------|-----|-------------|-----|---------------------|----|
|                         | Conv.       | ee  | Conv.       | ee  | Conv.               | ee |
| 1:1                     | 49%         | 49% | 92%         | 42% | 0%                  | Nd |
| 1:2                     | 74%         | 40% | 88%         | 43% | 12%                 | -  |
| 1:5                     | 54%         | 38% | 90%         | 34% | 71%                 | -  |
| 1:10                    | 55%         | 29% | 79%         | 26% | 98%                 | -  |

Conditions: 20 mM MOPS, pH 6.5, 0.67 mg/ml st-DNA, [Cu(dmbipy)(NO<sub>3</sub>)<sub>2</sub>], 1 mM **17a**, 4 °C, 1h.

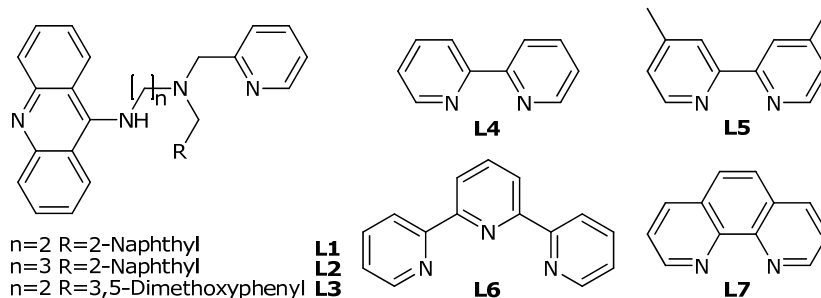
The pH of the buffer was varied in order to make sure that the product is completely protonated but also no Brønsted acid catalysis takes place. It was found that lowering the pH to 5.0 increased the enantioselectivity to 59% (Table 5.2). Although pH 5.0 is slightly below the buffering capacity of MOPS, the pH did not change during the reaction. Lowering the pH requires changing of the buffer to acetate and phosphate buffers, which are weakly copper binding. At this pH a decrease of selectivity was found. There are several possible explanations for this drop in enantioselectivity, 1) the weak binding of the buffer to the active copper complex might interfere with the reaction, 2) due to the lower pH, Brønsted acid catalysis of the conjugate addition starts to play a role in addition to the copper catalyzed reaction or 3) due to the lower pH the protonation step is accelerated thus causing a lower ee.

**Table 5.2.** Optimization of the pH.

| Buffer    | pH  | Conv | ee  |
|-----------|-----|------|-----|
| MOPS      | 7.5 | Full | 11% |
| MOPS      | 6.5 | 98%  | 27% |
| MES       | 5.5 | 87%  | 44% |
| MES       | 5.0 | Full | 59% |
| Phosphate | 4.5 | 86%  | 44% |
| Acetate   | 4.5 | 61%  | 46% |
| Phosphate | 4.0 | 94%  | 48% |
| Acetate   | 4.0 | 55%  | 51% |

Conditions: 20 mM buffer, 0.67 mg/ml DNA, 0.15 mM [Cu(dmbipy)(NO<sub>3</sub>)<sub>2</sub>], 1 mM **17a**, 1mM **25**, 4 °C.

Finally, a variety of ligands was screened for their performance in the enantioselective protonation. First generation ligands (Table 5.3, Entry 1-3) afforded hardly any enantioselectivity. The Cu<sup>II</sup> complex of 4,4'-dimethyl-2,2'-bipyridine (**L5**), which was also the ligand of choice for the enantioselective Friedel-Crafts alkylation, gave full conversion and 59% ee after 2 hours, whereas other second generation ligands (Entry 4,5 and 6) gave poor enantioselectivities. Combining all these results it was decided that Cu(dmbipy) with a MES buffer at pH 5.0 and 1 equivalent of indole were giving the best results.

**Table 5.3.** Screening of ligands.

| Entry          | Ligand    | conv  | ee   |
|----------------|-----------|-------|------|
| 1 <sup>a</sup> | <b>L1</b> | 57%   | -1%  |
| 2 <sup>a</sup> | <b>L2</b> | 67%   | 16%  |
| 3 <sup>a</sup> | <b>L3</b> | 63%   | -17% |
| 4              | <b>L4</b> | 34%   | 36%  |
| 5              | <b>L5</b> | Full% | 59%  |
| 6              | <b>L6</b> | 73%   | 9%   |
| 7              | <b>L7</b> | 98%   | 11%  |

Conditions: 20 mM MES pH 5.0, 0.67 mg/ml DNA, 0.15 mM [Cu(NO<sub>3</sub>)<sub>2</sub>], 0.15 mM ligand, 1 mM **17a**, 1 mM **25**, 4 °C. a; 0.165 mM ligand.

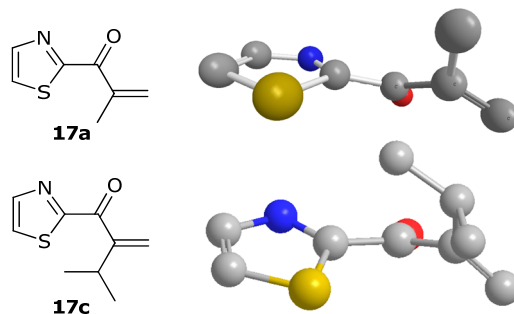
## 5.5 Substrate scope

With the optimal conditions in hand, a range of substrates (**17a-f**) was tested (Table 5.4). Using substrates with linear alkyl chains (**17a** and **b**) resulted in full conversion after 4h, with 59% and 58% ee, respectively. Using more bulky  $\alpha$ -substituents (Entries 4-7; **17c-f**), no conversion was obtained after 4h. After extended reaction time, some conversion could be obtained in case of **17c**. Furthermore, the hetero Diels-Alder product (**20**) was formed in the course of the reactions that did not reach full conversion within 4h. DFT calculations were performed to check whether the thiazole and carboxyl group in these substrates are still co-planar.\* In these calculations the minimal energy structure was determined for **17a** and **17c**. It was found that the dihedral angle between the thiazole and the carbonyl moieties was small for substrates bearing linear alkyl chains ( $22^\circ$ ) while the substrates with more bulky substituents showed a larger dihedral angle of  $46^\circ$  (Figure 5.2A). This geometry does not allow for a bidentate coordination of the substrate to the  $\text{Cu}^{\text{II}}$  center. Therefore, the  $\alpha,\beta$ -unsaturated substrates with bulky substituents in the  $\alpha$  position cannot be activated.

**Table 5.4.** Substrate scope.

| Entry | Substrate                            | Time | Conv | ee  | remarks |
|-------|--------------------------------------|------|------|-----|---------|
| 1     | Me                                   | 2h   | Full | 59% |         |
| 2     | Me <sup>a</sup>                      | 4h   | Full | 50% |         |
| 3     | Et                                   | 4h   | Full | 58% |         |
| 4     | <i>i</i> Pr                          | 3d   | 17%  | 32% | + dimer |
| 5     | Ph                                   | 3d   | 0%   | Nd  | + dimer |
| 6     | Bz                                   | 3d   | 0%   | Nd  |         |
| 7     | $\text{CH}_2\text{C}(\text{CH}_3)_3$ | 3d   | 0%   | Nd  |         |

Conditions: 20 mM MES pH 5.0, 0.67 mg/ml DNA, 0.15 mM  $[\text{Cu}(\text{dmbipy})(\text{NO}_3)_2]$ , 1 mM **17**, 1 mM **25**, 4 °C. a; reaction performed at -18 °C with 40% v/v MeOH.



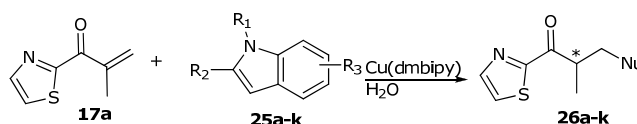
**Figure 5.2.** Substrate conformation calculations performed at the DFT B3-LYP 6-31G(d,p) level.

\* Calculations were performed by Jos Kistemaker.

As has been shown in chapter 3, the addition of a co-solvent allows for a lower reaction temperature. Therefore, the reaction of **17a** with indole **25** has been performed at  $-18\text{ }^{\circ}\text{C}$ . However a lower enantioselectivity was obtained in this case. This can either be caused by the addition of the co-solvent, or the isoinversion effect, as was explained in chapter 5.2.

## 5.6 Nucleophile scope

A large number of nucleophiles for the Friedel-Crafts alkylation (Scheme 5.20) was tested. The enantioselectivity decreased significantly when the electron donating group in the 5-position was removed (Entry 2-4). Furthermore, the enantioselectivity was completely lost when a N- or 2-substituted methylindole was used (Entry 5-7). The nucleophilicity of these indoles (**25b-g**) is lower compared to **25a**.<sup>47</sup> This results in a relatively slower alkylation and therefore the rates of the alkylation step approaches the rate of the protonation step. This will lead to a lower kinetic control over the protonation and thus enantioselectivity. Changing the electron donating group to either a hydroxyl, amino, chloride or bromide did give rise to enantioselectivity (Entry 8-11).



|   | R <sub>1</sub> | R <sub>2</sub> | R <sub>3</sub>    |
|---|----------------|----------------|-------------------|
| a | H              | H              | 5-MeO             |
| b | H              | H              | H                 |
| c | H              | H              | 6-MeO             |
| d | H              | H              | 7-MeO             |
| e | Me             | H              | H                 |
| f | H              | Me             | H                 |
| g | H              | Me             | 5-MeO             |
| h | H              | H              | 5-OH              |
| i | H              | H              | 5-NH <sub>2</sub> |
| j | H              | H              | 5-Cl              |
| k | H              | H              | 5-Br              |

| Entry | Nucleophile | Product    | time | Conv. | ee  |
|-------|-------------|------------|------|-------|-----|
| 1     | <b>25a</b>  | <b>26a</b> | 2h   | Full  | 59% |
| 2     | <b>25b</b>  | <b>26b</b> | 4h   | Full  | 32% |
| 3     | <b>25c</b>  | <b>26c</b> | 1d   | Full  | 11% |
| 4     | <b>25d</b>  | <b>26d</b> | 1d   | Full  | 29% |
| 5     | <b>25e</b>  | <b>26e</b> | 4h   | Full  | 6%  |
| 6     | <b>25f</b>  | <b>26f</b> | 4h   | Full  | 3%  |
| 7     | <b>25g</b>  | <b>26g</b> | 1d   | Full  | 5%  |
| 8     | <b>25h</b>  | <b>26h</b> | 1d   | Full  | 48% |
| 9     | <b>25i</b>  | <b>26i</b> | 1d   | 95%   | 52% |
| 10    | <b>25j</b>  | <b>26j</b> | 1d   | Full  | 27% |
| 11    | <b>25k</b>  | <b>26k</b> | 1d   | Full  | 29% |

Conditions: 20 mM MES pH 5.0, 0.67 mg/ml st-DNA, 0.15 mM [Cu(dmbipy)(NO<sub>3</sub>)<sub>2</sub>], 1 mM **17a**, 1mM **25**,  $4\text{ }^{\circ}\text{C}$ .

**Scheme 5.20.** Nucleophile scope.

More importantly, in the reactions with indoles **25h-k** in the absence of DNA the desired product could not be obtained: only in the presence of DNA the desired product was formed. Additionally, in the reaction with **25i** in the absence of DNA the aza-Michael addition product, from addition of the 5-amino group, was formed. This demonstrates the essential role of DNA in catalysis by causing a large rate acceleration of the rate of the conjugate addition, consistent with previous observations.<sup>48,49</sup>

### 5.7 DNA sequence selectivity

A preliminary study of the DNA sequence dependence of the enantioselective protonation, using various self-complementary oligonucleotides as catalyst scaffold was performed (Table 5.5). The oligonucleotide with a central GGG tract gave similar results compared to st-DNA. However other GC rich sequences and AT rich sequences showed significantly lower enantioselectivities. As is known from previous studies, some DNA sequences accelerate the reaction more than others. However, in the enantioselective protonation two processes are taking place: the Friedel-Crafts alkylation and the enantioselective protonation. Both steps of the process will be affected by the DNA sequence. The rate acceleration of the protonation step needs to be smaller than the rate acceleration of the alkylation step in order to maintain the kinetic control over the protonation step. Hence, the effect of the DNA sequence is not as simple as is found for the Friedel-Crafts alkylation itself. Another possible explanation would be that the sequence containing the central GGG tract is accelerating the reaction to such an extent, that also in st-DNA, this sequence is dominating the outcome of the reaction. In that case it is unlikely that higher ee's can be found by using defined DNA sequences.

**Table 5.5.** Sequence selectivity.

| Sequence     | Conv. | ee  |
|--------------|-------|-----|
| st-DNA       | Full  | 59% |
| TCAGGGCCCTGA | 96%   | 60% |
| GCGCGCGCGCGC | 85%   | 34% |
| CGGGATCCCGA  | 72%   | 17% |
| TCGGGGCCCCGA | Full  | 24% |
| CAAAAATTTTTG | 70%   | 26% |
| GCGCTATAGCGC | 94%   | 10% |

Conditions: 20 mM MES pH 5.0, DNA (1 mM in bp), 0.15 mM [Cu(dmbipy)(NO<sub>3</sub>)<sub>2</sub>], 1 mM **17a**, 1 mM **25**, 4 °C, 2h.

### 5.8 Conclusions

Using the DNA-based catalysis concept, we have developed the first catalytic enantioselective Friedel-Crafts alkylation/protonation cascade

of enones to indoles mediated by transition metal complexes in a protic solvent, *q.* water. Although the substrate scope is limited to enones carrying small substituents on the  $\alpha$ -position, a large variety of indoles can be used with up to 59% ee. This might be related to the hydrophobic environment that the DNA creates around the copper complex. Furthermore, some products can only be obtained in the presence of DNA, illustrating the importance of the DNA acceleration effect.

## 5.9 Experimental section

### General remarks

Salmon testes DNA was obtained from Sigma. Indoles were obtained from Aldrich and TCI Europe. Copper complexes<sup>50</sup>, **16**<sup>41</sup>, **19**<sup>40</sup>, **23f**,<sup>44</sup> and ligands<sup>51</sup> were synthesized according to literature procedures. <sup>1</sup>H-NMR and <sup>13</sup>C-NMR were recorded on a Varian 400 (400 MHz). Chemical shifts ( $\delta$ ) are quoted in ppm using residual solvent as internal standard ( $\delta_{\text{H}}$  7.26 and  $\delta_{\text{C}}$  77.0 for CDCl<sub>3</sub>). Enantiomeric excess determination was performed by HPLC analysis on a Shimadzu 10AD-VP system. Mass spectra were recorded on a LTQ ORBITRAP XL.

### Computational details

The Gaussian 03W (rev. B.03) software package was used for all calculations.<sup>52</sup> The structures (**17a**, **c**) were optimized using the DFT B3-LYP 6-31G(d,p) level. In these calculations only the local minimal energy structure was determined for the structures in which the nitrogen and carbonyl are in cisoid formation. Frequency analysis showed only positive eigenvalues, demonstrating that they are at energy minima.

### DNA-based catalysis, representative procedure

A buffered solution (20 mM MES, pH 5.0) of DNA bound catalyst (1 mM salmon testes DNA in basepairs and 0.15 mM [Cu(dmbipy)(NO<sub>3</sub>)<sub>2</sub>]) was prepared by mixing a solution of salmon testes DNA (5 ml of a 2 mg/ml solution in 60 mM MES pH 5.0, prepared 24 h in advance) with an aqueous solution of catalyst (10 ml of a 0.225 mM solution of [Cu(dmbipy)(NO<sub>3</sub>)<sub>2</sub>] in water). 15  $\mu$ mol of indole in 10  $\mu$ L MeCN was added and the mixture was cooled to 5 °C. The reaction was started by addition of 15  $\mu$ mol of substrate and mixed by continuous inversion for the indicated time, followed by extraction of the product with Et<sub>2</sub>O, drying (Na<sub>2</sub>SO<sub>4</sub>) and removal of the solvent. The crude product was analyzed by <sup>1</sup>H-NMR and HPLC.

### Enantioselective protonation, general synthesis of racemates

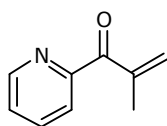
A buffered solution (20 mM MES, pH 5.0) of 0.15 mM [Cu(NO<sub>3</sub>)<sub>2</sub>] $\cdot$ 3 H<sub>2</sub>O and 1 mM of the corresponding indole was prepared. To this mixture 1 mM of enone dissolved in an appropriate amount of MeCN was added. The reaction was mixed by continuous inversion at room temperature, followed by extraction of the product with Et<sub>2</sub>O. After drying (Na<sub>2</sub>SO<sub>4</sub>) and removal of the solvent the crude product was purified by column chromatography (EtOAc/heptane 1:4).

### Reaction of **21** with acrylaldehydes, general procedure

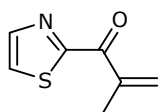
2-(trimethylsilyl)thiazole (1 g; 6.4 mmol) and the acrylaldehyde (6.4 mmol) were added to a round bottom flask and stirred for 4h. The mixture was diluted with 100 ml THF and treated with tetrabutylammoniumfluoride (TBAF) in THF (1 eq.) and stirred for 1 h. The solvent was removed and the residue was dissolved in EtOAc (50 ml) and washed with sat. NaHCO<sub>3</sub>, dried over Na<sub>2</sub>SO<sub>4</sub> and the solvent was removed. The brownish oil was purified by column chromatography (silica; pentane/Et<sub>2</sub>O, 7:3) to give the products as slightly yellow oils.

**Oxidation of 24a-f to 25a-f, general procedure**

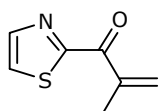
10 eq of MnO<sub>2</sub> was added to a solutions of the 1-(thiazol-2-yl)prop-2-en-1-ol in 10 ml CH<sub>2</sub>Cl<sub>2</sub> and stirred for 45 minutes. The black mixture was filtered over celite and the solvent was evaporated to afford the corresponding ketone.

**2-Methyl-1-(pyridin-2-yl)prop-2-en-1-one (16)**

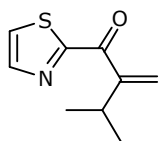
The product was obtained as a yellow oil. <sup>1</sup>H NMR (400 MHz, CDCl<sub>3</sub>) δ 8.65 (d, J=4.6 Hz, 1H), 7.82 (m, 2H), 7.42 (m, 1H), 6.03 (d, J=14.7 Hz, 2H), 2.09 (s, 3H). <sup>13</sup>C NMR (100 MHz, CDCl<sub>3</sub>) δ 173.5, 155.5, 148.4, 142.7, 136.9, 129.9, 125.7, 124.0, 18.5. HRMS: m/z: C<sub>9</sub>H<sub>10</sub>NO<sup>+</sup>, Calcd. 148.07569; found: 148.07614.

**2-Methyl-1-(thiazol-2-yl)prop-2-en-1-one (17a)**

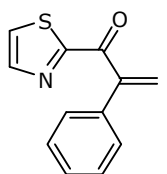
The product was obtained as a slightly yellow oil. <sup>1</sup>H NMR (400 MHz, CDCl<sub>3</sub>) δ 7.99 (d, J = 3.1 Hz, 1H), 7.64 (d, J = 3.1 Hz, 1H), 6.93 (br, 1H), 6.19 – 6.10 (br, 1H), 2.09 (s, 3H). <sup>13</sup>C NMR (100 MHz, CDCl<sub>3</sub>) δ 185.4, 167.5, 144.4, 141.6, 131.2, 125.6, 18.7. HRMS: m/z: C<sub>7</sub>H<sub>8</sub>NOS<sup>+</sup>, Calcd. 154.03211; found 154.03219.

**2-Methylene-1-(thiazol-2-yl)butan-1-one (17b)**

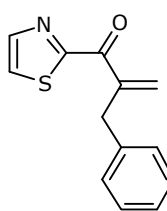
The product was obtained as a slightly yellow oil. <sup>1</sup>H NMR (300 MHz, CDCl<sub>3</sub>) δ 7.99 (d, J = 3.0 Hz, 1H), 7.64 (d, J = 3.1 Hz, 1H), 6.85 (br, 1H), 6.08 (br, 1H), 2.49 (q, J = 7.4 Hz, 2H), 1.12 (t, J = 7.4 Hz, 3H). <sup>13</sup>C NMR (100 MHz, CDCl<sub>3</sub>) δ 185.7, 167.8, 147.4, 144.4, 129.0, 125.6, 24.9, 12.4. HRMS: m/z: C<sub>8</sub>H<sub>10</sub>NOS<sup>+</sup>, Calcd. 168.04776; found 168.04750.

**3-Methyl-2-methylene-1-(thiazol-2-yl)butan-1-one (17c)**

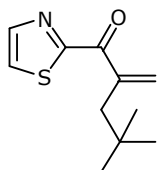
The product was obtained as a slightly yellow oil. <sup>1</sup>H NMR (400 MHz, CDCl<sub>3</sub>) δ 8.00 (d, J = 3.1 Hz, 1H), 7.65 (d, J = 3.1 Hz, 1H), 6.69 (br, 1H), 6.03 (br, 1H), 3.16 – 3.00 (m, 1H), 1.14 (d, J = 6.9 Hz, 6H). <sup>13</sup>C NMR (100 MHz, CDCl<sub>3</sub>) δ 186.4, 168.0, 152.2, 144.4, 126.6, 125.7, 29.2, 21.6. HRMS: m/z: C<sub>9</sub>H<sub>12</sub>NOS<sup>+</sup>, Calcd. 182.06341; found 182.06331.

**2-Phenyl-1-(thiazol-2-yl)prop-2-en-1-one (17d)**

The product was obtained as a slightly yellow oil. <sup>1</sup>H NMR (300 MHz, CDCl<sub>3</sub>) δ 8.00 (d, J=3.1 Hz, 1H), 7.64 (d, J=3.1 Hz, 1H), 7.26 (m, 5H), 7.07 (d, J=0.9 Hz, 1H), 6.02 (d, J=0.9 Hz, 1H). <sup>13</sup>C NMR (100 MHz, CDCl<sub>3</sub>) δ 188.9, 167.4, 147.8, 143.4, 132.3, 131.9, 129.1, 128.7, 128.4, 124.2. HRMS: m/z: C<sub>12</sub>H<sub>12</sub>NOS<sup>+</sup>, Calcd. 216.04831; found 216.05012.

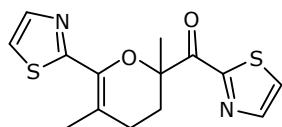
**2-Benzyl-1-(thiazol-2-yl)prop-2-en-1-one (17e)**

The product was obtained as a slightly yellow oil. <sup>1</sup>H NMR (300 MHz, CDCl<sub>3</sub>) δ 8.00 (d, J = 3.1 Hz, 1H), 7.64 (d, J = 3.1 Hz, 1H), 7.43 – 7.18 (m, 5H), 7.07 (d, J = 0.5 Hz, 1H), 6.02 (d, J = 0.9 Hz, 1H), 3.83 (s, 2H). <sup>13</sup>C NMR (75 MHz, CDCl<sub>3</sub>) δ 185.1, 145.5, 144.8, 138.8, 132.2, 129.5, 129.2, 128.7, 126.6, 126.1, 38.4. HRMS: m/z: C<sub>13</sub>H<sub>12</sub>NOS<sup>+</sup>, Calcd. 230.06341; found 230.06359.

**4,4-Dimethyl-2-methylene-1-(thiazol-2-yl)pentan-1-one (17f)**

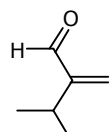
The product was obtained as a slightly yellow oil. <sup>1</sup>H NMR (400 MHz, CDCl<sub>3</sub>) δ 8.21 (d, J = 2.9 Hz, 1H), 7.84 (d, J = 3.0 Hz, 1H), 6.85 (br, 1H), 6.16 (br, 1H), 2.69 (s, 2H), 1.09 (s, 9H). <sup>13</sup>C NMR (100 MHz, CDCl<sub>3</sub>) δ 186.6, 167.5, 144.5, 144.1, 131.6, 125.7, 45.1, 31.6, 29.4. HRMS: m/z: C<sub>12</sub>H<sub>16</sub>NOS<sup>+</sup>, Calcd. 210.09471; found 210.09472.





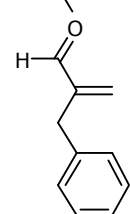
**(2,5-Dimethyl-6-(thiazol-2-yl)-3,4-dihydro-2H-pyran-2-yl)(thiazol-2-yl) methanone (20)**

The product was obtained as a slightly yellow oil.  $^1\text{H}$  NMR (400 MHz,  $\text{CDCl}_3$ )  $\delta$  = 8.01 (d,  $J$  = 3.1 Hz, 1H), 7.80 (d,  $J$  = 3.3 Hz, 1H), 7.64 (d,  $J$  = 3.1 Hz, 1H), 7.28 (d,  $J$  = 3.3 Hz, 1H), 3.05 – 3.01 (m, 1H), 2.19 – 2.14 (m, 1H), 2.09 (s, 3H), 2.07 – 2.06 (m, 1H), 2.04 – 2.03 (m, 1H), 1.85 (s, 3H).  $^{13}\text{C}$  NMR (100 MHz,  $\text{CDCl}_3$ )  $\delta$  = 191.9, 165.3, 163.9, 144.7, 142.6, 139.8, 126.3, 118.6, 111.3, 82.6, 30.7, 26.5, 24.7, 18.4. HRMS:  $m/z$ :  $\text{C}_{14}\text{H}_{15}\text{N}_2\text{O}_2\text{S}_2^+$ , Calcd. 307.05695; found 307.05653.



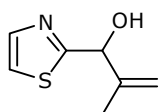
**3-Methyl-2-methylenebutanal (23c)**

The product was obtained as a colorless oil.  $^1\text{H}$  NMR (400 MHz,  $\text{CDCl}_3$ )  $\delta$  9.52 (s, 1H), 6.23 (br, 1H), 5.94 (br, 1H), 2.92 – 2.61 (m, 1H), 1.07 (m, 6H).  $^{13}\text{C}$  NMR (100 MHz,  $\text{CDCl}_3$ )  $\delta$  194.7, 156.4, 132.2, 26.1, 21.3.



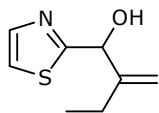
**2-Benzylacrylaldehyde (23e).**

The product was obtained as a colorless oil.  $^1\text{H}$  NMR (400 MHz,  $\text{CDCl}_3$ )  $\delta$  9.61 (s, 1H), 7.24 (m, 5H), 6.09 (br, 1H), 5.29 (br, 1H), 3.57 (s, 2H).  $^{13}\text{C}$  NMR (100 MHz,  $\text{CDCl}_3$ )  $\delta$  194.0, 149.7, 142.2, 135.2, 129.1, 128.5, 126.4, 34.1. HRMS:  $m/z$ :  $\text{C}_{10}\text{H}_{11}\text{O}^+$ , Calcd. 169.06239; found 169.06220.



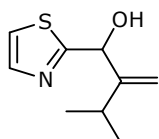
**2-Methyl-1-(thiazol-2-yl)prop-2-en-1-ol (24a)**

The product was obtained as a slightly yellow oil.  $^1\text{H}$  NMR (300 MHz,  $\text{CDCl}_3$ )  $\delta$  7.72 (d,  $J$  = 3.2 Hz, 1H), 7.32 (d,  $J$  = 3.2 Hz, 1H), 5.45 (br, 1H), 5.25 (s, 1H), 5.05 (d,  $J$  = 1.2 Hz, 1H), 1.72 (s, 3H).  $^{13}\text{C}$  NMR (75 MHz,  $\text{CDCl}_3$ )  $\delta$  151.4, 145.4, 142.4, 119.8, 114.2, 76.0, 17.5. HRMS:  $m/z$ :  $\text{C}_7\text{H}_{10}\text{NOS}^+$ , Calcd. 156.04776; found: 156.04784.



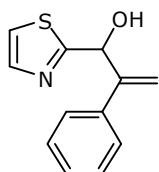
**2-Methylene-1-(thiazol-2-yl)butan-1-ol (24b)**

The product was obtained as a slightly yellow oil.  $^1\text{H}$  NMR (400 MHz,  $\text{CDCl}_3$ )  $\delta$  7.71 (s, 1H), 7.31 (s, 1H), 5.48 (br, 1H), 5.30 (s, 1H), 5.06 (br, 1H), 3.62 (s, 1H), 2.16 (m, 1H), 1.96 (m, 1H), 1.03 (td,  $J$  = 7.3, 1.7, 3H).  $^{13}\text{C}$  NMR (100 MHz,  $\text{CDCl}_3$ )  $\delta$  173.3, 151.0, 142.1, 119.6, 111.5, 75.4, 23.6, 11.9. HRMS:  $m/z$ :  $\text{C}_8\text{H}_{12}\text{NOS}^+$ , Calcd. 170.06341; found 170.06283.



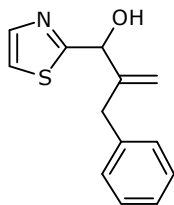
**3-Methyl-2-methylene-1-(thiazol-2-yl)butan-1-ol (24c)**

The product was obtained as a slightly yellow oil.  $^1\text{H}$  NMR (300 MHz,  $\text{CDCl}_3$ )  $\delta$  7.72 (d,  $J$  = 3.3 Hz, 1H), 7.31 (dd,  $J$  = 3.1, 1.7 Hz, 1H), 5.52 (d,  $J$  = 3.8 Hz, 1H), 5.30 (s, 1H), 5.12 (br, 1H), 2.46 – 2.25 (m, 1H), 1.09 (d,  $J$  = 6.8 Hz, 3H), 1.00 (d,  $J$  = 6.8 Hz, 3H).  $^{13}\text{C}$  NMR (100 MHz,  $\text{CDCl}_3$ )  $\delta$  173.2, 156.4, 142.1, 119.6, 110.5, 74.6, 29.8, 22.9, 22.6. HRMS:  $m/z$ :  $\text{C}_9\text{H}_{14}\text{NOS}^+$ , Calcd. 184.07906; found 184.07851.

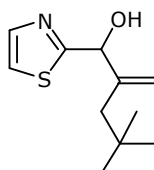


**3-Phenyl-2-methylene-1-(thiazol-2-yl)butan-1-ol (24d)**

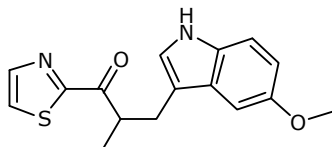
The product was obtained as a slightly yellow oil.  $^1\text{H}$  NMR (400 MHz,  $\text{CDCl}_3$ )  $\delta$  7.74 (d,  $J$  = 3.1 Hz, 1H), 7.25 (m, 6H), 5.98 (d,  $J$  = 5.2 Hz, 1H), 5.58 (s, 2H), 5.23 (d,  $J$  = 5.2 Hz, 1H).  $^{13}\text{C}$  NMR (100 MHz,  $\text{CDCl}_3$ )  $\delta$  172.1, 153.4, 142.4, 139.6, 128.2, 127.1, 126.4, 118.6, 112.9, 81.5. HRMS:  $m/z$ :  $\text{C}_{12}\text{H}_{12}\text{NOS}^+$ , Calcd. 218.06341; found 218.06341.

**2-Benzyl-1-(thiazol-2-yl)prop-2-en-1-ol (24e)**

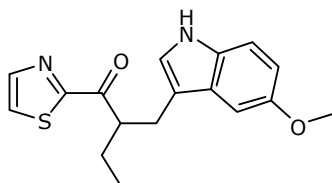
The product was obtained as a slightly yellow oil.  $^1\text{H}$  NMR (300 MHz,  $\text{CDCl}_3$ )  $\delta$  7.74 (d,  $J = 3.2$  Hz, 1H), 7.33 (d,  $J = 3.2$  Hz, 1H), 7.32 – 7.12 (m, 5H), 5.49 (d,  $J = 3.1$  Hz, 1H), 5.37 (s, 1H), 4.93 (br, 1H), 3.49 (d,  $J = 15.9$  Hz, 1H), 3.30 (d,  $J = 15.9$  Hz, 1H).  $^{13}\text{C}$  NMR (100 MHz,  $\text{CDCl}_3$ )  $\delta$  172.9, 149.0, 142.2, 138.7, 129.3, 128.4, 126.3, 119.7, 114.7, 74.6, 38.0. HRMS:  $m/z$ :  $\text{C}_{13}\text{H}_{14}\text{NOS}^+$ , Calcd. 232.07906; found 232.07904.

**4,4-Dimethyl-2-methylene-1-(thiazol-2-yl)pentan-1-ol (24f)**

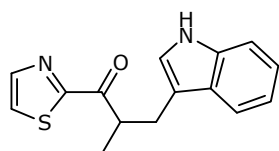
The product was obtained as a slightly yellow oil.  $^1\text{H}$  NMR (400 MHz,  $\text{CDCl}_3$ )  $\delta$  7.71 (d,  $J = 2.8$  Hz, 1H), 7.30 (d,  $J = 2.9$  Hz, 1H), 5.47 (d,  $J = 5.2$  Hz, 2H), 5.09 (br, 1H), 3.52 (s, 1H), 2.07 (d,  $J = 13.8$  Hz, 1H), 1.93 (d,  $J = 13.5$  Hz, 1H), 0.95 (s, 9H).  $^{13}\text{C}$  NMR (100 MHz,  $\text{CDCl}_3$ )  $\delta$  173.6, 147.3, 142.2, 119.6, 114.9, 74.6, 45.7, 31.7, 29.8. HRMS:  $m/z$ :  $\text{C}_{11}\text{H}_{18}\text{NOS}^+$ , Calcd. 212.11036; found 212.11031.

**3-(5-Methoxy-1H-indol-3-yl)-2-methyl-1-(thiazol-2-yl)propan-1-one (26a)**

Purification by column chromatography ( $\text{SiO}_2$ , EtOAc:heptane 1:4). The product was obtained as a slightly yellow oil.  $^1\text{H}$  NMR (400 MHz,  $\text{CDCl}_3$ )  $\delta$  8.01 (d,  $J = 3.0$  Hz, 1H), 7.83 (s, 1H), 7.66 (d,  $J = 3.0$  Hz, 1H), 7.27 – 7.24 (m, 1H), 7.22 (d,  $J = 8.7$  Hz, 1H), 7.00 (d,  $J = 2.4$  Hz, 1H), 6.84 (dd,  $J = 8.7$ , 2.5 Hz, 1H), 4.23 (m, 1H), 3.91 (s, 3H), 3.37 (dd,  $J = 14.4$ , 5.9 Hz, 1H), 2.83 (dd,  $J = 14.4$ , 8.1 Hz, 1H), 1.29 (d,  $J = 6.9$  Hz, 3H).  $^{13}\text{C}$  NMR (100 MHz,  $\text{CDCl}_3$ )  $\delta$  197.4, 167.0, 153.9, 144.6, 131.3, 127.9, 126.2, 123.3, 113.5, 112.3, 111.7, 101.0, 55.9, 42.3, 29.0, 16.5. HRMS:  $m/z$ :  $\text{C}_{16}\text{H}_{17}\text{N}_2\text{O}_2\text{S}^+$ , Calcd. 301.10052; found 301.10130. Ee's were determined by HPLC analysis (Chiralcel-AD, n-heptane/iPrOH 95:5, 1 mL/min). Retention times: 32.8 and 34.6 mins.

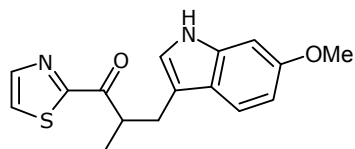
**2-((5-Methoxy-1H-indol-3-yl)methyl)-1-(thiazol-2-yl)butan-1-one (26Et)**

Purification by column chromatography ( $\text{SiO}_2$ , EtOAc:heptane 1:4). The product was obtained as a slightly yellow oil.  $^1\text{H}$  NMR (300 MHz,  $\text{CDCl}_3$ )  $\delta$  7.17 (d,  $J = 8.75$  Hz, 1H), 7.21 (d,  $J = 1.94$  Hz, 1H), 6.82 (dd,  $J = 8.78$ , 2.24 Hz, 1H), 6.95 (s, 1H), 7.61 (d,  $J = 3.02$  Hz, 1H), 7.97 (d,  $J = 3.01$  Hz, 1H), 8.03 (s, 1H), 4.18 (td,  $J = 10.51$ , 6.29 Hz, 1H), 3.90 (s, 3H), 3.30 (dd,  $J = 14.48$ , 6.91 Hz, 1H), 2.91 (dd,  $J = 14.48$ , 7.18 Hz, 1H), 1.93 (m, 1H), 1.73 (m, 1H), 0.92 (t,  $J = 7.40$  Hz, 3H).  $^{13}\text{C}$  NMR (75 MHz,  $\text{CDCl}_3$ )  $\delta$  197.6, 168.0, 154.1, 144.9, 131.6, 128.2, 126.5, 124.0, 113.7, 112.4, 112.0, 101.2, 56.1, 49.5, 28.4, 24.9, 12.0. HRMS:  $m/z$ :  $\text{C}_{17}\text{H}_{19}\text{N}_2\text{O}_2\text{S}^+$ , Calcd. 315.11672; found 315.11584. Ee's were determined by HPLC analysis (Chiralcel-AD, n-heptane/iPrOH 95:5, 1 mL/min). Retention times: 14.1 and 15.6 mins.

**3-(1H-Indol-3-yl)-2-methyl-1-(thiazol-2-yl)propan-1-one (26b)**

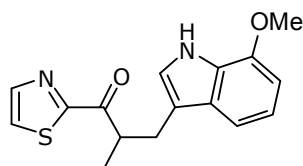
Purification by column chromatography ( $\text{SiO}_2$ ,  $\text{Et}_2\text{O}$ :n-pentane 1:1). The product was obtained as a slightly yellow oil.  $^1\text{H}$  NMR (400 MHz,  $\text{CDCl}_3$ )  $\delta$  8.02 (d,  $J = 2.9$  Hz, 1H), 7.94 (br, 1H), 7.74 (d,  $J = 7.8$  Hz, 1H), 7.65 (d,  $J = 2.9$  Hz, 1H), 7.33 (d,  $J = 8.0$  Hz, 1H), 7.18 – 7.13 (m, 2H), 7.02 (s, 1H), 4.38 – 4.12 (m, 1H), 3.40 (dd,  $J = 14.4$ , 6.3 Hz, 1H), 2.90 (dd,  $J = 14.4$ , 8.0 Hz, 1H), 1.30 (d,  $J = 6.9$  Hz, 3H).  $^{13}\text{C}$  NMR (100 MHz,  $\text{CDCl}_3$ )  $\delta$  197.4, 166.9, 144.7, 135.8, 127.6, 126.1, 122.5, 121.9, 121.2, 119.7, 119.3, 111.0, 42.4, 28.7, 16.8. HRMS:  $m/z$ :  $\text{C}_{15}\text{H}_{15}\text{N}_2\text{OS}^+$ , Calcd.

271.08996; found 271.09000. Ee's were determined by HPLC analysis (Chiralcel-AD, n-heptane/iPrOH 95:5, 1 mL/min). Retention times: 23.0 and 26.0 mins.



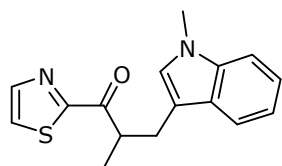
**3-(6-Methoxy-1H-indol-3-yl)-2-methyl-1-(thiazol-2-yl)propan-1-one (26c)**

The product was obtained as a slightly yellow oil. Purification by column chromatography (SiO<sub>2</sub>, Et<sub>2</sub>O:n-pentane 1:1). <sup>1</sup>H NMR (400 MHz, CDCl<sub>3</sub>) δ = 8.01 (s, 1H), 7.85 (br, 1H), 7.69 (s, 1H), 7.60 (s, 1H), 7.58 (s, 1H), 6.89 (s, 1H), 6.81 (s, 1H), 4.27 – 4.17 (m, 1H), 3.83 (s, 3H), 3.35 (dd, J = 14.5, 6.4 Hz, 1H), 2.84 (dd, J = 14.4, 8.0 Hz, 1H), 1.28 (d, J = 6.9 Hz, 3H). <sup>13</sup>C NMR (100 MHz, CDCl<sub>3</sub>) 197.8, 167.2, 153.4, 144.6, 131.4, 127.1, 126.0, 123.5, 114.6, 111.4, 110.7, 100.5, 57.3, 41.3, 30.1, 17.5. HRMS: m/z: C<sub>16</sub>H<sub>17</sub>N<sub>2</sub>OS<sup>+</sup>, Calcd. 301.10052; found 301.10025. Ee's were determined by HPLC analysis (Chiralcel-OD, n-heptane/iPrOH 90:10, 1 mL/min). Retention times: 20.2 and 25.8 mins.



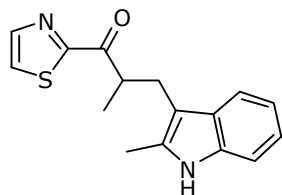
**3-(7-Methoxy-1H-indol-3-yl)-2-methyl-1-(thiazol-2-yl)propan-1-one (26d)**

Purification by column chromatography (SiO<sub>2</sub>, Et<sub>2</sub>O:n-pentane 1:1). The product was obtained as a slightly yellow oil. <sup>1</sup>H NMR (400 MHz, CDCl<sub>3</sub>) δ = 8.16 (br, 1H), 8.01 (s, 1H), 7.64 (s, 1H), 7.34 (d, J = 7.6 Hz, 1H), 7.04 (t, J = 7.9 Hz, 1H), 6.99 (s, 1H), 6.63 (d, J = 7.6 Hz, 1H), 4.23 – 4.21 (m, 1H), 3.94 (s, 3H), 3.37 (dd, J = 14.4, 6.1 Hz, 1H), 2.87 (dd, J = 14.3, 8.0 Hz, 1H), 1.28 (d, J = 6.9 Hz, 3H). <sup>13</sup>C NMR (100 MHz, CDCl<sub>3</sub>) δ = 197.4, 167.0, 146.1, 144.7, 128.9, 126.7, 126.1, 122.1, 119.7, 114.2, 111.9, 101.8, 55.3, 42.5, 28.8, 16.8. HRMS: m/z: C<sub>16</sub>H<sub>17</sub>N<sub>2</sub>OS<sup>+</sup>, Calcd. 301.10052; found 301.10038. Ee's were determined by HPLC analysis (Chiralcel-OD, n-heptane/iPrOH 90:10, 1 mL/min). Retention times: 19.1 and 23.6 mins.



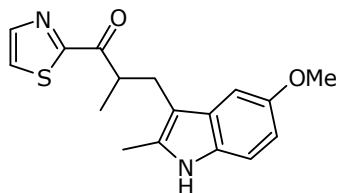
**2-Methyl-3-(1-methyl-1H-indol-3-yl)-1-(thiazol-2-yl)propan-1-one (26e)**

Purification by column chromatography (SiO<sub>2</sub>, Et<sub>2</sub>O:n-pentane 1:1). The product was obtained as a slightly yellow oil. <sup>1</sup>H NMR (400 MHz, CDCl<sub>3</sub>) δ = 8.01 (d, J = 1.8 Hz, 1H), 7.72 (d, J = 7.9 Hz, 1H), 7.64 (d, J = 1.8 Hz, 1H), 7.25 (s, 1H), 7.21 (t, J = 7.5 Hz, 1H), 7.11 (t, J = 7.4 Hz, 1H), 6.87 (s, 1H), 4.28 – 4.14 (m, 1H), 3.72 (s, 3H), 3.38 (dd, J = 14.4, 6.2 Hz, 1H), 2.87 (dd, J = 14.4, 8.0 Hz, 1H), 1.29 (d, J = 6.9 Hz, 3H). <sup>13</sup>C NMR (100 MHz, CDCl<sub>3</sub>) δ = 197.4, 166.9, 144.7, 142.6, 136.9, 127.3, 126.1, 121.4, 119.2, 118.7, 112.1, 109.0, 42.7, 32.6, 28.6, 16.8. HRMS: m/z: C<sub>16</sub>H<sub>17</sub>N<sub>2</sub>OS<sup>+</sup>, calcd. 285.10561; found 258.10554. Ee's were determined by HPLC analysis (Chiralcel-OD, n-heptane/iPrOH 98:2, 1 mL/min). Retention times: 13.6 and 15.0 mins.



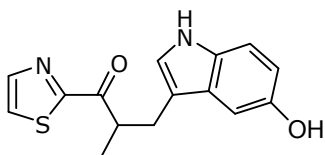
**2-Methyl-3-(2-methyl-1H-indol-3-yl)-1-(thiazol-2-yl)propan-1-one (26f)**

Purification by column chromatography (SiO<sub>2</sub>, EtOAc:n-pentane 1:3). The product was obtained as a slightly yellow oil. <sup>1</sup>H NMR (400 MHz, CDCl<sub>3</sub>) δ = 8.00 (d, J = 3.0 Hz, 1H), 7.82 (br, 1H), 7.69 – 7.67 (m, 1H), 7.62 (d, J = 3.0 Hz, 1H), 7.26 – 7.22 (m, 1H), 7.11 – 7.08 (m, 2H), 4.22 (dd, J = 14.0, 7.3 Hz, 1H), 3.30 (dd, J = 14.1, 5.6 Hz, 1H), 2.80 (dd, J = 14.2, 8.9 Hz, 1H), 2.39 (s, 3H), 1.24 (d, J = 6.9 Hz, 3H). <sup>13</sup>C NMR (100 MHz, CDCl<sub>3</sub>) δ = 196.5, 165.9, 143.7, 134.2, 131.1, 127.8, 125.0, 119.9, 118.2, 117.4, 109.0, 108.3, 41.7, 27.0, 15.2, 10.8. HRMS: m/z: C<sub>16</sub>H<sub>17</sub>N<sub>2</sub>OS<sup>+</sup>, calcd. 285.10561; found 258.10551. Ee's were determined by HPLC analysis (Chiralcel-AD, n-heptane/iPrOH 95:5, 1 mL/min). Retention times: 16.9 and 19.2 mins.



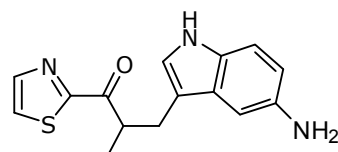
### 3-(5-Methoxy-2-methyl-1H-indol-3-yl)-2-methyl-1-(thiazol-2-yl)propan-1-one (26g)

Purification by column chromatography (SiO<sub>2</sub>, EtOAc:n-pentane 1:3). The product was obtained as a slightly yellow oil. <sup>1</sup>H NMR (400 MHz, CDCl<sub>3</sub>) δ = 8.00 (s, 1H), 7.65 (s, 2H), 7.25 (s, 1H), (7.12 (dd, *J* = 8.7, 2.0 Hz, 1H), 6.76 (d, *J* = 8.7 Hz, 1H), 4.29 – 4.12 (m, 1H), 3.91 (s, 3H), 3.28 (dd, *J* = 14.2, 5.2 Hz, 1H), 2.73 (dd, *J* = 14.2, 9.0 Hz, 1H), 2.38 (s, 3H), 1.22 (d, *J* = 6.8 Hz, 3H). <sup>13</sup>C NMR (100 MHz, CDCl<sub>3</sub>) δ = 197.5, 167.0, 153.9, 144.6, 133.0, 130.3, 129.2, 126.1, 110.7, 109.4, 105.9, 100.9, 55.9, 42.6, 28.3, 15.9, 11.9. HRMS: *m/z*: C<sub>17</sub>H<sub>19</sub>N<sub>2</sub>O<sub>2</sub>S<sup>+</sup>, calcd. 315.11617; found 315.11638. Ee's were determined by HPLC analysis (Chiralcel-AD, n-heptane/iPrOH 95:5, 1 mL/min). Retention times: 22.1 and 23.7 mins.



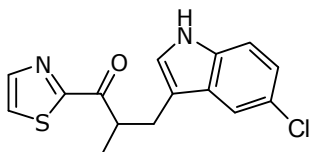
### 3-(5-Hydroxy-1H-indol-3-yl)-2-methyl-1-(thiazol-2-yl)propan-1-one (26h)

Purification by column chromatography (SiO<sub>2</sub>, Et<sub>2</sub>O:n-pentane 3:2). The product was obtained as a slightly yellow oil. <sup>1</sup>H NMR (400 MHz, CDCl<sub>3</sub>) δ = 8.02 (d, *J* = 3.0 Hz, 1 H), 7.81 (br, 1 H), 7.65 (d, *J* = 3.0 Hz, 1 H), 7.18 (d, *J* = 8.6 Hz, 1 H), 7.13 (d, *J* = 2.0 Hz, 1 H), 6.99 (d, *J* = 2.1 Hz, 1 H), 6.75 (dd, *J* = 8.6, 2.5 Hz, 1 H), 4.58 (br, 1 H), 4.26 – 4.15 (m, 1 H), 3.32 (dd, *J* = 14.4, 6.4 Hz, 1 H), 2.82 (dd, *J* = 14.4, 7.9 Hz, 1 H), 1.28 (d, *J* = 7.0 Hz, 3 H). <sup>13</sup>C NMR (100 MHz, CDCl<sub>3</sub>) δ = 197.3, 166.9, 149.2, 144.6, 131.4, 128.2, 126.1, 123.6, 113.1, 111.6, 111.5, 103.6, 42.2, 28.7, 16.7. HRMS: *m/z*: C<sub>15</sub>H<sub>15</sub>N<sub>2</sub>O<sub>2</sub>S<sup>+</sup>, calcd. 287.08487; found 287.08248. Ee's were determined by HPLC analysis (Chiralcel-OD, n-heptane/iPrOH 90:10, 1 mL/min). Retention times: 40.1 and 46.0 mins.



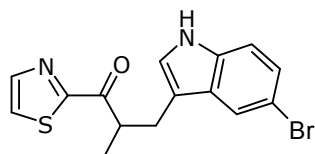
### 3-(5-Amino-1H-indol-3-yl)-2-methyl-1-(thiazol-2-yl)propan-1-one (26i)

Purification by column chromatography (SiO<sub>2</sub>, EtOAc:Et<sub>2</sub>O:pentane 2:6:1 and 5 vol% Et<sub>3</sub>N). The product was obtained as a slightly yellow oil. <sup>1</sup>H NMR (400 MHz, CDCl<sub>3</sub>) δ = 8.00 (d, *J* = 3.0 Hz, 1H), 7.91 (br, 1H), 7.63 (d, *J* = 3.0 Hz, 1H), 7.11 (d, *J* = 8.5 Hz, 1H), 7.01 (s, 1H), 6.91 (s, 1H), 6.63 (d, *J* = 8.5 Hz, 1H), 4.20 (m, 1H), 3.30 (dd, *J* = 14.3, 6.3 Hz, 1H), 2.80 (dd, *J* = 14.4, 8.0 Hz, 1H), 1.28 – 1.25 (m, 5H). <sup>13</sup>C NMR (100 MHz, CDCl<sub>3</sub>) δ = 197.5, 167.0, 144.7, 139.1, 131.1, 128.4, 126.2, 123.3, 112.8, 112.5, 111.6, 104.2, 42.4, 28.8, 16.8. HRMS: *m/z*: C<sub>15</sub>H<sub>15</sub>N<sub>3</sub>O<sup>+</sup>, calcd. 286.10148; found 286.10201. Ee's were determined by HPLC analysis (Chiralcel-AD, n-heptane/iPrOH 93:7, 1 mL/min). Retention times: 76.8 and 80.4 mins.



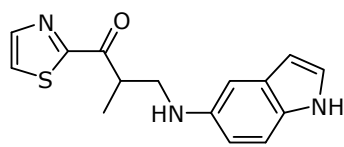
### 3-(5-Chloro-1H-indol-3-yl)-2-methyl-1-(thiazol-2-yl)propan-1-one (26j)

Purification by column chromatography (SiO<sub>2</sub>, Et<sub>2</sub>O:n-pentane 1:2). The product was obtained as a slightly yellow oil. <sup>1</sup>H NMR (400 MHz, CDCl<sub>3</sub>) δ = 8.03 (s, 1 H), 7.99 (br, 1 H), 7.70 (s, 1 H), 7.66 (s, 1 H), 7.26 (s, 1 H), 7.23 (d, *J* = 8.6, 1 H), 7.12 (d, *J* = 8.6, 1 H), 4.19 (dd, *J* = 14.0, 7.1 Hz, 1 H), 3.34 (dd, *J* = 14.4, 6.2 Hz, 1 H), 2.85 (dd, *J* = 14.5, 7.7 Hz, 1 H), 1.29 (d, *J* = 6.9, 3 H). <sup>13</sup>C NMR (100 MHz, CDCl<sub>3</sub>) δ = 192.3, 162.0, 140.0, 129.7, 123.9, 121.5, 120.4, 119.1, 117.5, 114.0, 108.9, 107.2, 61.1, 37.7, 23.9. HRMS: *m/z*: C<sub>15</sub>H<sub>14</sub>ClN<sub>2</sub>O<sup>+</sup>, calcd. 305.05156; found 305.05172. Ee's were determined by HPLC analysis (Chiralcel-AD, n-heptane/iPrOH 95:5, 1 mL/min). Retention times: 21.3 and 22.3 mins.



**3-(5-Bromo-1H-indol-3-yl)2-methyl-1-(thiazol-2-yl)propan-1-one (26k)**

Purification by column chromatography (SiO<sub>2</sub>, Et<sub>2</sub>O:n-pentane 1:1). The product was obtained as a slightly yellow oil. <sup>1</sup>H NMR (400 MHz, CDCl<sub>3</sub>) δ = 8.04 (d, J = 3.0 Hz, 1H), 7.96 (br, 1H), 7.87 (s, 1H), 7.66 (d, J = 3.0 Hz, 1H), 7.24 (d, J = 1.8 Hz, 1H), 7.20 (s, 1H), 7.02 (d, J = 1.8 Hz, 1H), 4.23-4.12 (m, 1H), 3.33 (dd, J = 14.5, 6.4 Hz, 1H), 2.85 (dd, J = 14.5, 7.7 Hz, 1H), 1.29 (d, J = 6.9 Hz, 3 H). <sup>13</sup>C NMR (100 MHz, CDCl<sub>3</sub>) δ = 197.0, 166.8, 144.7, 134.8, 129.4, 126.2, 124.8, 123.6, 121.9, 113.6, 112.7, 112.4, 42.4, 28.6, 16.7. HRMS: m/z: C<sub>15</sub>H<sub>14</sub>BrN<sub>2</sub>OS<sup>+</sup>, calcd. 349.00047; found 349.00057. Ee's were determined by HPLC analysis (Chiralcel-AD, n-heptane/iPrOH 95:5, 1 mL/min). Retention times: 21.4 and 22.4 mins.



**3-((1H-Indol-5-yl)amino-2-methyl-1-(thiazol-2-yl))propan-1-one (aza-Michael product)**

Product isolated from the reaction between **17a** and **25i** in the absence of DNA. Purification by column chromatography (SiO<sub>2</sub>, Et<sub>2</sub>O:n-pentane 4:1). The product was obtained as a slightly yellow oil. <sup>1</sup>H NMR (400 MHz, CDCl<sub>3</sub>) δ = 8.01 (d, J = 2.9 Hz, 1 H), 7.91 (br, 1 H), 7.65 (d, J = 2.9 Hz, 1 H), 7.16 (d, J = 8.6 Hz, 1 H), 7.09 (s, 1 H), 6.89 (s, 1 H), 6.59 (d, J = 8.6 Hz, 1 H), 6.37 (s, 1 H), 4.31 - 4.12 (m, 1 H), 3.69 (dd, J = 12.6, 7.6 Hz, 1 H), 3.38 (dd, J = 12.6, 5.5 Hz, 1 H), 2.43 (s, 1 H), 1.37 (d, J = 7.0 Hz, 3 H). <sup>13</sup>C NMR (100 MHz, CDCl<sub>3</sub>) δ = 196.6, 167.0, 144.7, 141.8, 130.2, 128.8, 126.4, 124.4, 112.3, 111.6, 102.6, 101.8, 48.4, 41.7, 15.1. HRMS: m/z: C<sub>15</sub>H<sub>16</sub>N<sub>3</sub>OS<sup>+</sup>, calcd. 286.10141; found 286.10168 Ee's were determined by HPLC analysis (Chiralcel-AD, n-heptane/iPrOH 93:7, 1 mL/min). Retention times: 53.0 and 57.8 mins.

## 5.10 References

1. C. Fehr, *Angew. Chem. Int. Ed.* **1996**, *35*, 2567.
2. S. Kobayashi, Y. Yamashita, *Acc. Chem. Res.* **2011**, *44*, 58.
3. J. T. Mohr, A. Y. Hong, B. M. Stoltz, *Nature Chem.* **2009**, *1*, 359.
4. J. Eames, M. Suggate, *Angew. Chem. Int. Ed.* **2005**, *44*, 186.
5. L. Duhamel, P. Duhamel, J. Plaquevent, *Tetrahedron-Asym.* **2004**, *15*, 3653.
6. L. Duhamel, J. Plaquevent, *Bull. Soc. Chim. Fr.* **1982**, *II*, 75.
7. E. Vedejs, - J. Org. Chem. **1998**, *63*, 2792.
8. H. Buschmann, H. Sharf, N. Hoffmann, P. Esser, *Angew. Chem. Int. Ed.* **1991**, *30*, 477.
9. F. Cavellier, S. Gomez, R. Jacquier, J. Verducci, *Tetrahedron Lett.* **1994**, *35*, 2891.
10. D. Uraguchi, N. Kinoshita, T. Ooi, *J. Am. Chem. Soc.* **2010**, *132*, 12240.
11. E. M. Beck, A. M. Hyde, E. N. Jacobsen, *Org. Lett.* **2011**, *13*, 4260.
12. C. H. Cheon, O. Kanno, F. D. Toste, *J. Am. Chem. Soc.* **2011**, *133*, 13248.
13. C. H. Cheon, H. Yamamoto, *J. Am. Chem. Soc.* **2008**, *130*, 9246.
14. C. H. Cheon, T. Imahori, H. Yamamoto, *Chem. Commun.* **2010**, *46*, 6980.
15. M. Morita, L. Drouin, R. Motoki, Y. Kimura, I. Fujimori, M. Kanai, M. Shibasaki, *J. Am. Chem. Soc.* **2009**, *131*, 3858.
16. O. Roy, F. Loiseau, A. Riahi, F. Hémin, J. Muzart, *Tetrahedron* **2003**, *59*, 9641.

17. O. Roy, A. Riahi, F. Hénin, J. Muzart, *Eur. J. Org. Chem.* **2002**, 3986.
18. M. A. Baur, A. Riahi, F. Hénin, J. Muzart, *Tetrahedron-Asym.* **2003**, *14*, 2755.
19. M. Hayashi, S. Nakamura, *Angew. Chem. Int. Ed.* **2011**, *50*, 2249.
20. N. Reynolds, T. Rovis, *J. Am. Chem. Soc.* **2005**, *127*, 16406.
21. M. Sibi, H. Tatamidani, K. Patil, *Org. Lett.* **2005**, *7*, 2571.
22. L. Navarre, R. Martinez, J. Genet, S. Darses, *J. Am. Chem. Soc.* **2008**, *130*, 6159.
23. C. G. Frost, S. D. Penrose, K. Lamshead, P. R. Raithby, J. E. Warren, R. Gleave, *Org. Lett.* **2007**, *9*, 2119.
24. N. Fu, L. Zhang, J. Li, S. Luo, J. Cheng, *Angew. Chem. Int. Ed.* **2011**, *50*, 11451.
25. M. P. Sibi, J. Coulomb, L. M. Stanley, *Angew. Chem. Int. Ed.* **2008**, *47*, 9913.
26. Y. Hamashima, H. Somei, Y. Shimura, T. Tamura, M. Sodeoka, *Org. Lett.* **2004**, *6*, 1861.
27. Y. Hamashima, S. Suzuki, T. Tamura, H. Somei, M. Sodeoka, *Chem. Asian J.* **2011**, *6*, 658.
28. Y. Hamashima, T. Tamura, S. Suzuki, M. Sodeoka, *Synlett* **2009**, 1631.
29. Y. Belokon, S. Harutyunyan, E. Vorontsov, A. Peregudov, V. Chrustalev, K. Kochetkov, D. Pripadchev, A. Sagyan, A. Beck, D. Seebach, *Arkivoc* **2004**, 132.
30. T. Poisson, Y. Yamashita, S. Kobayashi, *J. Am. Chem. Soc.* **2010**, *132*, 7890.
31. K. Matsumoto, S. Tsutsumi, T. Ihori, H. Ohta, *J. Am. Chem. Soc.* **1990**, *112*, 9614.
32. T. Hirata, K. Shimoda, T. Kawano, *Tetrahedron-Asym.* **2000**, *11*, 1063.
33. T. Sakai, A. Matsuda, Y. Tanaka, T. Korenaga, T. Ema, *Tetrahedron-Asym.* **2004**, *15*, 1929.
34. K. Miyamoto, H. Ohta, *Eur. J. Biochem.* **1992**, *210*, 475.
35. K. Matoishi, M. Ueda, K. Miyamoto, H. Ohta, *J. Mol. Catal. B* **2004**, *27*, 161.
36. Y. Ijima, K. Matoishi, Y. Terao, N. Doi, H. Yanagawa, H. Ohta, *Chem. Commun.* **2005**, 877.
37. Y. Terao, Y. Ijima, K. Miyamoto, H. Ohta, *J. Mol. Catal. B* **2007**, *45*, 15.
38. K. Miyamoto, S. Hirokawa, H. Ohta, *J. Mol. Catal. B* **2007**, *46*, 14.
39. D. Geerdink, Master research report: The catalytic asymmetric 1,4-addition of water, **2008**.
40. J. Easmon, G. Puerstinger, K. Thies, G. Heinisch, J. Hofmann, *J. Med. Chem.* **2006**, *49*, 6343.
41. Y. Hon, T. Hsu, C. Chen, Y. Lin, F. Chang, C. Hsieh, P. Szu, *Tetrahedron* **2003**, *59*, 1509.
42. A. Dondoni, G. Fantin, M. Fogagnolo, A. Medici, P. Pedrini, *J. Org. Chem.* **1988**, *53*, 1748.
43. A. Erkkila, P. Pihko, *J. Org. Chem.* **2006**, *71*, 2538.
44. I. Piras, R. Jennerjahn, R. Jackstell, A. Spannenberg, R. Franke, M. Beller, *Angew. Chem. Int. Ed.* **2011**, *50*, 280.
45. K. Guckian, B. Schweitzer, R. Ren, C. Sheils, D. Tahmassebi, E. Kool, *J. Am. Chem. Soc.* **2000**, *122*, 2213.
46. E. Kool, J. Morales, K. Guckian, *Angew. Chem. Int. Ed.* **2000**, *39*, 990.

47. S. Lakhdar, M. Westermaier, F. Terrier, R. Goumont, T. Boubaker, A. R. Ofial, H. Mayr, *J. Org. Chem.* **2006**, *71*, 9088.
48. A. J. Boersma, B. L. Feringa, G. Roelfes, *Angew. Chem. Int. Ed.* **2009**, *48*, 3346.
49. E. W. Dijk, A. J. Boersma, B. L. Feringa, G. Roelfes, *Org. Biomol. Chem.* **2010**, *8*, 3868.
50. G. Roelfes, A. J. Boersma, B. L. Feringa, *Chem. Commun.* **2006**, 635.
51. G. Roelfes, B. L. Feringa, *Angew. Chem. Int. Ed.* **2005**, *44*, 3230.
52. M. J. Frisch, *et al.*, Gaussian 03, revision B.03. 340 Quinnipiac St Bldg 40: Gaussian Inc., **2004**.







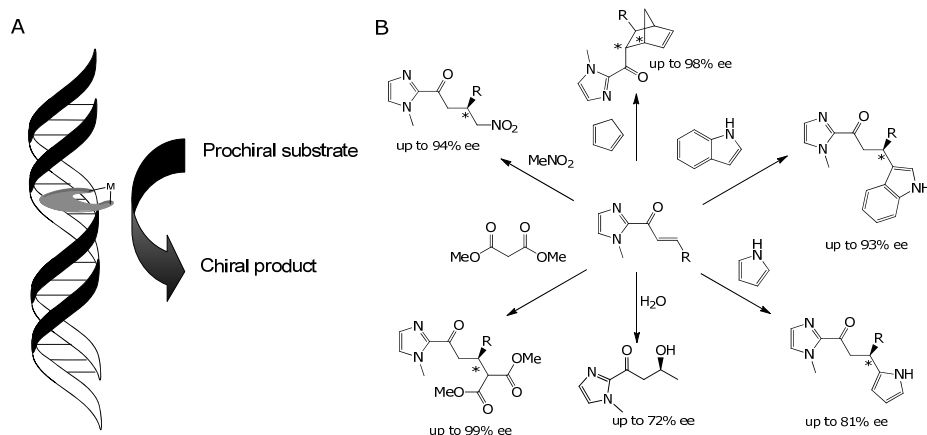
## **Chapter 6**

# **Conclusions and Perspective**

*In this chapter the results described in this thesis are summarized and a general discussion will be presented about DNA-based catalysis and what the present work adds to this. Furthermore, future perspectives are presented on the basis of ongoing projects.*

## 6.1 Introduction

The research described in this thesis was initiated by the discovery of DNA-based asymmetric catalysis.<sup>1</sup> This concept is based on the use of an achiral metal complex that binds to DNA in a non-covalent fashion (Figure 6.1A). Upon binding of the complex a chiral micro-environment is created around the metal complex. This chiral environment has been used to induce enantioselectivity in a variety of reactions, like the Diels-Alder reaction,<sup>1-5</sup> Michael addition,<sup>6</sup> Friedel-Crafts alkylation<sup>7</sup> and the *syn*-hydration reaction<sup>8</sup> (Figure 6.1B).



**Figure 6.1.** A; Concept of DNA-based catalysis, B; reaction scope.

The goal of the research described in this thesis was to develop this method into a synthetically useful technique. The specific aims were to use this approach for larger scale reactions, development of an easy recycling method of the catalyst and discovery of novel reactivities.

The main achievements reported in this thesis are:

- Water miscible organic co-solvents can be used in DNA-based catalysis. The ee was not affected and in several cases faster reactions were found, due to an increase of the rate of product dissociation. The enantioselectivity of these reactions was further enhanced since the co-solvent allowed for lowering the reaction temperature to -18 °C.
- The development of the first transition metal catalyzed enantioselective intermolecular oxa-Michael addition of alcohols.
- The development of the first catalytic enantioselective protonation of  $\alpha$ -substituted enones in water.

In the present chapter, the reactivity of DNA-based catalysts will be discussed and combined with new insights generated in the present work. This discussion will be based on a distinction between 1<sup>st</sup> and 2<sup>nd</sup> generation catalyst and their different reactivity profile. Furthermore,

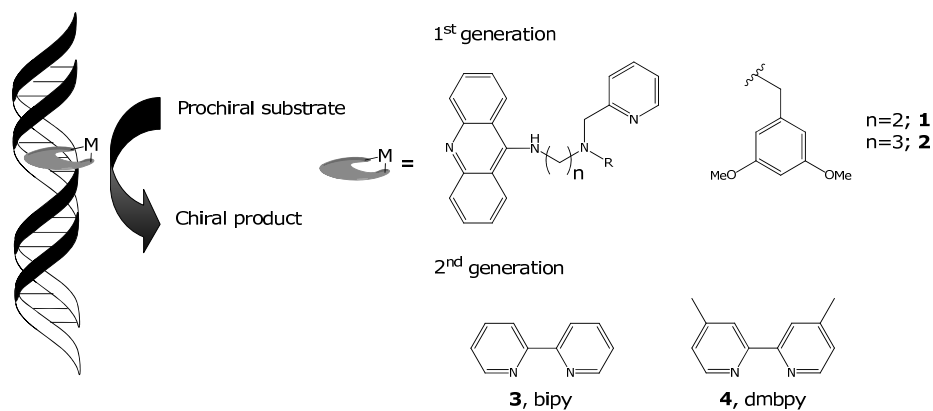
future prospects will be presented on the basis of additional experiments.

## 6.2 DNA-based catalysis

Over the last years, DNA-based catalysis has evolved into a promising technique for enantioselective organic synthesis. In this period, two generations of DNA-based catalysts have been developed, which differ in the type of ligands used: the acridine based ligands, which have a DNA intercalating part attached to a metal binding part (1<sup>st</sup> generation)<sup>1</sup> and ligands that combine the DNA binding part and the metal binding (2<sup>nd</sup> generation).<sup>2</sup> It has been shown that both types of ligands exhibit different characteristics and perform best in separate classes of reactions. In this chapter, I will discuss the different reactivity and present a model that gives a possible explanation for their different behavior.

### 6.2.1 1<sup>st</sup> generation vs. 2<sup>nd</sup> generation ligands

The first generation ligands comprise an acridine moiety, responsible for DNA intercalation, tethered to a metal binding domain via a small linker. The design of the ligand has an important influence on the enantioselectivity of the catalyzed reaction (Figure 6.2). Generally ligands containing a (substituted) arylmethyl group give rise to the best results. One of the characteristics of these ligands is that the outcome of the reaction can be influenced by the length of the spacer.<sup>1,2</sup> It has been shown in the Diels-Alder reaction that different enantiomers could be obtained by extending the linker with one extra carbon atom (48% (n=2; **1**), -49% (n=3; **2**)).



**Figure 6.2.** Concept of DNA-based catalysis with examples of 1<sup>st</sup> and 2<sup>nd</sup> generation ligands.

In the second generation ligands the DNA-binding moiety is combined with the metal-binding region into one structural unit, hence the linker is no longer required. With this class of ligands a dramatic

increase in enantioselectivity was observed in the Diels-Alder reaction (up to 99% ee for 4,4'-dimethyl-2,2'-bipyridine (dmbpy)), however only one enantiomer of the product can be generated.<sup>2</sup> Using terpyridine, instead of dmbpy, made it possible to obtain the opposite enantiomer of the product.<sup>9</sup>

### 6.2.2 Reactivity

1<sup>st</sup> and 2<sup>nd</sup> generation metal-ligand complexes are active in a wide variety of reactions. However, there is a striking difference in their reactivity and (enantio-)selectivity. The second generation copper complexes give rise to excellent ee's in C-C bond-forming reactions, like the Diels-Alder reaction,<sup>2</sup> the Michael addition,<sup>6</sup> the Friedel-Crafts alkylation<sup>7</sup> and the Friedel-Crafts alkylation/enantioselective protonation cascade reaction (Chapter 5). The first generation copper complexes can also catalyze these reactions albeit with much lower enantioselectivities. However, these are more successful in catalyzing reactions with oxygen based nucleophiles, like the oxa-Michael addition (Chapter 4) and the *syn* hydration reaction, resulting in good ee's.<sup>8</sup>

This can be explained by the difference in interaction of the metal complexes with the DNA. In the case of the 2<sup>nd</sup> generation ligands the reaction is proposed to take place in the minor and major groove of the DNA.<sup>10</sup> It is thought that in these cases the tighter microenvironment provided by the binding of the complex into the DNA ensures the higher enantioselectivity. Hydrophilic nucleophiles like alcohols and water are less present in the DNA core, due to the hydrophobicity of the DNA core.<sup>11,12</sup> Hence the low reactivity of these catalysts in the oxa-Michael addition.

The 1<sup>st</sup> generation ligands are based on the intercalating acridine which is tethered via a carbon spacer to the metal-binding domain. Due to the linker, the active copper centre is partially located in the hydration shell of the DNA. As a consequence, the conjugate addition of oxygen based nucleophiles can take place with high selectivity. This hypothesis is also in agreement with the observed decrease in enantioselectivity in the Diels-Alder reaction when using 1<sup>st</sup> generation ligands with a longer spacer.

### 6.2.3 Role of DNA

The role of DNA is not unambiguous. The DNA does not only act as chiral scaffold but also plays an important role for the rate of the reaction. For the Diels-Alder reaction,<sup>4</sup> the Michael addition<sup>13</sup> and the Friedel-Crafts alkylation<sup>7</sup> the DNA accelerates the reaction in case of the 2<sup>nd</sup> generation ligands. A rate increase of up to 58-fold was found for the Diels-Alder reaction. It is possible that this rate acceleration is caused by favorable arene-arene interactions of the substrate bound Cu<sup>II</sup>-complex with the nucleobases of the DNA.<sup>4</sup>

The favorable arene-arene interactions might also play an important role in the product dissociation step (Chapter 3). A kinetic study of the Michael addition and the Friedel-Crafts alkylation showed a decrease in the overall rate ( $k_{app}$ ) upon using water miscible organic co-solvents, while higher conversions were found under catalytic conditions. These observations were only made in the case of substrates with an aromatic or methyl substituent. Due to the fact that in the kinetic study the dissociation step is left out of consideration; the addition of water miscible co-solvents has to accelerate the dissociation step. However these observations were only made in the case of substrates with aromatic or methyl substituents. This suggests that the product bound  $Cu^{II}$ -complex is stabilized, possibly by the favorable arene-arene interaction, and thus becomes rate limiting.

Also in the Friedel-Crafts alkylation/enantioselective protonation cascade reaction the DNA is of utmost importance for enantioselectivity in this reaction (Chapter 5). The protonation needs to be the rate determining step in order to obtain high enantioselectivity. However, due to the large concentration of protonating agent and the fact that protonation is generally very fast, this can only be achieved by acceleration of the Friedel-Crafts alkylation step. Up to 60% ee was obtained in this cascade reaction demonstrating the acceleration of the Friedel-Crafts alkylation step by the DNA. Furthermore, we hypothesize that the difference in enantioselectivity obtained with different  $\pi$ -nucleophiles is partly caused by the difference in reactivity of these  $\pi$ -nucleophiles: with the less reactive indoles the DNA accelerating effect is not sufficient to make the protonation step rate limiting. The formation of products which are not formed under catalytic conditions without DNA already suggests that the rate of the Friedel-Crafts alkylation step is accelerated. However, a kinetic study is necessary in order to prove this hypothesis.

#### 6.2.4 Importance of DNA sequence

1<sup>st</sup> and 2<sup>nd</sup> generation metal-ligand complexes also show a large difference in their DNA sequences dependence. The 2<sup>nd</sup> generation metal-ligand complexes display a preference for sequences containing G-trimers. It has been shown that these sequences do not only induce the highest enantioselectivity but also accelerate the reaction more than sequences without this G-trimer. These results are most likely related to the structure of the DNA. The CD-spectra showed that all sequences still show a CD-signal similar to B-type DNA.<sup>10</sup> However, the sequences containing the G-trimer showed a CD spectrum that is indicative of a small distortion towards A-type DNA.

The sequence dependence has an important implication for the reactions catalyzed by st-DNA. As mentioned before, the sequence of st-DNA can be considered as a random sequence. Therefore, the obtained ee is a weighted average of the outcome of all sequences. However,

since sequences containing G-trimer accelerate the reaction most, they will dominate the outcome of the reaction.

Also in the case of the Friedel-Crafts alkylation/enantioselective protonation cascade, the optimal sequence contained a G-trimer (Chapter 5). However, among the tested sequences there was not a clear trend to be found. This can be attributed to the fact that this cascade reaction requires two different steps. The first step involves the addition of the neutral  $\pi$ -nucleophile to the  $\alpha,\beta$ -unsaturated ketone and the second step involves the asymmetric protonation of the formed enolate. In order to obtain high enantioselectivity the protonation step needs to be rate-determining. Therefore, a sequence that accelerates the addition of the  $\pi$ -nucleophile but does not, or to a lesser extent, accelerate the protonation step, would be suitable. However, due to this conflicting argument, sequences suitable for this purpose may be limited.

The 1<sup>st</sup> generation metal-ligand complexes showed a preference for AT-rich sequences in the *syn* hydration reaction.<sup>8</sup> However, in the case of the oxa-Michael addition of alcohols, lower enantioselectivities were found upon using specific DNA sequences (Chapter 4). The presence of the alcohol destabilizes the duplex formation of the oligonucleotides and thereby also influences the outcome of the reaction. However, sequences containing a central ATAT segment tend to show the highest enantioselectivities, although, these are considerably lower compared to the results obtained with st-DNA.

### 6.2.5 Recycling of the DNA-based catalyst

In order to optimize the recyclability of the catalyst after use a DNA-functionalized gold nanoparticles (DNA-Au np's) have been synthesized and tested in catalysis. However, when using these DNA-Au np's in the DNA-based catalyzed Diels-Alder reaction and Michael addition, no enantioselectivity could be obtained. This is attributed to the blocking of the active copper centre by neighbouring DNA strands, since unfunctionalized Au np's did not influence the catalysis. Alternative approaches for such a recyclable catalyst should be based on mixed monolayers or the use of a different solid support, such as glass.

### 6.2.6 Water-miscible organic co-solvents

Water-miscible organic co-solvents can be used in DNA-based catalysis and can even be beneficial for it. Chapter 3 describes the use of up to 33 v/v% of water-miscible organic co-solvents without a loss in conversion and enantioselectivity. In the case of substrates with an aromatic or methyl substituent even higher conversions were found compared to the reactions in water alone. However, a kinetic study revealed that the use of water miscible organic co-solvents result in a decrease in the overall rate ( $k_{app}$ ). This can only be explained by the product dissociation step, which is not taken into consideration under kinetic conditions. Organic co-solvents accelerate the product

dissociation and thereby the overall reaction rate. Moreover, the use of water-miscible organic co-solvents has made it possible to reduce the catalyst loading down to 0.75 mol% and has as additional advantage that it allows for lower reaction temperatures. This has been used in the Friedel-Crafts alkylation. By performing the reaction at  $-18\text{ }^{\circ}\text{C}$  the enantioselectivity was increased from 83% to 93%. However, this was achieved at the expense of the reactivity.

The use of water-miscible organic co-solvents has also led to the development of the oxa-Michael addition of alcohols (Chapter 4). The combination of the water and alcohol is crucial for this reaction to take place even though it also gives rise to the *syn*-hydration product as side product. The alcohol is required as nucleophile whereas water seems to be important for reverting unwanted side reactions such as 1,2-additions, resulting in higher overall yields. The formation of the *syn*-hydration product could be reduced by performing the reaction at  $-18\text{ }^{\circ}\text{C}$ . Apparently, the rate of the hydration reaction depends much stronger on the temperature than the oxa-Michael reaction. Hence, even though the requirement for aqueous conditions causes the formation of a side product resulting from hydration of the enone, the reaction can be made chemoselective by lowering the reaction temperature.

## 6.3 Future prospects

### 6.3.1 DNA-based catalysis as synthetic tool

DNA-based catalysis has made an impressive progress since its discovery in 2005. However, as a tool for organic synthesis it has not made its entrance yet. This is probably due to the fact that DNA is not commonly used in organic synthesis and presents a mental barrier for the synthetic chemist. DNA-based catalysis has however a great potential and shows several advantages which make it suitable as a synthetic tool.

- DNA is, compared to other chiral ligands, relatively inexpensive and can be obtained from natural sources.
- DNA-based catalysis is performed in water. Water is a "green" solvent and is one of the most inexpensive and safe solvents imaginable. Moreover, whenever water is problematic, due to solubility issues, water miscible organic co-solvents can be added in order to improve the solubility.
- DNA-based catalysis shows interesting reactivities. Using DNA-based catalysis unusual enantioselective reactions, like the oxa-Michael addition of alcohols and the *syn*-hydration reaction, can be performed. These reactions are problematic using conventional catalysis.

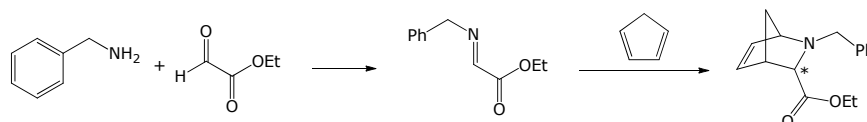
- DNA-based catalysis is performed under ambient conditions. Generally, the reactions are performed at 5 °C without a protective atmosphere. However, by the addition of a water miscible organic co-solvent the temperature can be lowered to -18 °C. which can be beneficial for either the enantioselectivity or chemoselectivity.
- Although an auxiliary group is required, for the coordination to the copper, it can be readily replaced by a variety of functional groups, such as carboxylic acids, esters, aldehydes and ketones.<sup>14,15</sup> Still, the use of substrates without the auxiliary group would be desirable.

Of course, there is still room for improvement. Challenges remain, they will be discussed in combination with some insights obtained from ongoing projects.

### 6.3.2 Challenges

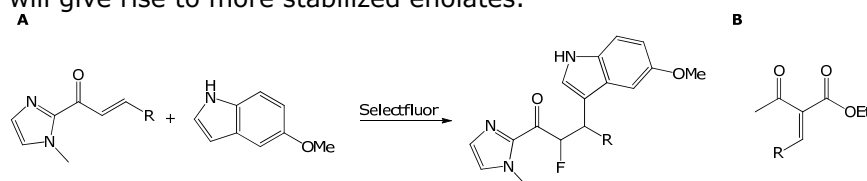
- *Recycling*  
One of the challenges mentioned before is still to improve the recyclability of the catalyst after use. The most suitable method is the covalent attachment of a short duplex of DNA to a solid support. However, the problem here is the blocking of the catalyst by the dense coverage of DNA on the solid support. This could be solved in two possible ways. Firstly, by making a mixed monolayer of alkanethiols and thiol modified DNA on gold nanoparticles. One possible problem could be that the cooperative binding of DNA on the gold support results in domains of DNA and thus not in reducing the packing of the DNA. The second solution would be to switch to a gold support with a mixed monolayer of alkanethiols and alkanethiol with a functional group and attach the DNA to these functionalized alkane thiols in a second step. This will result in separated duplexes of DNA on the solid support, however at the expense of the duplex stabilization induced by the cooperativity.
- *Expanding the scope of reactions*  
Although DNA-based catalysis has shown its power in several reactions, there is still plenty of room for the development of reactions. The asymmetric addition of thiols and amines are obvious but one could also think of cascade reactions like an aza-Diels-Alder reaction in which the dienophile is *in situ* formed from an amine and an aldehyde. Such a reaction would benefit from the addition of an organic co-solvent since the formed imine would readily hydrolyse in water. An aza-Diels-Alder reaction of cyclopentadiene with an *in situ* formed imine from benzylamine and ethylglyoxylate was performed (Scheme 6.1) with 33 v/v% of dioxane.<sup>16</sup> Unfortunately, even though the product could be isolated, no separation could be found on chiral HPLC.





**Scheme 6.1.** Aza-Diels-Alder reaction of cyclopentadiene with an *in situ* formed imine from benzylamine and ethylglyoxylate.

An alternative cascade reaction could make use of two previously developed reactions for DNA-based catalysis. In this cascade a conjugate addition is followed by the trapping of the enolate with an electrophile, such as for example an electrophilic fluorine source.<sup>17</sup> Such a cascade reaction was attempted by performing a Friedel-Crafts alkylation followed by the trapping with selectfluor (Scheme 6.2A). However, after the reaction only the Friedel-Crafts alkylation product could be obtained. Probably the lifetime of the enolate is too short to allow for an efficient fluorination of the intermediate enolate. A  $\beta$ -ketoester substrate (Scheme 6.2B) could be an interesting alternative substrate for this cascade reaction, since this will give rise to more stabilized enolates.



**Scheme 6.2.** A; Friedel-Crafts alkylation followed by the trapping with selectfluor, B; Alternative substrate,  $\beta$ -ketoester.

- *Transition metal catalysis other than copper catalysis*

Until now, all examples of DNA-based catalysis are based on  $\text{Cu}^{\text{II}}$ -complexes. However, the use of additional types of transition metal complexes should be possible. One of the major challenges in finding new metal complexes for DNA-based catalysis is the DNA itself. DNA has a large amount of free amines and alcohol groups capable of binding to the metal and thereby blocking its activity. In my opinion, especially hard metals pose problems in combination with DNA, since the large amount of free alcohols on the sugar moieties and phosphates can chelate the metal strongly. However, with this in mind, new metal complexes can be envisioned. A Pd-Bpy complex would be a suitable candidate to start with. They form, like  $\text{Cu}^{\text{II}}$ , square planar complexes,<sup>18</sup> bind to DNA,<sup>18</sup> and can be used in water. Furthermore, they already showed activity in a boronic acid addition to cyclohexenone. Under unoptimized conditions, Pd-Bipy showed 25% ee; however, due to hydrolysis of the boronic acid the conversion was only 5%. Altogether this would be a promising start for a new catalyst in DNA-based catalysis.

## 6.4 Concluding remarks

All in all, DNA-based catalysis displays interesting reactivities and high enantioselectivities, which make it interesting for organic synthesis. The present work represents a major step towards its application in organic synthesis.

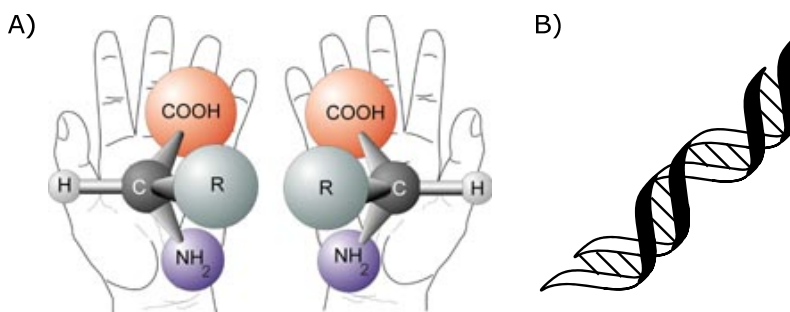
## 6.5 References

1. G. Roelfes, B. L. Feringa, *Angew. Chem. Int. Ed.* **2005**, *44*, 3230.
2. G. Roelfes, A. J. Boersma, B. L. Feringa, *Chem. Commun.* **2006**, 635.
3. A. J. Boersma, B. L. Feringa, G. Roelfes, *Org. Lett.* **2007**, *9*, 3647.
4. A. J. Boersma, J. E. Klijn, B. L. Feringa, G. Roelfes, *J. Am. Chem. Soc.* **2008**, *130*, 11783.
5. F. Rosati, A. J. Boersma, J. E. Klijn, A. Meetsma, B. L. Feringa, G. Roelfes, *Chem. Eur. J.* **2009**, *15*, 9596.
6. D. Coquière, B. L. Feringa, G. Roelfes, *Angew. Chem. Int. Ed.* **2007**, *46*, 9308.
7. A. J. Boersma, B. L. Feringa, G. Roelfes, *Angew. Chem. Int. Ed.* **2009**, *48*, 3346.
8. A. J. Boersma, D. Coquière, D. Geerdink, F. Rosati, B. L. Feringa, G. Roelfes, *Nature Chem.* **2010**, *2*, 991.
9. A. J. Boersma, B. de Bruin, B. L. Feringa, G. Roelfes, *Chem. Commun.* **2012**, *48*, 2394.
10. A. J. Boersma, **2009**, DNA-based asymmetric catalysis, Thesis, University of Groningen.
11. K. Guckian, B. Schweitzer, R. Ren, C. Sheils, D. Tahmassebi, E. Kool, *J. Am. Chem. Soc.* **2000**, *122*, 2213.
12. E. Kool, J. Morales, K. Guckian, *Angew. Chem. Int. Ed.* **2000**, *39*, 990.
13. E. W. Dijk, A. J. Boersma, B. L. Feringa, G. Roelfes, *Org. Biomol. Chem.* **2010**, *8*, 3868.
14. D. H. Davies, J. Hall, E. H. Smith, *J. Chem. Soc. Perkin Trans. 1* **1991**, 2691.
15. D. A. Evans, K. R. Fandrick, H. J. Song, K. A. Scheidt, R. Xu, *J. Am. Chem. Soc.* **2007**, *129*, 10029.
16. P. Bailey, R. Wilson, G. Brown, *Tetrahedron Lett.* **1989**, *30*, 6781.
17. N. Shibata, H. Yasui, S. Nakamura, T. Toru, *Synlett* **2007**, 1153.
18. M. Yodoshi, N. Okabe, *Chem. Pharm. Bull.* **2008**, *56*, 908.

## Nederlandse samenvatting

Katalyse is een belangrijk gereedschap voor het synthetiseren van moleculen. Bij katalyse worden reacties versneld of mogelijk gemaakt zonder dat de katalysator zelf wordt verbruikt. Katalysatoren zijn bv. zuren, basen, metaal complexen of organische verbindingen.

Bij enantioselectieve katalyse is het doel om één spiegelbeeldvorm van een molecuul te maken. Dit kan erg belangrijk zijn voor het maken van bv. medicijnen, omdat deze verschillende reacties kunnen hebben in het lichaam. Deze spiegelbeeldvormen van moleculen zijn te vergelijken met een linker- en een rechterhand, beide bevatten dezelfde groepen (vingers) maar zijn elkaars spiegelbeeld (Figuur 1A). Bij enantioselectieve katalyse wordt daarom vaak gebruik gemaakt van een structuur die één van de twee spiegelbeelden herkent. Om weer terug te komen bij het voorbeeld van de handen, in een rechterhandschoen past slecht een linkerhand. Hoe goed een katalysator is in het selecteren van een spiegelbeeld wordt uitgedrukt in enantiomere overmaat (ee). Een ee van 80% betekent dat er 90% van het juiste spiegelbeeld wordt gemaakt ten opzichte van 10% van het andere spiegelbeeld, oftewel hoe hoger de ee hoe beter de katalysator is.

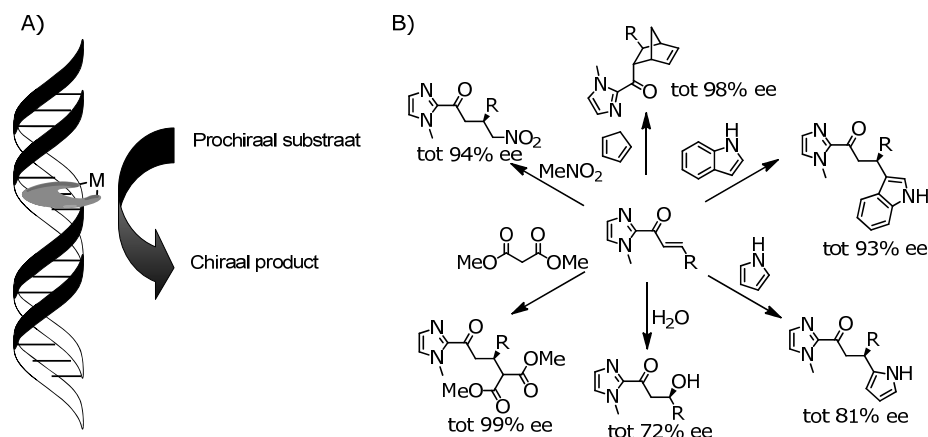


**Figuur 1.** A; spiegelbeeldvormen, B; dubbele DNA-helix

In het onderzoek beschreven in dit proefschrift wordt DNA in combinatie een metaalcomplex gebruikt als katalysator. In de natuur is DNA de drager van alle genetische informatie en verantwoordelijk voor het functioneren van alle levende organismen. DNA is opgebouwd uit twee lange polymeren. DNA bevat een ruggegraat van fosfaat en suikergroepen waaraan de nucleobasen zijn bevestigd. De nucleotiden zijn adenine (A), cytosine (C), guanine (G) en thymine (T). De genetische informatie is opgeslagen in de volgorde van deze vier

nucleobasen. De twee lange polymeren binden elkaar op een antiparallele manier waarbij ze om elkaar heen draaien tot een mooie rechtshandige dubbele helix (Figuur 1B). De dubbele DNA-helix wordt bijeen gehouden door twee krachten, namelijk, waterstof bruggen tussen de nucleotiden en "base-stacking" interacties tussen de nucleobasen.

De helische structuur van DNA heeft altijd al aantrekkingskracht gehad op chemici. In onze groep hebben we DNA-gebaseerde katalyse ontwikkeld. Dit concept is gebaseerd op een achiraal metaal complex dat kan binden aan DNA (Figuur 2A). Hierdoor wordt het beïnvloed door de chirale omgeving die door het DNA gevormd wordt en die kan worden overgedragen op verschillende asymmetrisch gekatalyseerde reacties zoals de Diels-Alder reactie, Michael additie, Friedel-Crafts alkylering en meer recent de *syn*-hydratie reactie (Figuur 2B).



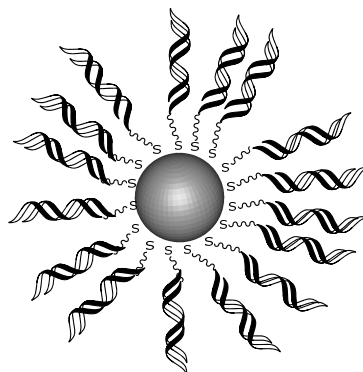
**Figuur 2.** A; algemene concept van op DNA-gebaseerde katalyse, B; overzicht van DNA-gebaseerde katalyse reacties

Het doel van het onderzoek dat in dit proefschrift gepresenteerd wordt is om het gebruik van DNA-gebaseerde katalyse verder uit te werken voor het gebruik in synthetisch interessante reacties. Het onderzoek was gericht op twee gebieden, namelijk, 1) optimalisatie van de reactiecondities met betrekking tot de reactieschaal en het recyclen van de DNA-koper katalysator, 2) de ontwikkeling van nieuwe reacties die hiervoor onbekend of moeilijk uit te voeren waren.

Hoofdstuk 1 geeft een algemeen overzicht van het gebruik van helix-vormige polymeren in asymmetrische katalyse.

In hoofdstuk 2 wordt een aanpak voor de covalente binding van DNA- strengen aan goud nanodeeltjes beschreven voor het gebruik in enantioselectieve katalyse. Het covalent binden van DNA aan een vaste ondergrond zou het recyclen van DNA vergemakkelijken. Het DNA werd succesvol gekoppeld aan de goud nanodeeltjes (Figuur 3) en liet een scherpe smelt transitie zien. Dit is bekend voor dit soort systemen. Bij het gebruik van deze deeltjes werd er echter geen katalytische activiteit

voor de Michael additie en de Diels-Alder reactie waargenomen. Ook het verlengen van de linker met als doel om de DNA verder van het oppervlak te krijgen resulteerde niet in katalyse. Waarschijnlijk is het DNA te dicht open gepakt op de goud nanodeeltjes en kunnen de reagentia niet bij het actieve koper complex komen.

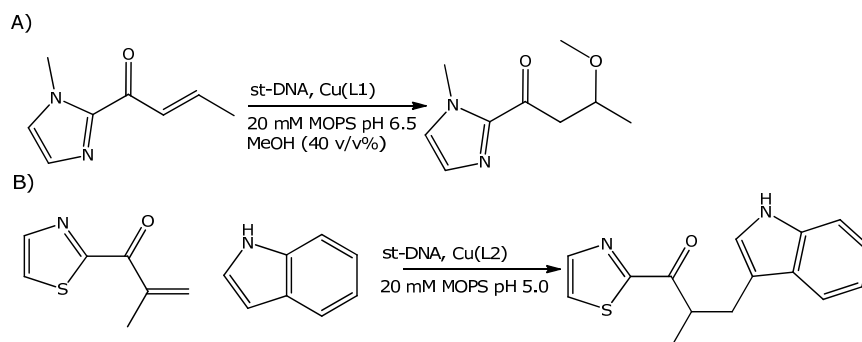


**Figuur 3.** DNA op goud nanodeeltjes

Hoofdstuk 3 beschrijft de invloed van een organisch mede-oplosmiddel op DNA-gebaseerde katalyse. Dit onderzoek richtte zich op het effect van deze mede-oplosmiddelen op de DNA-structuur, en de opbrengst, enantioselectiviteit en kinetiek van de gekatalyseerde reactie. Aangetoond werd dat tot 33 v/v% van een water oplosbaar organisch mede-oplosmiddel kon worden gebruikt in de Diels-Alder reactie zonder dat de opbrengst of de enantioselectiviteit werd beïnvloed. In de Michael additie en Friedel-Crafts alkylering kon maximaal 10 v/v% worden gebruikt zonder de opbrengst of de enantioselectiviteit negatief te beïnvloeden. Een kinetische studie toonde aan dat de bindingsconstante van het koper-complex aan het DNA niet veranderd werd door de toevoeging van een water oplosbaar organisch mede-oplosmiddel. Verder bleek dat de totale reactiesnelheid van de reacties wel werd verminderd. Dit terwijl onder katalytische condities hogere omzettingen bleken te zijn behaald. De hypothese is dat de toevoeging van een water oplosbaar organisch mede-oplosmiddel de dissociatie constante van het product met de katalysator wordt verlaagd en dat daardoor de reactie onder katalytische condities wordt versneld.

Het gebruik van een water oplosbaar organisch mede-oplosmiddel heeft als extra voordeel dat het de oplosbaarheid van reagentia verhoogd. Dit voordeel werd gebruikt om een hogere concentratie van substraten te bereiken. Hierdoor was het mogelijk om de katalysator lading te verlagen naar 0.75 mol%. Verder maakt het gebruik van water oplosbaar organisch mede-oplosmiddelen het ook mogelijk om de temperatuur waarbij de reactie wordt uitgevoerd te verlagen. Hierdoor kon de Friedel-Crafts alkylering worden uitgevoerd bij  $-18\text{ }^{\circ}\text{C}$ , wat leidde tot een toename van de enantioselectiviteit van 83% tot 93%.

Hoofdstuk 4 beschrijft de eerste overgangsmetaal gekatalyseerde asymmetrische intermoleculaire oxa-Michael additie van alcoholen (Schema 1A). Deze reactie werd gekatalyseerd door een eerste generatie ligand. Tot 86 % ee kon worden behaald in deze reactie. Echter bleek het gebruik van water ook te leiden tot de vorming van het *syn*-hydratie product. Gelukkig kon de chemo-selectiviteit van deze reactie worden beïnvloed door de reactie bij  $-18\text{ }^{\circ}\text{C}$  uit te voeren. Het gebruik van water bleek echter wel belangrijk voor het reduceren van extra ongewenste reacties zoals 1,2-addities. De behaalde ee's representeren de hoogste enantioselectiviteiten die tot nog toe zijn behaald in een katalytische intermoleculaire oxa-Michael additie.



**Schema 1.** A; intermoleculaire oxa-Michael additie. B; Friedel-Crafts alkylering/enantioselectieve protonering cascade reactie

In hoofdstuk 5 wordt een nieuwe benadering voor de asymmetrische protonering in water beschreven. Normaal wordt deze reactie uitgevoerd met lage concentraties protonen om de protonering te kunnen controleren. In ons systeem kan de concentratie van de protonen echter niet worden gereduceerd omdat de reactie wordt uitgevoerd in water. Het is echter bekend dat het gebruik van DNA de Friedel-Crafts alkylering versnelt. Wij hebben hiervan gebruik gemaakt door een cascade reactie uit te voeren waarin een enolaat *in situ* wordt gevormd door de additie van een  $\pi$ -nucleofiel (Schema 1B). Door de versnelling van de Friedel-Crafts alkylering wordt de protonering de snelheidbepalende stap. Met behulp van een tweede generatie koper complex kon de Friedel-Crafts alkylering/enantioselectieve protonering cascade reacties worden uitgevoerd met een grote verscheidenheid aan indolen waarbij de producten konden worden gesynthetiseerd met maximaal 59% ee. Verdere kinetische studies zijn belangrijk om de hypothese te onderbouwen.

Tenslotte worden in hoofdstuk 6 de resultaten van het in dit proefschrift beschreven onderzoek samengevat en conclusies getrokken. Verder wordt er een perspectief voor verder onderzoek gegeven.

# Dankwoord

Bijna vijf jaar na het begin van mijn promotieonderzoek kijk ik met veel plezier terug op een periode van een beetje bloed, zweet en tranen maar vooral veel plezier. Daarom wil ik een aantal mensen bedanken voor hun bijdrage aan deze mooie periode. Zoals jullie weten ben ik een persoon van weinig woorden dus ik houd het kort, maar allereerst wil ik me wel verontschuldigen voor mijn practical jokes en soms slechte muziekkeuze.

Allereerst wil ik mijn promotor Gerard Roelfes bedanken. Gerard, je bent een uitstekend voorbeeld van een groepsleider, ik heb dan ook erg veel van je geleerd. Bedankt voor de dagelijkse begeleiding, de altijd openstaande deur en het creëren van een kritische, creatieve maar toch vooral gezellige onderzoeksgroep.

Graag wil ik de leden van de leescommissie, prof. dr. F.P.J.T. Rutjes, prof. dr. B.L. Feringa en prof. dr. J.G. de Vries, bedanken voor hun vlotte en positieve beoordeling van dit proefschrift. Verder wil ik jullie ook bedanken voor de discussies aangaande het in dit proefschrift gepresenteerde onderzoek.


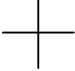
Verder wil ik Theodora Tiemersma-Wegman, Monique Smith, Albert Kiewiet, Hans van de Velde, Ebe Schudde, Wim Kruizinga voor het uitvoeren van de analyses of hulp bij het uitvoeren daarvan.

Jos, bedankt voor het uitvoeren van de berekeningen in hoofdstuk 5.

Wesley, thanks for the discussions and help involving spectroscopic techniques. Also I want to thank you for the suggestion to run the reaction with organic co-solvents in the freezer. I know you enjoyed the thought of me working at  $-18\text{ }^{\circ}\text{C}$ .

Almudena, thank you for joining up on the enantioselective protonation reaction project. I really enjoyed working together with you, the discussions and laughters. I am glad that you want to be one of my paranymphs and look forward to join you on a trip to Asturias someday.

Jeffrey, waar zal ik beginnen? Bedankt voor alle, soms verhitte, discussies, je "voorzetten", de filmpjes, je eigenaardigheidjes, maar bovenal voor de gezelligheid. Het is een eer om je als paranimf te hebben en ik wens je alle succes toe met het afronden van je eigen promotie.



Tijdens mijn promotie heb ik het plezier gehad om een drietal studenten te mogen assisteren, namelijk Wienand, Ruben en Pim. Ik heb veel van jullie geleerd over het begeleiden van verschillende type mensen. Succes met het vervolg of afronden van jullie Master.

Nuria, I see the two of us as Pinky and the Brain, everyday a new 'plan' to conquer the Ruffles group. It was a great pleasure to share the lab with you and I have missed you a lot since you left.

Lorina, Qian, Fiora, Jens, Almudena Lueje Alonso, Bea, Arjan, Jorrit, Ruben, Pim, Wienand, Arnold, Davide, Ewold, Ana, Sambika, Massimo, Diane, Sylvia, and all other people that have passed during my promotion period in the Ruffles group. Thank you all for participating in Ruffles activities and making the Ruffles group such a fun group to work in.

De deelnemers van de spelavonden voor de benodigde ontspanning buiten het lab. Bedankt Tim, Chris, Bart, Danny, Arjen, Jeroen, Kerwin en Mark.

Then I would like to thank all participants of the football subgroup and borrels. Although my ankle did not always enjoy the football I would like to thank you all for the nice after worktime laughs and widely ranged conversations

Dan wil ik mijn vrienden en (schoon)familie erg bedanken voor hun interesse en steun wanneer dat nodig was.

Als laatste natuurlijk Ellen. Ellen bedankt voor alle support en we gaan een spannende maar mooie tijd tegemoet.